Journal of Marine Technology and Environment

Vol. II, year 2012

ISSN 1844-6116

CONTENTS

THE ENVIRONMENTAL IMPACTS OF EMMISIONS GENERATED BY ROUTINE OPERATION ON PORTS

[1]ABDUL CHALID, [2]ABD SAMAN BIN AB KADER, [3]AHMAD KHAIRI BIN ABD WAHAB, MUHAMAD HANIS

[1]Staff of Coastal & Offshore Engineering Institute UTM, [2]Staff of Dept. Marine Technology, Faculty of Mechanical UTM, [3]Director of Coastal & Offshore Engineering Institute UTM, [4]Graduated Master Student, Dept of Hydraulic & Hydrology, Malaysia

The expansion of international trade arising from globalization has led to a substantial increase in goods transshipment between ports. This has led to increased emissions from ships in ports, and trucks traveling to and from ports. Increment of ship traffics and machineries could be a source of gaseous emissions and particulate pollutants. This study attempt to investigate the problems in Johor Port. Emission sources concentration of sulphur dioxide (SO_2), nitrogen dioxide (NO_2), carbon oxides (CO, CO_2) and particulate matter less than 10 µm (PM10) in port were obtained. From the results obtained based on the comparison with Recommended Malaysian Air Quality Guidelines (RMAQG), NO_2 concentration surprisingly exceed the limit by 5.9 percent in sampling station 2 while highest SO_2 concentration were detected in sampling station 1 and 3 with a value of 0.2 ppm exceeding the RMAQG limits of 0.13 ppm by 53.8 percent for both stations. Other gaseous at station 1, 2 and 3 are still within the recommended guidelines. Based on the computation of Ocean-Going Vessels (OGVs) emissions estimate and later compiled as inventory, the results clearly shows that major pollutants contributor in Johor Port are oxides of nitrogen (NOx) and sulphur dioxide (SO_2) with a percentage value of 60 and 27 percent for maneuvering mode while 60 and 28 percent for berthing mode. Other pollutants contribute below than 10 percent for both modes.

***Keywords**:* Inland Port, Environment, Emission source, Pollutants

1. INTRODUCTION

What is contamination and what constitutes pollution are commonly asked questions and the view taken by some scientists is that a distinction must be made between contamination and pollution. Contamination is the presence of elevated concentrations of substances in the environment that are above the natural background level for the area and for the organism. Pollution on the other hand is the introduction by humans, directly or indirectly, of substances or energy into the water, resulting in such deleterious effects as harmful to living resources and hazard to human health. The objective is to have health, hygiene and waste disposal issues addressed by port planners when designing new ports and upgrading existing facilities as well as by port managers at all times. Thus, the standards for sanitary water that

should be used in all aspects of fisheries, including the routes of contamination, are reviewed and solutions proposed. In particular, methods for the disposal of all types of waste likely to arise from fishing operations are discussed. Consequently, the readership, port engineers, port managers and those responsible for safety and health would be better equipped to design systems that can withstand the rigours of a new modern fishing port and, with regard to existing ports, to identify potentially weak points in their public health applications as well as waste disposal systems. The ultimate beneficiaries will be the consumers of fish and fish products.

1.1. Environmental Impacts of Pollutants

Problems concerning environmental issues have received more and more attention during the last decades. Transportation sector is one of the major polluting sectors and it is the only sector that has not yet been able to reduce its emission levels if compared to earlier years [1]. In addition, transportation sector is the only sector with increasing carbon dioxide emission amounts

Figure 1 presents the extend of port generated pollution. On the basis of an IAPH (International Association of Ports & Harbors) survey, filled in by 183 ports, the crucial areas were three: (1) dangerous materials, (2) water pollution, and (3) dredging and dumping of dredged waste. The third factor is connected to port expansion or conservation as a great danger for oil pollution. However, maritime transport is responsible for only 12% of all pollution though in terms of quantity this figure cannot be underestimated. Handling of cargo generates dust, especially dust coming from phosphates [2]. The loss of product is most likely at storage and handing places, i.e. in ports with a product loss is 1% of traffic flow. The liquid products are flammable and toxic with vapour emissions. Common causes of accidents are due to rupture of connecting hoses or pipelines, bursting of valves or manifolds and failure of coupling between ship and shore[3].

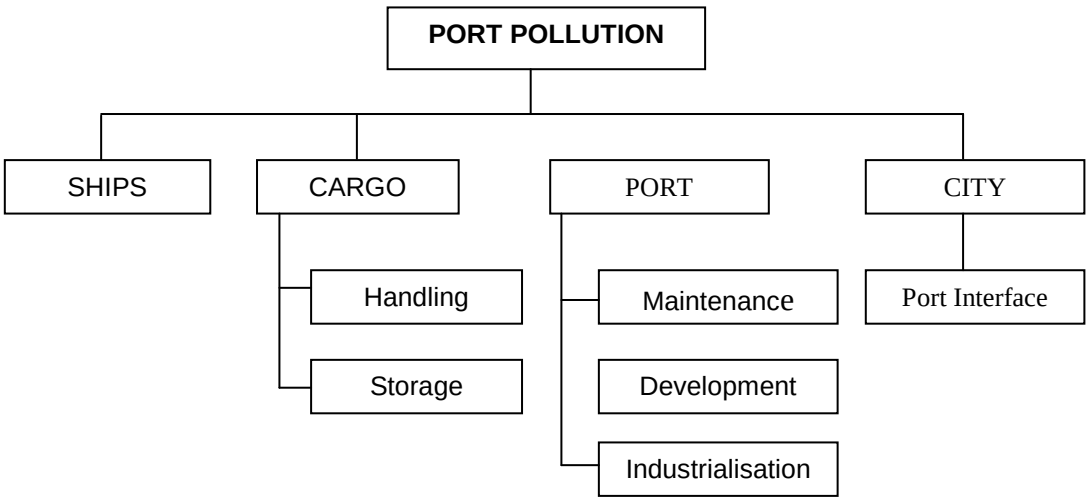

Fig. 1. Port Pollution and its causes (UNCTAD, 1993)

There is also the turbidity effect [3]. Possible pollution may come from maintenance of port's equipment and superstructure due to grit blasting and spray painting or from ship

repairs in the port area. If port is of a third (or even a second) generation, pollution may come from maintenance and repair works to the industrial plants located in the port. Very important is the relationship between port development and environment [4-6], as traffic (demand) expands and the roles of port change from a simple hinterland terminal to a complex nodal point n the logistics chain. This last fact requires also change in port's infrastructure layout [3]. Apart from investment cost for dredging facilities, the infrastructure should now take into account environmental impact and environment restoration to ecological standards. Environment requirements are now part of the investment cost and this may be quite high for a port, even for those owned by the public sector [7].

Although the social needs of the Community should be supported by ports, conflicts are inevitable because the concentration of cargo in a limited number of ports makes the whole situation more suitable and viable for high-volume modes like rail, except road, which may be the candidate for next use. This is a negative factor for the policy of shifting freight transport from road to sea. Smaller ships could increase their direct port calls in the future. It is thought that this attitude will permit a more balanced traffic flow and port development in Euro. Ports are to help congestion and bottleneck phenomena of the main land-corridors and minimize external [8].

1.2. Environmental Impacts of Port Development

Major sources of port development adverse effects can be categorized into three types: (a) location of port; (b) construction; and (c) port operation, including ship traffic and discharges, cargo handling and storage, and land transport. Location of port connotes the existence of structures or landfills, and the position of the development site. Construction implies construction activities in the sea and on land, dredging, disposal of dredged materials, and transport of construction materials. Port operation includes ship-related factors such as vessel traffic, ship discharges and emissions, spills and leakage from ships; and cargo-related factors such as cargo handling and storage, handling equipment, hazardous materials, waterfront industry discharges, and land transport to and from the port.

Environmental facets to be considered in relation to port development are categorized into nine groups: (a) water quality; (b) coastal hydrology; (c) bottom contamination; (d) marine and coastal ecology; (e) air quality; (f) noise and vibration; (g) waste management; (h) visual quality; and (i) socio-cultural impacts.

Water quality includes five elements: (a) general features such as temperature, salinity, pH, colour, transparency, oil and grease, and organic material concentration measured by total organic carbon (TOG), chemical oxygen demand (GOD) or biochemical oxygen demand (BOD); (b) turbidity measured by suspended solids (SS); (c) eutrophication-related factors measured by dissolved oxygen (DO), nitrogen (N) and phosphorus (P); (d) harmful or toxic substances including heavy metals such as mercury, cadmium, lead, and pesticides; and (e) sanitation-related factors determined by measuring the amount of coliform bacteria.

1.3. Checklist of Potential Adverse Effects

The list of categorizes environmental resources concerning port development into the following types: (a) Coastal marine ecology; (b) Recreation/Resort/Beach areas; (c) Sanitation in harbor area; (d) Hazardous cargo; (e) Materials to and from harbor, (f) Local socio-economics, etc., and has an indication of feasible protection measures against each action. The Japanese Transport Ministry also furnishes a check list of environmental impacts

concerning port development, which is classified from a viewpoint of environmental components, viz. water quality, air quality, living characteristics (noise, odour, vibration, etc.) topographical features, ocean graphical features, hazardous material contamination, natural habitat (land and marine), landscape, and socio-cultural features [9]. As indicated in these check lists, the potential adverse effects of port development embrace a wide range of environmental issues like water pollution, contamination of bottom sediment, loss of bottom biota, damage to fisheries, beach erosion, current pattern changes, waste discharges, waterfront drainage, oil leakage and spillage, hazardous materials, emissions of dust and gases, smoke and other air pollution, noise, odour, traffic increases, landfills, landscape, socio-cultural impacts, and so forth.

These probable adverse effects of port development are usually assessed by the magnitude of impacts, however, there is no established criteria to evaluate whether or not these adverse effects fall within an acceptable range as such criteria will vary by countries or ports depending on local and regional characteristics. In case the background pollution levels in a project area exceeded their standards, a development project could be evaluated from a viewpoint whether the project is included in the environment management plan of the region. Evaluation procedures are the key to successful implementation of EEA [10].

1.4. Waste Water Limit Parameters of Port

The uses limitation of sludge, or potentially hazardous exposure levels are based on local limits requirements by the city of Port Angeles established in cooperation with the Department and codified in the city's ordinance. The existing permit does not require a monitoring for the pollutant parameters. This proposed permit requires the city to monitor certain parameters to verify that the presence of certain parameters is below the local limits. The city of Port Angeles does have limits on certain pollutants. The new maximum limits in this permit are derived from the city of Port Angeles local limits. Current and proposed applicable limits for this discharge are included in Table 1.

Table 1: Local (The city of Port Angeles), Existing and Proposed Limits Parameters

	Units	Local Limits	Existing Limits	Proposed Limits
pH	S.U	5-9	None	5.0-9.0
Oil and Grease	mg/L	100	None	100
TSS	mg/L	400	None	400
BOD_5	mg/L	400	None	400
Arsenic	mg/L	0.1	None	0.1
Cadmium	mg/L	0.1	None	0.1
Total Chromium	mg/L	2	None	2
Copper	mg/L	1	None	1
Lead	mg/L	0.5	None	0.5
Nickel	mg/L	1.5	None	1.5
Silver	mg/L	0.5	None	0.5

Zinc	mg/L	1.5	None	1.5
Cyanide	mg/L	1	None	1
Mercury	mg/L	0.05	None	0.05

2. METHODOLOGY

2.1. Location Study

This study was conducted at Johor Port (It can be seen in Figure 2). The location was chosen based on the study whereby today, emissions from ships have been recognized as one of the important sources of air pollution and it is apparent that air pollution from shipping activities is a growing problem that is drawing increased attention around the world. Johor Port is located in area whereby it is very well known for its industrial activities and the air quality condition which is closely related to the smoke or air pollutants emitted from industries and vehicles. Therefore, the study locations for sampling should follow the following criteria: (1) The selection of sampling stations should only consider the emissions from vessels.(2) Sampling stations must be as near as possible to the vessels emissions sources in port area, and (3) the closest sources to collect the concentration of gaseous from vessels emission will be on the pier/wharf/dock.

Based on the above, it can be assumed that the gas concentrations that are collected mainly coming from the vessels emission. For this study, there are three sampling stations selected for the purpose of data sampling, the port indicates the locations of sampling stations namely: Station 1 : Pier 10 **[**N 01°25'52.5"**,** E 103°55'14.0"**]**, Station 2 : Pier 3 **[**N 01°26'00.4"**,** E 103°54'29.1"**]**, and Station 3 : Container Terminal 3 (CT3) **[**N 01°26'18.6"**,** E 103°53'15.2" The factors of working day and working time are not an issue due to inland port activities running 24 hours a day throughout the year. For this study, the sampling was carried out during office hours from 0900 hours till 1700 hours with a data frequency collected every 5 minutes for every sampling station. Sampling and monitoring were only conducted on bright and sunny days.

Fig. 2. Johor Port of Johor State Map in Malaysia

2.2. Data Collection

The data collection focuses on two primary areas; vessel or equipment details and operational profiles that were collected from Johor Port Authority to be used in this study include the parameters such as; port vessels statistics, Vessel type (e.g., container vessel, bulk carrier, general cargo), No, type and rated power (kilowatts) of main engine, No, type

and rated power of auxiliary engine, Hours of operation annually in port, Engine model years, and Types of fuel used

2.3. Equipments

There are three types of equipment used for collecting the concentration of gas and total suspended particulate in the atmosphere. The equipment used to measure the concentration of suspended particulate is MiniVol Portable Air Sampler whereas to measure the concentration of gas is by using Graywolf Direct Sense Monitoring Kit (Toxic Gas TG-501 PROBE) and TSI IAQ-Calc. These equipments are the property of Environmental Engineering Lab, Faculty of Civil Engineering, Universiti Teknologi Malaysia.

2.4. Total Suspended Particulate Equipment

Equipment used to measure the concentration of total suspended particulate (TSP) is the MiniVol Portable Air Sampler. This unit is a product of Air metrics 2121 situated in Franklin Boulevard, Eugene, USA. This unit can also be used to collect the concentration of gas in the air instead of only being used for collecting the concentration of TSP. However, this study only uses the equipment to trace the concentration of TSP. This unit operated on four alkaline batteries with the power of 12 Volts. After every sampling, the battery must be charged with a minimum charging time of 18 hours. The size of TSP that can be collected on the filter paper is bigger than 2.5 μm. The diameter of filter paper is 47 mm and the weight is within 0.0815 to 0.0916 g. The filter paper is made of quartz paper or pure Teflon and must be stored inside petri slides, before and after use.

3. RESULTS AND DISCUSSION

The analyses are conducted based on firstly: Comparison between stations based on Recommended Malaysian Air Quality Guidelines (RMAQG) in Johor Port area. Secondly: The emission inventory for Johor Port Table 2 shows NO_2 concentrations in relation to the recommended guidelines. The highest NO_2 concentration was detected in sampling Station 2, with a concentration of 0.18 ppm, exceeding the RMAQG limits of 0.17 ppm by 5.9 percent. Apart from Station 2 that is high in concentration, Station 3 also detects a high value of NO_2 concentration as well, even though the concentration is at par with the RMAQG limits of 0.17 ppm. Such high concentration in both Station 2 and 3 are due to heavy vessels operation of cargo loading and unloading during the sampling process. For Station 1, the concentration of 0.12 ppm is considered acceptable and is still within the RMAQG limits. Overall NO_2 concentration for Johor Inland Port area is in the range of 0.01 ppm to 0.18 ppm. By referring to the trends of NO_2 concentration levels in Johor, based on sampling stations, the concentration level can be considered as high, thus contributing to the poor air quality in the area.

Table 2: Recommended Malaysian Air Quality Guidelines (RMAQG) (DOE, 2006)

Pollutant	Averaging Time	RMAQG
NO2	1 hour	0.17 ppm
SO2	1 hour	0.13 ppm
CO	1 hour	30 ppm
PM10	24 hour	150 μg/m3

The SO_2 concentrations for all sampling stations with the RMAQG limit. In the case of SO_2 concentration, the highest concentrations were detected in Station 1 and 3 with a value of 0.2 ppm exceeding the RMAQG limits of 0.13 ppm by 53.8 percent for both stations. Such a big differences is mainly caused by the emission from vessels manoeuvring towards the pier/wharf/dock and it might also be contributed by pilot and tug boat which assist the vessels during manoeuvring period. For sampling Station 2, the SO_2 concentration of 0.1 ppm is within the recommended guideline limits and this value is acceptable. For the low concentration levels that give a reading of zero for all three stations mainly caused by the sensitivity of the sampling equipment. By looking at the limits set by the RMAQG of 0.13 ppm, the concentration value is in point two decimal places (0.xx) whereas for the equipment that was used, the concentration reading only give up to point one decimal place (0.x). Any SO_2 concentration detected less than 0.1 ppm cannot be detected thus giving the zero reading as in Figure 4. Overall SO_2 concentration for Johor Port area is in the range of 0.0 ppm to 0.2 ppm. As a remark, the air quality in Johor Port based on SO_2 concentrations remain below than average.

Table 3 present the emission estimate of OGVs by mode in Johor Port which later was compiled as inventory for the year 2007. With a total number of 9176 vessels in 2007 as in Figure 4, the type of vessel, the activity duration, based on the selected factors being considered, the above inventory are the results of emission that were computed using the emission rate estimate. Each pollutants and gaseous emits such emission in a year.

Table 3: 2007-OGVs emission inventory by mode in Johor Port

Mode	NOx	VOC	CO	SO2	PM10	PM2.5	CO2	N2O	CH4
	kT yr-1								
Manoeuvering	13,698	489	1,076	6,301	802	641	62,425	29	39
Berthing	15,234	441	1,130	7,138	849	679	748,249	31	41

The emission estimates of OGVs by mode in Johor Port for the year 2008 are compiled in Table 4. In 2008, a total number of 8241 vessels were recorded in Johor Port area. Basically, some decrease was observed in emission for every pollutant and gaseous in year 2008 when compared to the year 2007. The decrease was possibly caused by the amount of vessel in 2008 which decreasing by 11.3 percent from year 2007. However, if the numbers of vessels keep on growing, the emission rate can be decreased by installing reduction technologies onto the vessels that were going to enter the Johor Port boundaries. Besides, the inventory in Table 3 and 4 can act as a baseline of emission in Johor Port for future planning and references.

Table 4: 2008-OGVs emission inventory by mode in Johor Port

Mode	NOx	VOC	CO	SO2	PM10	PM2.5	CO2	N2O	CH4
	kT yr-1								
Manoeuvring	11,203	400	880	5,153	656	524	541,781	24	32
Berthing	12,458	339	932	5,837	694	555	611,926	25	33

Table 4 is from the emission inventory, the overall percentage contribution of pollutants in manoeuvring mode in Johor Port area. As we can see from the pie chart, oxides of

nitrogen contribute 60 percent out of all pollutants emission while sulphur dioxide contributes 27 percent. Carbon monoxide contributes 5 percent out of total pollutants emission and particulate matters, both contribute 3 percent each and lastly volatile organic compound is the smallest percentage pollutants contributor to Johor Port.

The overall percentage contribution of pollutants in berthing mode in Johor Port area based on the emission inventory. The pie chart shows the contribution of oxides of nitrogen as much as 60 percent while sulphur dioxide is as much as 28 percent out of all the pollutants emission. Sulphur dioxide increases in hotel mode due to longer period needed for running the auxiliary engine to produce electricity for the vessels purposes. Other gaseous contributes below than 10 percent out of total OGVs emissions.

From this table 5, it is obvious that the highest NO_2 detected in Station 2 with a concentration of 0.18 ppm exceeding the RMAQG limits of 0.17 ppm by 5.9 percent while highest SO_2 concentration were detected in Station 1 and 3 with a value of 0.2 ppm exceeding the RMAQG limits of 0.13 ppm by 53.8 percent for both stations. Other gaseous at Station 1, 2 and 3 are still within the recommended limits. Basically the limits of NO_2 in Station 2 exceeded the RMAQG due to heavy operation (cargo loading and unloading) during the sampling process and as for high SO_2 reading that were detected were also caused by vessel manoeuvring towards pier/wharf/dock. From this table, CO values were not detected. The possibilities that CO was not detected are due to the sensitivity of the equipment used because, theoretically, CO should be at a certain value when there is an emission. As a whole, Johor Port should look into methods on how to reduce the concentration based on the sampling done, and the values that were recorded with such a value.

Table 5. Summary of result for NO_2, SO_2, PM10, CO and CO_2

Station	Sampling Range	NO_2	SO_2	PM_{10}	CO	CO_2	RMAQG	Comment
1	High	0.12	0.2	4.8	ND*	353	NO_2= 0.17 $S0_2$ = 0.13 PM_{10}= 150 C0 = 30	Highest $S0_2$ (0.2) > 0.13
	Low	0.01	0.0	2.3	ND*	351		
2	High	0.18	0.1	9.6	ND*	364	NO_2= 0.17 $S0_2$ = 0.13 PM_{10}= 150 C0 = 30	Highest $N0_2$ (0.18) > 0.17
	Low	0.02	0.0	2.4	ND*	350		
3	High	0.17	0.2	9.5	ND*	385	NO_2= 0.17 $S0_2$ = 0.13 PM_{10}= 150 C0 = 30	Highest $S0_2$ (0.2) > 0.13
	Low	0.02	0.0	2.2	ND*	351		

ND* = not detected

Figure 3 presents the numbers of vessel that were in Johor Port in the year 2007 till mid 2009. The vessel data in the year 2010 cannot be found. Based on the graph, the increase and decrease number of vessel for a certain month in a certain year depends much on the consumer needs or market demands. In 2007, the highest number of vessel count was recorded in the month of April with a total number of 875 vessels while in 2008, the highest number of vessel was recorded in the month of July with a total number of 761 vessels, in which showing a decrease of about 15 percent based on the highest number of vessels that was recorded between years. The statistic pattern of year 2008 shows some plunges due to economic downturn in the beginning of the year and started to show some growth by July

2008. Year 2009 showed some growth for vessel statistic and this statistic later on will relate to the emission estimate or inventory which will be discussed later.

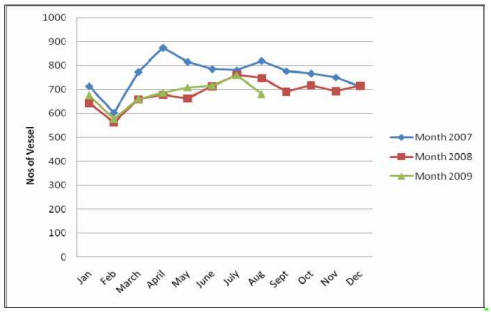

Fig.3. Vessel Statistic in Johor Port for Year 2007-2009

Vessel activity which consist of 'berthing' and 'maneuvering' mode in terms of time (hours) are presented in Figure 4. Based on the graph above, a similar pattern of statistic can be seen for both modes. What makes the difference is that these graphs were given a unit in terms of time duration (hours) whereby Figure 4 shows a graph in terms of number of vessels. The time period for each mode what makes the berthing graphs is higher than the maneuvering graphs. Based on some consideration, this study used the average berthing time of 9.6 hours while the average maneuvering time of 4 hours were used, and these time duration was provided by the Johor Port Authority for consistency in calculating the emission estimation later on. In 2007, the total numbers of vessels count in Johor Port has 9176 while in 2008, the total vessels count decreased to 8241 with a difference of 935. The most dominant vessels in Johor Port were container vessels and bulk carrier vessels. These vessels were mostly equipped with bigger horsepower engine which most probably emits greater emission than other vessels in OGVs categories. Based on the figure above, container vessel decreases by 4 percent in 2008 from 3395 to 3132 meanwhile bulk carrier vessels decreases by 6 percent in 2008 from 5781 to 5109.

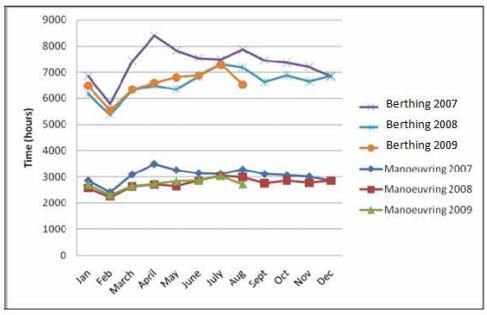

Fig. 4. Vessel Activities in Johor Port

4. CONCLUSIONS

Maritime pollutants generated by routine shipping operations can lead to both natural damages and economic losses to a coastal area. The results obtained, it can be concluded that NO_2 produce some high values of concentration even though two of its which are from Station 1 and 3 are still below and par with the limits, this condition should be a concern. It should be a concern for the high concentration value of SO_2 which exceeded the RMAQG

limits at Station 1 and 3. As for Station 2, the NO_2 values exceeded the limits mainly caused by pack vessels in operation. These high NO_2 values were recorded during sampling work which is during cargo loading and unloading is in heavy operation. Apart from that, gaseous like SO_2 at Station 2 and CO was detected at low concentration values and are not caused by very low emission. The biggest factors causing such value are because of strong wind which depletes the concentration. Theoretically, CO should be at a certain value when there is an emission. As for particulates and carbon dioxide, the value recorded does not differ as much and the particulates are well below the limits of 24-hour averaging time when compared to RMAQG. As a whole, NO_2 is a major pollutant in Johor Port and SO_2 in port area are mainly contributed by the combustion of fuel.

The Johor Inland Port ocean-going vessels emission inventory shows that manoeuvring mode contributes NOx(60%), SO_2(27%), CO(5%), PM10(3%), PM2.5(3%) and VOC(2%) while berthing mode contributes NOx(60%), SO_2(28%), CO(4%), PM10(3%), PM2.5(3%) and VOC(2%). Surprisingly, NO_x emissions from OGVs are relatively high because most marine engines operate at high temperature and pressures without effective reduction technologies. Besides, SO_2 emissions are also high because of the high average sulphur content (2.5%) of marine fuels used by most OGVs within Johor Inland Port boundaries. As a conclusion based on the emission estimation of OGVs, NO_2 and SO_2 is the major pollutant in Johor Inland Port contributing 60 and 28 percent out of other pollutants.

Given uncertainties in all emissions inventories, the best estimate for major greenhouse gas contributor like carbon dioxide (CO_2) for year 2007 to 2008 in Johor Port is within the bounded range of 1,100,000-1,500,000 kilotons per year (kT yr-1) while major pollutant contributor such as NO_2 is within the bounded range of 23,000-29,000 kT yr-1 and for SO_2 is at 10,000-14,000 kT yr-1.

Railway connections to Johor ports can reduce freight emissions of CO_2 and local air pollution through a modal shift that reduces the number of long-haul trucks plying on roads. Investment in railway infrastructure ports can encourage modal shifts to greener modes of transport. In order to improve the operational efficiency, the modernization of facilities and the use of cleaner and greener fuels are necessary. Detailed studies of the environmental benefits of ports are needed for future research.

REFERENCES

[1]. Aronsson, H. and Brodin, M.H.- ***The environmental impact of changing logistics structures***, The International Journal of Logistics Management, Vol. 17 No. 3; 394-415. 2006
[2]. Farthing, B. and Brownrigg, M.- ***Farthing on International Shipping***, LLP, London. 1997
[3]. UNCTAD,. - ***Sustainable Development for Ports, Report UNCTAD (SDD/Port)*** 1, 27/8, 1993, Geneva, Switzerland
[4]. Finney, N. and Young, F. - ***Environmental zoning restrictions on port activities and development, Maritime Policy and Management Journal***, 22; 319-329, 1995
[5]. Vandermeulen, J.H.- ***Environmental trends of ports and harbours: implications for planning and management***, 23; 55-66. 1996
[6]. Guhnemann, A. and Rothengatter, W. - ***Strategic Environmental Assessment of Transport Infrastructure Investments***, 8th World Conference on Transport Research, Antwerp, Belgium, 12-17 July. 1998
[7]. Gibb, B. - ***Dredging, environmental issues and port experience in the United States***, Maritime Policy and Management Journal, 24; 313-318, 1997
[8]. Commission of the European Communities. - ***Green Paper on Sea Ports and Maritime Infrastructure***, Com (97) 678 final, 10/12, 1997 Luxembourg.
[9]. Economical Social Commission for Asia and Pacific. - ***Assessment of the Environmental Impact of Port Developments***. An IMO/ESCAP seminar, Yokohama 31/8-4/9, 1992
[10]. EEA. - **European *Union Emissions Trading Scheme (EU ETS) data viewer***, available at: http://dataservice.eea.europa.eu/PivotApp/pivot.aspx?pivotid=473 accessed December, 2010.

MODELING AND ANALYSIS OF A RECONSTRUCTION OF SHIP SEARCHLIGHT USING LED MATRIX

[1]BOHOS APRAHAMIAN, [2]BORISLAV DIMITROV, [3]LYUBOMIR DANKOV

[1,2]*Technical University – Varna, Bulgaria,* [3]*Nicola Vaptsarov Naval Academy, Varna, Bulgaria*

The searchlights of the ships and the lifeboats are designed to help in the rapid identification of people fallen overboard and to communicate with other ships and shore. To safely perform these functions, they need to be powered from independent sources, and their capacity is determined by SOLAS (International Convention for the Safety of Life at Sea), according to the required duration of illumination. Although light communication is shifting from various forms of radio communication, it is still indispensable element of navigation equipment of each vessel. New LED light sources provide high brightness, high efficiency (the ratio of light to electricity usage) and responsiveness (the transition from off in a state of maximum brightness). This allows for the construction of relatively small-sized searchlights with multiple parameters exceeding the requirements of SOLAS.

Keywords*:* ship searchlight, LED matrix, model, process simulation, reconstruction

1. INTRODUCTION

Chapter III of the SOLAS Convention [1] includes requirements for life-saving appliances and arrangements, including requirements for life boats, rescue boats and life jackets according to type of ship. The International Life-Saving Appliance (LSA) Code [2] gives specific technical requirements for LSAs and is mandatory under Regulation 34, which states that all life-saving appliances and arrangements shall comply with the applicable requirements of the LSA Code.

The parameters for a searchlight in a SOLAS lifeboat is defined in the IMO Life Saving Appliance Code (LSA), and specifies luminous intensity of 2,500 cd, a horizontal and vertical sector of 6 degrees and be able to work continuously for 3 hours. There are many low-cost searchlights available, of high intensity with narrow beams, suitable for search and rescue and basic signalling. It is suggested that where a SOLAS searchlight or lifeboat searchlight cannot be specified, then to borrow a phrase from the UK MCA[3] (UK Maritime and Coastguard Agency), a searchlight of a type considered suitable for search and rescue purposes under NSCV (Australian National Standard for Commercial Vessels) Clauses 2.16 - 2.17. It may be portable or fixed, but where fixed, its beam position should be controllable from the control position of the vessel.

According UK MCA the searchlight should be of substantial construction. The light should be supplied by a gas-filled filament of at least 30 watts. The lamp and electrical connections should be waterproof. An efficient reflector should be provided so that the searchlight can

produce beam of light with a divergence of about 6 degrees, and apparatus must be capable of giving illumination of a light-colored object over a width of about 18 m at a distance of 180 m. There should be focusing arrangements to increase divergence to about 30 degrees.

In this paper experimentally is studied ship searchlight type MSNP 250M (220V AC, 300W) – Russian construction, widely used in Bulgarian Navy, shown in Figure 1. The searchlight is designed to carry out light communication using Morse code and search persons fallen overboard. It is realized with incandescent lamp, representing outdated design and works with low energy efficiency.

Fig. 1. Sketch and photo of the investigated searchlight type MSNP-250M

The thermographic analysis of the searchlight shows that most of the energy is lost as heat. The result of the thermographic analysis is shown in Figure 2. According to the results the temperature of the searchlight body is above the acceptable level under current standards.

In this paper an available reconstruction of the ship searchlight with replacement of the used incandescent lamp with LED matrix is proposed and analyzed. By achieving such modernization reduced power consumption, high reliability and extended life cycle of the facility is meant. For this purpose we performed a comprehensive analysis of the searchlight to the standard form and then reconstructing it.

An appropriate installation mode of the LED matrix providing the required optical characteristics of the searchlight is proposed and comparative analysis of the results is done, arguing the relevance of the reconstruction.

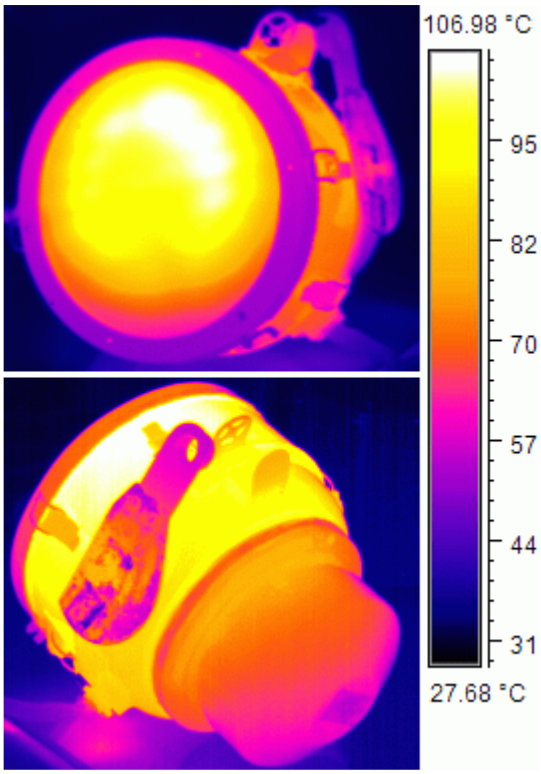

Fig. 2. Photo with thermography camera of ship searchlight type MSNP-250M

2. SOME CALCULATIONS REQUIRED FOR THE IMPLEMENTATION OF THE RECONSTRUCTION

One candela (Cd) emits 1 lumen (Lm) luminous flux in one steradian solid angle. The requirement for the searchlight is to cover an angle of 6 degrees. If **π** (pi) radians equate 180 degrees we would have one radian = 180/3.14 = 57.3 degrees. So the spatial radian has 57,3x57,3=3286 degrees, then for six spatial degrees one candela will emit approximately 100 times less, or more precisely 3286/36 = 91.3 times.

The searchlight has a requirement to provide a luminous flux of 2500 Cd. Then 2500/91, 3 = 27.4 Lm. In this case, the reconstruction of the searchlight will need 3 LEDs with 10 lumens each or about 0,1 W each.

Let's take as an example an incandescent lamp, filled with inert gas. For example, 30 W x 12-36 Lm/W = 360-1000 Lm. The reflector of the lamp has efficiency 80-95%, i.e. remaining 300 to 950 Lm. It follows that the reconstructed searchlight can be performed with one 10 W LED matrix. Spot with a diameter of 18 meters has an area of about 250 sq.m. or 250 Lm are needed for a one Lux (Lx) illumination of this spot. If about the same amount is diffused, even 5W LED matrix is sufficient.

In fact the marketed searchlights went far beyond the requirements of LSA. In practice the required by SOLAS searchlights are now widely replaced by Chinese portable devices. The searchlights are waterproof and offer a brightness of 100 000 to 1 million Cd with diffusion angle of about 3-6 degrees - Fig.3.

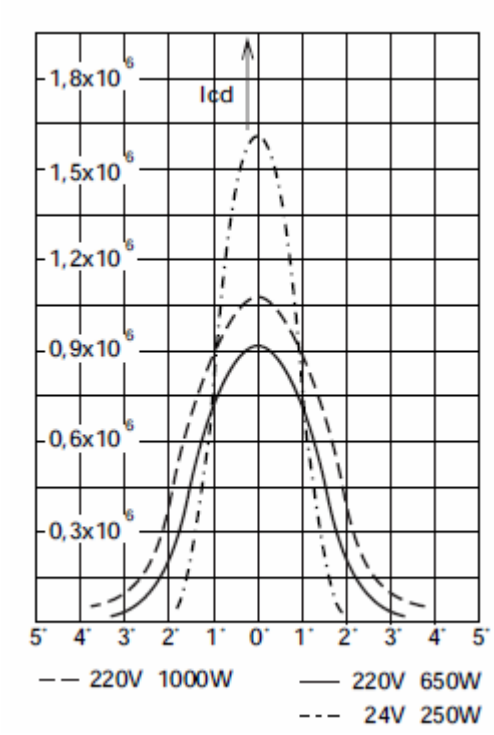

Fig. 3. Dependence of the luminous flux emitted by the searchlight on the angle of diffusion

3. MODEL OF THE RECONSTRUCTED SHIP SEARCHLIGHT

The developed model of LED searchlight [4,5,6,7] is shown in Figures 4-7 as follows:

- Figure 4 – searchlight model developed in two versions - using heat pipes and through the direct use of the back cover as a cooling system of the LED matrix.
- Figure 5 – model of the system LED matrix – back cover, serving for cooling. The latter is made of anodized aluminum and in fact is a cooling radiator.
- Figure 6 – model of the construction of the cooling system realized with heat pipes.
- Figure 7 – model of the construction of the back cover, realized with ribbed surface.

The LED matrix has electric power of 90W and is composed of nine LEDs 10W each. The geometry of the searchlight is not significantly different from the original design. The necessary installed power and the number and location of the LED matrices are determined experimentally. Performed by measuring the light output of the original model of the searchlight (Fig. 1) the following parameters of the matrices were selected: Lens Color: Water Clear; Emitted Color: Cool White; Intensity: 700-900 Lm; Viewing Angle: 160°; Color Temperature: 6000 K-7000 K; Forward Voltage: 9-12V; Forward Current: 1000 mA.

Fig. 4 Model of the searchlight with LED matrix.

Fig. 5 Structure of the system LED matrix – cooling body.

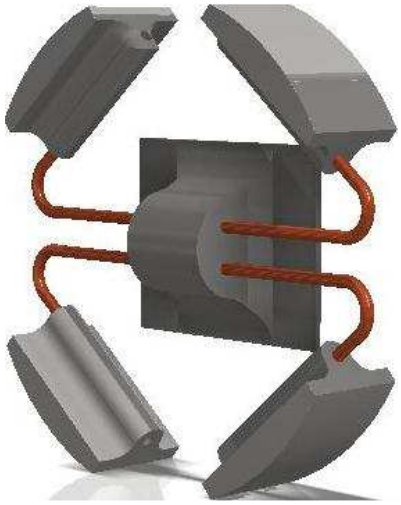

Fig. 6. Heat pipes used for cooling the LED matrix.

Fig. 7. Back cover of the searchlight.

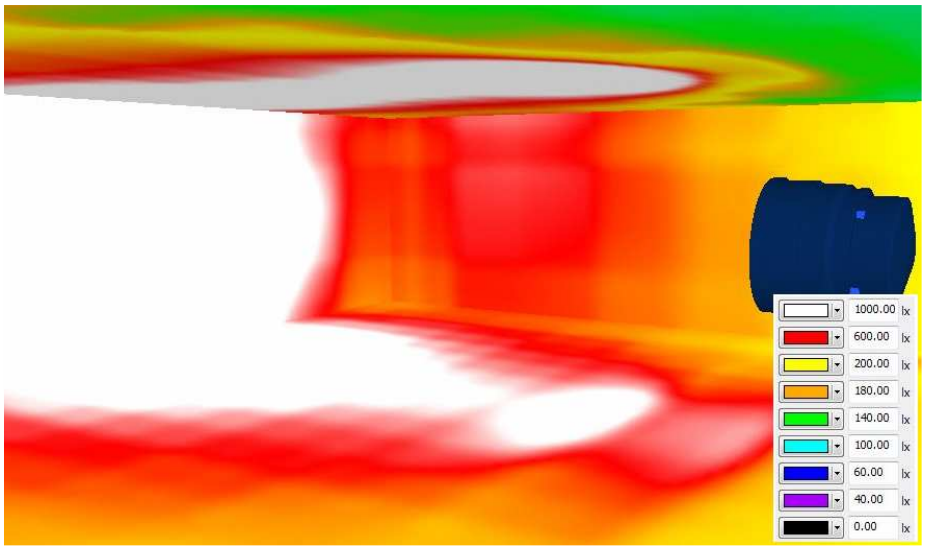

Fig. 8 Simulation of the work of the reconstructed LED searchlight.

The lighting capacity of the searchlight is studied through the model shown in Figure 8. The results show that the reconstructed device can fully replace the searchlight presented in Figure 1. The model is made using specialized software that allows conducting simulation procedure and determination of the optical and thermal parameters of the modelled object.

4. THE SEARCHLIGHT SUPPLY SYSTEM.

The operation of lights, realized with LED elements is provided by electronic circuits with the required properties.

One of the requirements for the proposed reconstructed searchlight with LED matrix, is to ensure a wide range of supply voltages (85 - 230V AC), low losses and high energy efficiency. Thus is provided by special power supply block designed for the specific task. Thus offers a complete turn-key system: lighting - power supply bock, meeting the regulatory requirements for this class of equipment.

The supply system is based on the product range of Power Integration [8] (Figure 9), and as a power element is used TopSwitch. The scheme is designed using the software PIExpert, and experimentally studied without introducing significant changes.

The main elements of the experimentally studied prototype are as follows:

- Input filter and rectifier: R1, R2, L1, BR1, C2. These elements provide electromagnetic compatibility of the device so that interference with other working devices is not distorting the supply voltage. Bulgarian Register of Shipping limits the level of high harmonics in the voltage, none to be no effective value greater than 5% of the effective value of the first harmonic and total harmonic distortion (THD) shall not exceed 8%.
- Power element and feed circuit to it: TopSwitch-HX, R3-R11, C3-C5.
- Ferrite transformer T1.
- Rectifier and filter on the secondary side: D3, R12, C7, C9-C16, L2, C17.
- Feedback: D2, C8, U2, R13-R16, C18, U3.

The proposed feeder scheme has small dimensions, allowing installation in the searchlight housing. The efficiency depending on the supply voltage is shown in Figure 10. At rated voltage 220V AC, the efficiency reach 93.5%.

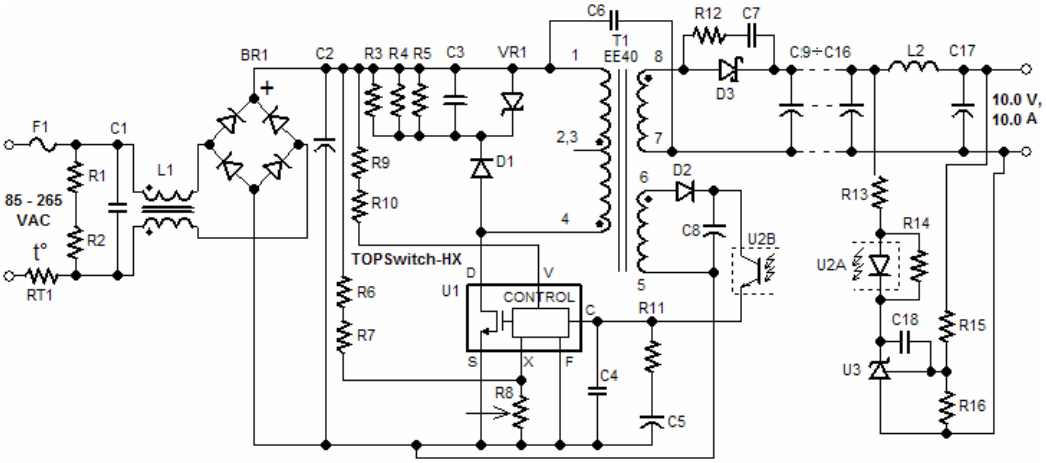

Fig.9. Power supply system of the LED matrix based on TOP Switch

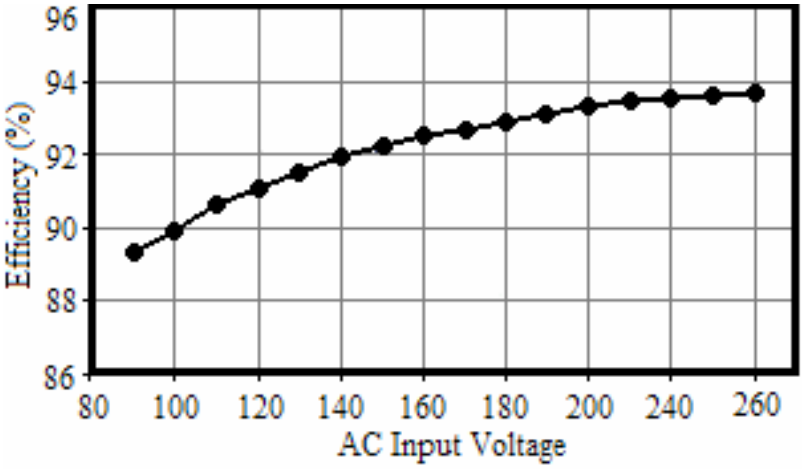

Fig. 10. Efficiency of the power supply system in function of supply voltage.

Additional experiments were conducted changing the circuit design (Figure 11) for DC supply voltages from battery 24 – 48 V DC. A transformer with several secondary windings is used, supplying each matrix separately. This requires two power supply blocks. The power element is from the DPA-Switch family. A detailed description of the proposed schemes is not necessary as PI Expert gives enough detailed information in their design.

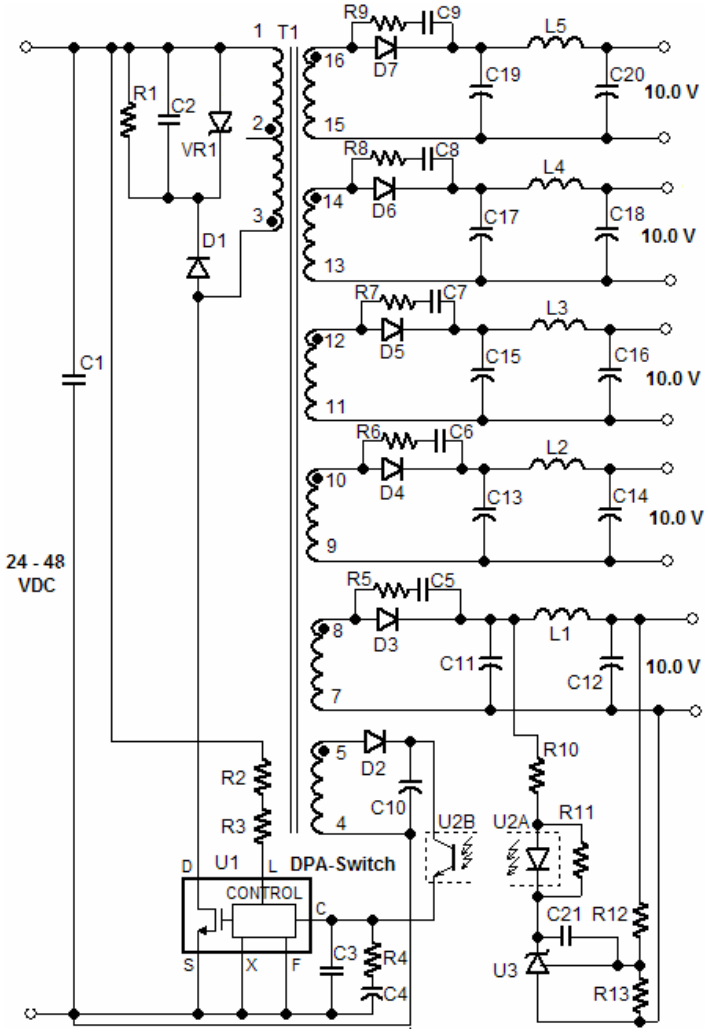

Fig. 11. Power supply system with constant input voltage of the battery.

5. CONCLUSIONS

The proposed lighting is designed as a model representing a conceptual option for modernizing widely used ship searchlight. A prototype of the searchlight can be fabricated and experimentally studied. At this stage of the conducted experimental and numerical procedures can be drawn:

- The created models (Figure 4, Figure 8), and the results of the thermographic investigation of the original searchlight (Figure 1, Figure 2), lead to the conclusion that the LED matrices can be used for modernization of the device, providing the increase of the light output, despite the reduced consumption of 300W to 90 W.
- The experimentaly studied power system (Figure 9, Figure 10) works with high efficiency. The conducted tests show that is suitable for powering LED matrices and in practice the system can operate continuously throughout all the night.

- The power to the searchlight can be supplied from a battery, using the proposed scheme in Figure 11.
- The expectations are that the reconstruction will increase the reliability of the device, and will get a much better spot illumination, facilitating the search and rescue at sea and increase the distance of the light communication.
- These assumptions have to be experimentally proven after the investigation of the prototype of a searchlight with LED matrix, which is under construction.

REFERENCES

[1]. ***International Convention for the Safety of Life at Sea (SOLAS)***, 1974
[2]. ***International life-saving appliance (LSA) code***, http://edpashipping.com/lsacode.pdf
[3]. ***Maritime and Coastguard Agency regulations***, http://www.dft.gov.uk/mca/lsa1ch12-2.pdf
[4]. Lenk R, C Lenk, ***Practical Lighting Design With LEDs***. A John Wiley & Sons, Inc. 2011
[5]. Schubert F. ***Light-Emitting Diodes***, Cambridge University Press, 2006
[6]. http://www.power-mag.com
[7]. http://hadco.com
[8]. http://powerint.com

RADAR IMAGE DESCRIPTION USING TIME SERIES AND HIGH ORDER SPECTRAL MOMENTS APPROACH

[1]BOZHIDAR DOYNOV, [2]ZACHARY POPOV, [3]CHAVDAR ALEXANDROV
[1,2]Technical University of Varna, Bulgaria, [3]'Nikola Vaptsarov' Naval Academy Varna, Bulgaria

This paper describes an attempt for modeling and estimation of a target under radar observation. High order spectral moments and time series are applied. Experiment with real target is conducted and autoregressive model is used to describe the target.

***Keywords**:* radar image, spectral moments, time series, estimation

1. INTRODUCTION

Main tasks of radar observation are detection and identification of targets. As is known [7], solving these problems involves the analysis and processing of returned from the target signal, transmited by radar. Receiving and storing information is a complicated task, depending on radar target scattering surface and additional external factors varying widely (viewing conditions, geographical coordinates, radar jamming devices, etc.). Getting quick and correct decisions about the type of the target of observation requires using of complex mathematical apparatus.

It is known that historically [7], the first characterization of radar targets, which is the most used in practice these days is the effective area of scattering (EAS) [11]. With the development of radar and considering the statistical features of radar signals EAS concept introduced early to describe the reflection properties of a fixed point of view is summarized case of fluctuating point object [7, 11].

Increasing radar resolution and reducing errors in the measurement equipment, the parameters of targets led to the introduction of the concept of a complex target, which consists of separate elementary reflectors, named main scattering centers [11].

Theoretical foundations for the description of such goals appears to be methods of physical theory of diffraction: Keller's diffraction geometry and Ufimtsev's finite waves, and on this basis has introduced the concept of target local radar performance [7,11]. Radar image is an expression of space-time scattering properties of targets. Space-time processing methods applied to signals reflected by the object allow to measure the target's local radar characteristics [1,11].

Mathematical apparatus used in these tasks requires consideration of complex spectral establishment of radar signal. The correct determination of the local dynamic and static characteristics of the radar targets allow detection and classification of relevant objects [1, 7, 11]. There are many well known developments in this matter based on the theory of time series [5].

The aim of this paper is estimation of radar image parameters using time series and high order spectral moments approach. This approach allows to reduce the amount of data, obtained by radar observation and measurement.

2. SPECTRAL INVARIANTS DESCRIBING RADAR IMAGE

Consider a 2D homogeneous process $Y(x, t)$, where x and t are spatial and temporal coordinates. They can be natural coordinates, when applied to a real physical surface. Homogeneity is an extension of the concept of stationarity to higher dimensionality [2, 8].

This means that the covariance function of $Y(x, t)$ depends only on the lag vector, i.e. the differences $(t - t')$ and $(x - x')$ in the case of 2D process. Spectral moments of such a process $Y(x, t)$ can be defined in the most general form as follows [8]:

$$\lambda_{jn} = \int_{-\infty}^{\infty} \int_{-\infty}^{\infty} \omega^j . k^n . Szz(\omega, k) . d\omega . dk \tag{1}$$

where Szz is bilateral spectral power density of $Y(x, t)$.

The homogeneity of $Y(x, t)$ includes [2, 4, 8]:

$$Szz(\omega, k) = Szz(-\omega, -k) \tag{2}$$

Hence the $(j + n)$ odd integral (1) has zero value [2, 8].

The 2D homogeneous process described above, represents a radar image, which is the description of surface. Heights measured in any direction I set in the horizontal plane, marked as $Z(I)$ determine the profile of the surface roughness. This profile can be viewed as a stationary random sample with autocorrelation function:

$$R_{zz}(l) = E\{Z(I) . Z(I - l)\} \tag{3}$$

and power spectral density

$$S_{zz}(\omega) = \frac{1}{2.\pi} . \int_{-\infty}^{\infty} R_{zz}(l) . e^{-j.l.\omega} . dl \tag{4}$$

Surface height $Z(I1, I2)$ measured along two directions $I1$ and $I2$ in the horizontal plane is stationary random function of two variables (stochastic field). Therefore the dual dimensional autocorrelation function is:

$$R_{zz}(l_1, l_2) = E\{Z(I_1, I_2) . Z(I_1 - l_1, I_2 - l_2)\} \tag{5}$$

and the dual dimensional power spectral density is

$$S_{zz}(\omega_1, \omega_2,) = \frac{1}{4.\pi^2} . \int_{-\infty}^{\infty} \int_{-\infty}^{\infty} R_{zz}(l_1, l_2) e^{-j.(l_1.\omega_1 + l_2.\omega_2)} . dl_1 . dl_2 \tag{6}$$

where $E\{\}$ is the mathematical expectation operator, l - lag, ω - frequency.

All important features of stationary random fields can be described by their spectral moments [2-4] defined as follows:

$$m_r = \int_{-\infty}^{\infty} \omega^r . S_{zz}(\omega) . d\omega \tag{7}$$

$$m_{pq} = \int_{-\infty}^{\infty} \int_{-\infty}^{\infty} \omega_1^p . \omega_2^q . Szz(\omega_1, \omega_2) . d\omega_1 . d\omega_2 \tag{8}$$

Autocorrelation function and power spectral density are Fourie couple and for single dimensional profile

$$R_{zz}(l) = \int_{-\infty}^{\infty} S_{zz}(\omega) . e^{j.l.\omega} . d\omega \tag{9}$$

and for random field:

$$R_{zz}(l_1,l_2,) = \int_{-\infty}^{\infty}\int_{-\infty}^{\infty} S_{zz}(\omega_1,\omega_2)e^{j.(l_1.\omega_1+l_2.\omega_2)}.d\omega_1.d\omega_2 \tag{10}$$

After differentiating equations (9) and (10) on the relevant lags for odd exponents follows:

$$m_r = (-1)^{\frac{r}{2}}.\frac{d^r R_{zz}(l)}{dl^r}\Big|_{l=0} \tag{11}$$

$$m_{pq} = (-1)^r.\frac{d^r R_{zz}(l_1,l_2)}{dl_1^p.dl_2^q}\Big|_{l_1=l_2=0} \tag{12}$$

where $r = p+q$.

From equation (11) follows that $m_0 = R_{zz}(0)$ which is a variation of the surface elevation, equal to the area under the curve of power spectral density.

It is proved that the moments of the power spectral density profiles measured in the direction forming an angle θ with the abscissa $I1$, are related to the moments of the power spectral density of the surface by the following equation [6, 9, 10]:

$$m_r(\theta) = m_{r,0}.\cos^r(\theta) + \binom{r}{1}.m_{r-1,1}.\cos^{r-1}(\theta).\sin(\theta) + m_{1,r-1}.\sin^{r-1}(\theta) + m_{0,r}.\sin^r(\theta) \tag{13}$$

So if we have estimates of the moments of the spectrum profile, then using (13) we can find estimates of spectral moments of the surface. Moreover, if $r = 0$, it is easy to see that the moments of the power spectral density of the surface profile and the same, i.e.

$$m_{00} = m_0(\theta_i), \quad i = 1,2,.....,n \tag{14}$$

Equation (14) can be used as a criterion of homogeneity, indicating that variations of the profiles measured in different random directions are equal to the variation of the surface roughness. Since the estimates of $m_0(\theta i)$ vary m_{00} assessment should take the average $E\{m_0(\theta_i)\}$. Assume that we have a sample of a surface profiles measured in three different directions at angles θ_1, θ_2, θ_3 against abscissa $I1$. Using equation (13) when $r = 2$, it results:

$$m_2(\theta) = m_{20}.\cos^2(\theta) + 2.m_{11}.\cos(\theta).\sin(\theta) + m_{02}.\sin^2(\theta) \tag{2.15}$$

When calculate the one-dimensional second-order moments $m_2(\theta_1)$, $m_2(\theta_2)$, $m_2(\theta_3)$ we can find a two-dimensional second-order moments of the spectrum of surface m_{20}, m_{11}, m_{02} , simultaneously solving the equations:

$$\begin{bmatrix} m_{21} \\ m_{11} \\ m_{02} \end{bmatrix} = T_2^{-1}.\begin{bmatrix} m_2(\theta_1) \\ m_2(\theta_2) \\ m_2(\theta_3) \end{bmatrix} \tag{16}$$

where:

$$T_2 = \begin{bmatrix} \cos^2(\theta_1) & 2.\sin(\theta_1).\cos(\theta_1) & \sin^2(\theta_1) \\ \cos^2(\theta_2) & 2.\sin(\theta_2).\cos(\theta_2) & \sin^2(\theta_2) \\ \cos^2(\theta_3) & 2.\sin(\theta_3).\cos(\theta_3) & \sin^2(\theta_3) \end{bmatrix} \tag{17}$$

For the purpose of calculations it is convenient to choose $\theta_1=0°$, $\theta_2=45°$ and $\theta_3=90°$. In this case the matrix T_2 significantly simplifies (17), giving the following:

$$m_{20} = m_2(0^\circ) \tag{18}$$

$$m_{11} = m_2(45^\circ) - \frac{1}{2}.m_2(0^\circ) - \frac{1}{2}.m_2(90^\circ) \tag{19}$$

$$m_{02} = m_2(90^\circ) \tag{20}$$

Both spectral moments m_{20} and m_{02} currently represent the variance of the gradient profile at 0° and 90° with respect to $I1$ and m_{11} moment is coefficient of correlation between these gradients. In case of random isotropic surface $m_2(\theta)$ does not depend on θ and the following relationship can serve as a criterion for isotropy of the surface:

$$m_{00}=m_0 \tag{21}$$

$$m_{20}=m_{02}=m_2 \tag{22}$$

$$m_{11}=0 \tag{23}$$

Surfaces not satisfying equations (21÷23) are anisotropic. Their statistical properties can be divided into two classes.

Surface spectral invariants from the first class are independent of the rotation of the coordinate axes and characterize common geometric surface properties, regardless of the law of probability distribution of the surface roughness.

The second class includes various stochastic quantitative indicators such as density peaks for area of surface, variation of the absolute surface slope, main directions, minimum and maximum rms roughness gradient, number of crossings with a positive sign for the derivative-configured profile including zero and the average maximum density per unit length of the profile.

3. EVALUATION OF SPECTRAL MOMENTS THROUGH TEMPORARY AUTOREGRESSIVE MODELS AND TIME SERIES

In [3] and [9] is proposed a method to obtain the optimal estimates of spectral densities and hence the moments of the spectral densities. The method is based on the provisional application of the least squares method to construct mathematical models.

The meaning of the model parameters obtained by the least squares satisfies maximum likelihood criterion, i.e. has the property of optimality.

A stationary random function, such as the surface of the radar image can be presented, with any degree of accuracy, as a solution of the differential equation

$$\frac{d^n.X(l)}{dl^n} + \alpha_{n-1}.\frac{d^{n-1}.X(l)}{dl^{n-1}} + ... + \alpha_1.\frac{d.X(l)}{dl} + \alpha_0.X(l) = \beta m.\frac{d^m.Z(l)}{dl^m} + ... + \beta_1.\frac{d.Z(l)}{dl} + Z(l) \tag{24}$$

where:

$m \le n\text{-}1$

$E\{Z(l)\} = 0$

$E\{Z(l).Z(l-u)\} = \delta(u).\sigma_2^2$

$X(l)$ – profile height ;

$Z(l)$ – random process with properties of white noise (having a normal distribution)

$\delta(u)$ – delta function;

$\alpha_0, \alpha_1, \alpha_{n-1}$ – autoregression coefficients;

$\beta_0, \beta_1, \beta_{m-1}$ – moving average coefficients.

Model (24) is known as model with Autoregression Moving Average of order (n, m), or ARMA(n, m). Particularly, when $m = 0$ it is referred to as Autoregression Model of order n, or AR(n). Dependence, with which displayed moments of the power spectral density define the parameters of the ARMA(n, m) has the form

$$f(\lambda)=\frac{\sigma_2^2.\Delta t}{2.\pi}.\frac{\left[1+\sum_{k=1}^{m}\beta_k.\exp(j.\lambda_k.\Delta t)\right]^2}{\left[1+\sum_{k=1}^{n}\alpha_k.\exp(j.\lambda_k.\Delta t)\right]^2} \tag{25}$$

Substitution of the above expression in (7) shows that the integrand is a polynomial of degree *(r + 2)* of *λ*. Therefore limited in polynomial $\lambda \rightarrow \infty$ and executed the following inequality:

$$r < 2.(n - m) \tag{26}$$

Thus, for power spectral density there exist final moments of row for which the inequality (26) is satisfied. General ARMA (n, m) model and its application procedures can be applied to radar images.

It is known [4, 6] that if a random function *Z(X)*, which represents the height profile of a surface in a direction *X*, has Fourier transform and k number of consecutive derivatives, its one-dimensional spectral moment of order k is defined as:

$$m_k=(2.\pi)^{(k+1)}.\int_{-\infty}^{+\infty}F^k.S_z(f).df \tag{27}$$

where: $S_z(f)$ is the power spectral density of *Z(X)*, *f* - frequency, and k = 0, 1, 2 .

Actualy the samples of data *Z(X)* are limited in size, and the necessary spectral moments can be evaluated by formula (27) once over *Z(X)* is applied discrete Fourier transform with the resulting constraints, and the integral is replaced by a sum. Thus the obtained spectral estimates are generally inconsistent [9]. Although to improve the accuracy of measurement we resort to repetition and averaging the results. Rich amount of spectral estimates can be obtained if over the data for *Z(X)* parameter identification is conducted by the least squares of linear stochastic differential equation of fourth order [6]

$$\frac{d^4Z}{dX^4}+a_3.\frac{d^3Z}{dX^3}+a_2.\frac{d^2Z}{dX^2}+a_1.\frac{dZ}{dX}+a_0.Z=U(X) \tag{28}$$

where: *U(X)* is a random function, uncorrelated with *Z(X)*, and having the normal law of distribution. Both two functions *U(X)* and *Z(X)* have zero mean and known variances, i.e. $E[Z(X)] = 0$, $E[U(X)] = 0$, $E[U_2(X)] = \sigma^2_u$.

Power spectral density of *Z (X)* is defined by the formula

$$Sz(f)=\frac{\sigma_u^2}{2.\pi.\left[(jf)^4+a_3.(jf)^3+a_2.(jf)^2+a_1.j.f+a_0\right]^2} \tag{29}$$

If the conditions for the differential equation are satisfied, autocorrelation function of *Z (X)* satisfies the differential equation [9]:

$$\frac{d^4R_z}{dX^4}+a_3.\frac{d^3R_z}{dX^3}+a_2.\frac{d^2R_z}{dX^2}+a_1.\frac{dR_z}{dX}+a_0.R_z=0 \tag{30}$$

where: $R_z(x)$ is the autocorrelation function of *Z(X),* and *x* is the independent variable expressed offset (lag) in the direction *X*.

In particular, this equation holds true when lag $x = 0$. Then we can use the relationship between the spectral moments and the derivatives values of the autocorrelation function when $x = 0$, which are given by

$$m_k=(j)^k.\frac{d^kR_z}{dx^k}\Big|x=0 \tag{31}$$

where *j* is the imaginary unit.

It is easy to see that the differential equation is transformed into the following form:

$$m_4 - j.a_3.m_3 - a_2.m_2 + j.a_1.m_1 + a_0.m_0 = 0 \quad (32)$$

Since the random function $Z(X)$ is real spectral density appeared as an even function of the frequency, the above equation is reduced to:

$$m_4 - a_2.m_2 + a_0.m_0 = 0 \quad (33)$$

According to the results published in [7] formulas for m_2 and m_4 are as follows:

$$m_2 = m_0.\frac{a_0.a_3}{a_2.a_3 - a_1} \quad (34)$$

$$m_4 = m_2.\frac{a_3}{a_1} \quad (35)$$

where m_0 is the empirical estimation of the dispersion of the measurements of $Z(X)$.

Such relations enable us not to resort to the Fourier transform when studying the topography of a surface. Instead, computational algorithms can be applied to identify the stochastic differential equation, which provides independent estimates of spectral moments needed to determine statistical geometrical properties of the surface.

4. EXPERIMENTAL RESULTS

Experimental data are from a coastal surveillance radar over Port Varna. The parameters of the radar are as follows:

- Height	200m above sea level
- Azimuth resolution	0.8˚ at 3dB
- Rotation speed	20 rpm
- Operating frequency	9410 MHz (X band);
- Transmitter Type	Simple pulse
- PRF	750 Hz, 1500Hz and 3000Hz
- Pulse duration	0.7μs, 0.25μs and 0.07μs
- Transmitter pulse power	12KWt
- Receiver Type	Superhet. Log
- Bandwidth	6 MHz or 14 MHz

The object of study is presented in Fig.1 and its reflection surface on Fig 2.

Fig. 1. AEGIS Cruiser

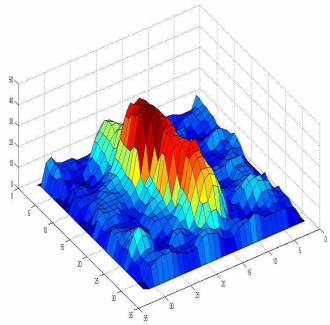

Fig. 2. Reflection surface of AEGIS

The results obtained by the stochastic geometry approach, applied for description of radar images in two different positions are presented in Table 1 and Table 2.

Table 1. Results AR(2) estimation

θ 0°	0.0000	a 0°	1.0000
θ 45°	0.7854		465.2871
θ 90°	1.5708		106833.6311
φ 0°	1.0000	a 45°	1.0000
	-1.5433		516.0080
	0.6280		132049.0808
φ 45°	1.0000	a 90°	1.0000
	-1.4949		891.0132
	0.5969		45528.6644
φ 90°	1.0000	m 2	16286959.3801
	1.3802		17840256.7744
	0.4102		5226984.4012
μ 0°	-2.3264e2+2.2958e2i	SDg 0°	0.7575
	-2.3264e2-2.2958e2i	α 0°	0.0065
μ 45°	-2.5800e2+2.5589e2i	SDg 45°	0.7237
	-2.5800e2-2.5589e2i	α 45°	0.0060
μ 90°	-54.4216	SDg 90°	1.3370
	-836.5916	α 90°	0.0204
M 2		21513943.7814	
δ 2		34958757879855.4000	
θ 2		26.0103	

Table 2. Results AR(2) estimation

θ 0°	0.0000	a 0°	1.0000
θ 45°	0.7854		289.7057
θ 90°	1.5708		99604.8050
φ 0°	1.0000	a 45°	1.0000
	-1.6627		1046.2067
	0.7485		187813.4134
φ 45°	1.0000	a 90°	1.0000
	-1.2366		773.0652
	0.3513		26020.2977
φ 90°	1.0000	m 2	16286959.3801
	-1.4435		17840256.7744
	0.4616		5226984.4012
μ 0°	-1.4485e2+2.8039e2i	SDg 0°	0.8406
	-1.4485e2-2.8039e2i	α 0°	0.0081
μ 45°	-230.1465	SDg 45°	0.6754
	-816.0602	α 45°	0.0052
μ 90°	-35.2675	SDg 90°	1.5487
	-737.7977	α 90°	0.0274
M 2		17119637.1762	
δ 2		-90636879744060.2000	
θ 2		34.3171	

5. CONCLUSIONS

The results in Table 1 and Table 2 summarize images estimation based on mathematical equations described above.

Image properties varay with direction change in plane. That is obviouse from estimation of m_0 and m_2.

The average values of surfece gradient α are close to each other in diferent directions. The statistical characteristics in Table 1 and Table 2, based on the second-order spectral moment estimation also show that surfaces have clearly expressed anisotropy.

Stochastic geometry aproach applied to analyze of radar image yields to great number of characteristics , which give a comprhensive description of the target.

Detailed consideration of data could be used for recognition of the principal direction of objects from target.

The results obtained by the high-order spectral moments and autregressive models will be published.

REFERENCES

[1]. Skolnik M. , - ***Introduction to Radar Systems***, Third Edition, McGraw-Hill, 2001
[2]. Bendat J. S , - ***Principles and applications of* random noise theory**, Wiley,1958
[3]. Jenkins G., Watts D., - ***Spectral Analysis with application***, 1971
[4]. Longuet-Higgins M. S,. - ***The Statistical Analysis of Random Moving Surface,*** Phil.Trans. of the Royal Society. Ser. A. Vol. 249. 1957
[5]. Moses R., Carrere R., - ***Autoregressive moving average modeling of radar targrt signature***,. IEEE. 1988
[6]. Nayak R., - ***Random process model of rough surfaces***, Journal Lubrication Tech, 1971
[7]. Peebles P. , - ***Radar Principles*** ,Wiley,1998
[8]. VanMarcke E., - ***Random fields: Analysis and synthesis***, MIT,1983
[9] Wu S.M. at , - ***Stochastic Geometry of Anisotropic Random Surfaces With Application to Coated Abrasives***, ASME 5, 1976
[10]. Popov Z.,Junkar M.,- ***Some stochastic geometrical properties of planar surfaces with regularly arranged surface roughness***, Machines and mech.,ISSN 0861-9727, Varna, 2003
[11] Nebabin V., Sergeev V., - ***Methods and techniques of radar recognition***, Artech House, 1984

OPTIMIZATION OF A METAL MATRIX COMPOSITE HYPERSONIC MISSILE AERODYNAMIC SHAPE AND STRUCTURE BASED ON THE ADVANCED TECHNIQUES

[1]CALIMANESCU IOAN, [2]STAN LIVIU-CONSTANTIN

[1,2]*Constanta Maritime University, Romania*

Applied aerodynamics has, historically, involved a very strong mix of theory and experiment. This is partly because experiments can be very costly and computations are rarely sufficiently sophisticated. This will continue to be the case. Computational Fluid Dynamics (CFD) is playing an ever increasing role in aerodynamic design for advanced missiles either for performance improvement of the existing system for new missions or for new concept development for future missions. A cost effective design process is to judiciously combine the wind tunnel tests and CFD studies that exploit the inherent strengths of each of these. Hypersonic missile flight is characterized by a high flight Mach number (usually greater than 5), thin shock layers and high viscous loads. The missile aerodynamic geometry has high impact on different missile systems such as control, propulsion, structure, and warhead. The objective of the current paper is to present a reliable Finite Element Analysis/CFD and Fluid Structure Interaction (FSI) advanced technique for obtaining hypersonic missile aerodynamics and use this technique for finding optimal hypersonic missile shape based on best structural behavior (the lowest von Mises stress will play the role of Objective Variable), and, secondly, based on the best aerodynamic behavior (the highest V∞ fluid velocity will play the role of Objective Variable).

Keywords: Fluid Solid Interaction, Optimisation, Hypersonic Missile, Metal Matrix Composite

1. INTRODUCTION

Applied aerodynamics has, historically, involved a very strong mix of theory and experiment. This is partly because experiments can be very costly and computations are rarely sufficiently sophisticated. This will continue to be the case. A recent, very simple, wind tunnel model with a few control surfaces but no pressure measurements, cost $200,000 to build. That would buy a fair amount of computer time. It also took several months for the model to be delivered. There is great motivation to use computational methods when possible and the numeric shape and structure Optimisation is by far the sole conceivable and reasonable approach, at least for these days.

On the other hand, the missile geometry is quite complicated and one may be interested in the behavior of a leading edge vortex, the onset of flow separation, and the spanwise flow of the boundary layer. Such features require solution of the complex Navier-Stokes equations. Even the NS code which can predict wing-alone characteristics takes weeks before one can get a converged solution.

Perhaps the ideal method of predicting the aerodynamics of a vehicle is flight test in real conditions. There are several reasons why this is not always the ideal method of aerodynamic testing. The cost involved in building and changing full scale designs and making repeated flights is extremely high; the instrumentation is generally not as good as ground-based instrumentation; the atmosphere is not static and it does not take much convective activity in the atmosphere to introduce significant errors in the results

Computational Fluid Dynamics (CFD) is playing an ever increasing role in aerodynamic design for advanced flight vehicles either for performance improvement of the existing system for a new missions or for new concept development for future missions. A cost effective design process is to judiciously combine the wind tunnel tests and CFD studies that exploit the inherent strengths of each of these.

Hypersonic missile flight is characterized by a high flight Mach number (usually greater than 5), thin shock layers and high viscous loads.

The missile aerodynamic geometry has high impact on different missile systems such as control, propulsion, structure, and warhead.

But in order to select between many possible candidates to be designed/tested/computed, an optimization study must be conducted, and this may be done only using dedicated software and a big computing power. Missile aerodynamicists aim to find the optimal external aerodynamic configuration. Missiles have to travel at varying speeds. The optimal aerodynamic configuration has to work efficiently at these variable speeds. The optimization process requires many iterations which makes computationally expensive CFD models unappealing to be used in such calculations. In the existing bibliography, a fast and reliable method such as build-up components method is used to predict performance for hypersonic missiles quickly and reliably [Hemsch, 1992], [Chin, 1961] and [Fleeman, 2006]. Keshavarz [13] presented formulations for different multidisciplinary design optimization (MDO) and two MDO formulations are applied to a sounding missile in order to optimize the performance. Three disciplines have been considered, trajectory, propulsion and aerodynamics.

Sooy and Schmidt [15] presented a study on aerodynamic predictions, comparisons and validations using Missile Datcom (97) and Aero-prediction 98 (AP98) numerical prediction codes. They evaluated the accuracy of each code compared to experimental wind tunnel data for a variety of missile configurations and flight conditions. The missile configurations included axisymmetric body, body wing tail and body tail.

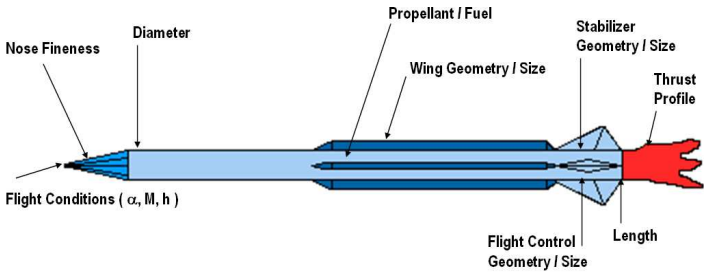

Fig.1. Parameters that Drive Missile Flight Performance

Hypersonic missile technologies, in the last decades, have been developed to include enhanced flight performance, reduced weight, increased Mach's number reduced costs, higher reliability, and reduced observables. Their increased performance depends on various parameters which affect the flight performance, their tradeoff in the context of aerodynamic shape optimization being of paramount importance (Figure.1).

New missile airframe materials technologies have arisen lately. These are hypersonic special dedicated structural materials as composite structure materials, hypersonic insulation materials, multi-spectral domes and so on.

Composite materials are a new technology that will find an increased use in new missile airframe structure. High temperature composites have particular benefits for hypersonic missiles, providing weight reduction. Titanium alloy technology also enables lighter weight missiles in a hypersonic, high temperature flight environment.

At subsonic and low supersonic Mach's number, graphite epoxy and aluminum or aluminum alloys are attractive choices for lighter weight structure. Graphite epoxy and aluminum alloys have high strength to weight ratio, are easily fabricated, have a good corrosion resistance, and are low in cost.

For higher Mach's numbers, graphite polyimide composite structure has an advantage of high structure efficiency at higher temperature for short duration flight Mach's numbers to about Mach 4.

For flight at about Mach 4.5, without external insulation, the titanium structure and its alloys are preferred. A disadvantage of a titanium structure is higher material and machining cost. However, the cost to cast a part made of titanium is comparable to the cost to cast an aluminum part.

At Mach 5, although it is heavier, a steel structure would probably be used. Up to Mach 5.7 without external insulation, at about 1093 degrees Celsius, super nickel alloys such as Inconel, Hastelloy may be used. Above Mach 5.7 the super alloys require either external insulations or active cooling.

The Mach's number and temperature application relationships are somehow dependent upon the temperature recovery factor.

At stagnation region, such as the nose or leading edges, the recovery factor is about 1, resulting in the highest stagnation temperature. A turbulent or laminar boundary layer downstream of the nose or leading edge will have temperature recovery factors of about 0.9 and 0.8 respectively, with local temperatures less than stagnation.

The objective of the current paper is to present a reliable Finite Element Analysis (FEA) and Fluid Structure Interaction (FSI) advanced technique for obtaining hypersonic missile aerodynamics and use this technique for finding optimal hypersonic high technology missile shape based on best structural behavior (the lowest von Mises stress will play the role of Objective Variable), and, secondly, based on the best aerodynamic behavior (the highest V_∞ fluid velocity will play the role of Objective Variable). In achieving these goals, state of the art software was involved: Ansys 9 and all its facilities.

2. THE MISSILE BODY STRUCTURE MATERIALS

The strength to weight capability of advanced composites is very high. For example, as shown in Figure 2, the unidirectional tensile strength of a small diameter graphite (carbon) fiber is more than 400000 PSI (2.757903e+009 Pa). In addition, to small diameter fibers, advanced composite structures have long, continuous fibers and a fiber/matrix ratio that is greater than 50% fibers by volume.

Fibers can be: carbon (graphite), kevlar, boron, ceramic, silicon carbide quartz, glass, polyethylene and others.

As an example of strength at the structure level, 50% of the volume of the graphite composite structure can have strength in a tailored laminate which is above 1.378e9 Pa, much greater than that of aluminum or even steel.

Also the low density of composites further reduces the weight compared to metals. Graphite fiber composite materials have extremely high modulus of elasticity resulting in low strain and deflection compared to metals.

However, a note of caution, unlike metals that generally yield before ultimate failure, composite fibers generally fail suddenly without yield.

For a short duration, temperatures up to 204^0 Celsius, graphite epoxy is a good candidate material based on its characteristics of high strength and low density. Graphite polymide can be used at even higher temperatures, up to 593^0 Celsius, short duration temperature. Over 593^0 Celsius, titanium and steel are the best materials based on strength to weight ratio. An area of enabling capability hypersonic precision of striking missiles is short duration insulation technology. Because hypersonic precision of striking missiles has stringent volume and weight constraints, higher density, external airframe and internal insulation, materials are in development. Higher density insulation materials permit more fuel resulting in longer range.

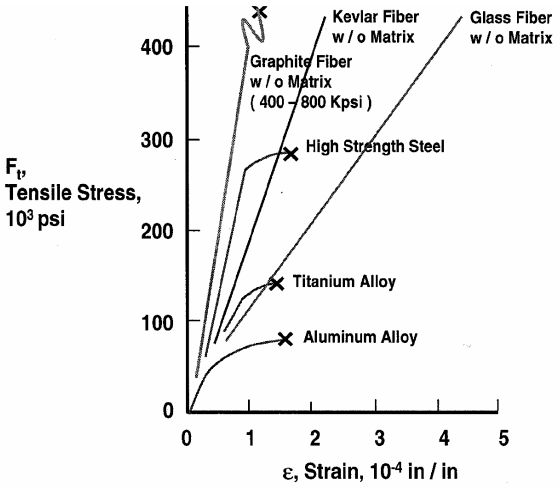

Fig.2. Materials Used in Missile Technology [1]

Thermal insulators are used to provide short duration protection for structural materials from either the aerodynamic heating of a hypersonic free stream or from propulsion heating of the combustion chamber and exhaust gases of the nozzle.

Ceramic refractory materials and graphite materials are also candidate insulators for high speed airframes, engines and motor cases.

Although ceramic refractory materials and graphite have high temperature capability, the insulation efficiency for a given weight of a material is not as good as that of plastic composite materials.

At high temperature, the resin melts providing cooling for the structure. Example of bulk ceramics are zirconium ceramic and hafnium ceramic. Bulk ceramics are capable of withstanding height temperatures but like porous ceramics they have relatively poor insulation efficiency.

Finally, graphite insulators provide the highest temperature capability. However, graphite has relatively poor insulation efficiency.

A good combination of materials for hypersonic missiles seems to be the Metal Matrix Composite (MMC) for the nose and fins and Inconel X-750 for the rest of the body.

2.1 The Nose and Fins Metal Matrix Composite Structure

A metal matrix composite (MMC) is a composite material with at least two constituent parts, one being a metal. The nose and the fins of the considered missile are made out of MMC. The other material may be a different metal or another material, such as a ceramic or organic compound. When at least three materials are present, it is called a hybrid composite

MMCs are made by dispersing a reinforcing material into a metal matrix. The reinforcement surface can be coated to prevent a chemical reaction with the matrix. For example, carbon fibers are commonly used in aluminium matrix to synthesize composites showing low density and high strength. However, carbon reacts with aluminium to generate a brittle and water-soluble compound Al_4C_3 on the surface of the fiber. To prevent this reaction, the carbon fibers are coated with nickel or titanium boride.

The matrix is the monolithic material into which the reinforcement is embedded, and is completely continuous. This means that there is a path through the matrix to any point in the material, unlike two materials sandwiched together. In structural applications, the matrix is usually a lighter metal such as aluminium, magnesium, or titanium, and provides a compliant support for the reinforcement. In high temperature applications, cobalt and cobalt-nickel alloy matrices are common.

The reinforcement material is embedded into the matrix. The reinforcement does not always serve a purely structural task (reinforcing the compound), but is also used to change physical properties such as wear resistance, friction coefficient, or thermal conductivity. The reinforcement can be either continuous, or discontinuous. Discontinuous MMCs can be isotropic, and can be worked with standard metalworking techniques, such as extrusion, forging or rolling. In addition, they may be machined using conventional techniques, but commonly would need the use of polycrystaline diamond tooling (PCD).

Continuous reinforcement uses monofilament wires or fibers such as carbon fiber or silicon carbide. Because the fibers are embedded into the matrix in a certain direction, the result is an anisotropic-orthotropic structure in which the alignment of the material affects its strength. One of the first MMCs used boron filament as reinforcement. Discontinuous reinforcement uses "whiskers", short fibers, or particles. The most common reinforcing materials in this category are alumina and silicon carbide.

In the modeled application was considered the following MMC:

- Matrix : Titanium (Ti); Young's Modulus = 110 GPa ; Poisson's Ratio = 0.25 ; Yield Stress = 300 MPa
- Reinforcements: Silicon Carbide (SiC) ; Young's Modulus = 410 GPa ; Poisson's Ratio = 0.17
- Design Parameters: Fibers': Aspect Ratio (AR=50); Volume Fraction (VF=8% or 12%); Orientation (8 layers symmetric φ=0°, 90°, 45°, -45° and symmetric); Basic layer thickness=0.00025 m for the initial model.

The Orthotropic Elastic Material model used in FEA has the main mechanical characteristics as following:

Table 1: Considered MMC Mechanical Characteristics

Ex=1.1e11 Pa	Ey=1.1e11 Pa	Ez=4.1e11
Gxy=0.44e11 Pa	Gxz=1.75e11 Pa	Gyz=1.75e11 Pa
vxz=0.17	vxy=0.25	vyz=0.17

2.2 The Missile Body Inconel Structure

Inconel alloys are oxidation and corrosion resistant materials well suited for service in extreme environments. The body of the considered missile is made out of Inconel X-750. When heated, Inconel forms a thick, stable, passivating oxide layer protecting the surface from further attack. Inconel retains strength over a wide temperature range, attractive for high temperature applications where aluminum and steel would succumb to creep as a result of thermally-induced crystal vacancies. Inconel's high temperature strength is developed by solid solution strengthening or precipitation strengthening, depending on the alloy. In age hardening or precipitation strengthening varieties, small amounts of niobium combine with nickel to form the intermetallic compound Ni_3Nb or gamma prime (γ'). Gamma prime forms small cubic crystals that inhibit slip and creep effectively at elevated temperatures. Inconel is a difficult metal to shape and machine using traditional techniques due to rapid work hardening. After the first machining pass, work hardening tends to elastically deform either the workpiece or the tool on subsequent passes. For this reason, age-hardened Inconels such as 718 are machined using an aggressive but slow cut with a hard tool, minimizing the number of passes required. Alternatively, the majority of the machining can be performed with the workpiece in a solutionised form, with only the final steps being performed after age-hardening. External threads are machined using a lathe to "single point" the threads, or by rolling the threads using a screw machine. Holes with internal threads are made by welding or brazing threaded inserts made of stainless steel. Cutting of plate is often done with a waterjet cutter. Internal threads can also be cut by single point method on lathe, or by threadmilling on machining center. New whisker reinforced ceramic cutters are also used to machine nickel alloys. They remove material at a rate typically 8X faster than carbide cutters.

In our FEA model, the body material was considered isotropic elastic Inconel X-750.

Alloy X-750 is a precipitation-hardenable alloy which has been used in applications such as high temperature structural members for gas turbines, jet engine parts, nuclear power plant applications, heat-treating fixtures, forming tools, and extrusion dies. The alloy is highly resistant to chemical corrosion and oxidation and has high stress-rupture strength and low creep rates under high stresses at temperatures up to 1500℉ (816℃) after suitable heat treatment.

Alloy X-750 work hardens quickly and is more difficult to machine than most standard ferritic and martensitic alloys. The alloy is most easily machined in the stress-equalized condition.

Because specific cutting forces are high, the machine tools used must have ample power and the cutting speed should be slow. The tools must have smooth finishes, be sharp, and be very rigid. To avoid work hardening, a continuous, smooth cutting action should be maintained; thus, the machines must have a minimum of backlash and the tool and work-piece must be rigidly supported. If at all possible, avoid very small cuts and feeds.

Table 2: Inconel X-750 Mechanical Properties

Test Temperature		Short-Time Tensile Properties Tests					
		Yield Strength 0.2% offset		Ultimate Tensile Strength		% Elongation in 2" (50.8 mm)	% Reduction of Area
℉	℃	ksi	MPa	ksi	MPa		
70	21.1	92	634	161	1110	22	30
1000	538.0	83	572	140	965	20	30

1200 1400 1500	649.0 760.0 816.0	82 68 45	565 469 310	120 80 47	827 552 324	10 10 20	21 22 32
Young Modulus=2.1e11 Pa							
Poisson's Ratio=0.29							

3. NUMERICAL INVESTIGATION

3.1. CAD Geometry and FEA mesh

The declared goal of generating CAD geometry and FEA mesh is to save as much of computing power we can, due to the high complexity of the simulation. Even the optimization using Subproblem method was selected taking into account the same goal, this method being less expensive in terms of the number of iterations needed to obtain the convergence.

The missile was considered a double symmetric body and the fluid domain and the solid one as well, was deemed to generate acceptable results even if was considered only ¼ of both domains and imposing proper symmetry boundary conditions. The CAD geometry is given in the figure 3:

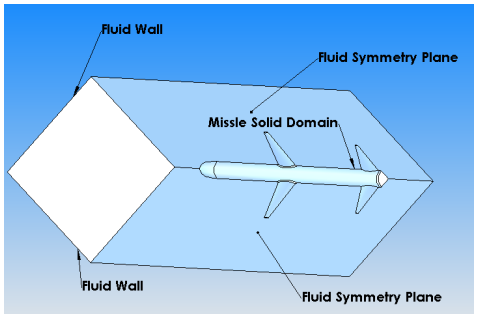

Fig.3. CAD geometry of the fluid and solid domains

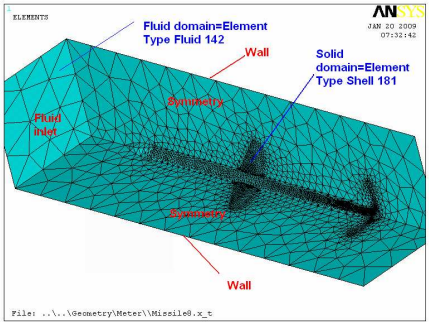

Fig.4. FEA mesh and boundary conditions

In the igure 4, there are visible the symmetry planes, the inlet region of the fluid where the velocity which was imposed being 1000 m/sec, the outlet region for the fluid opposed to the inlet region where the pressure was imposed being slightly under atmospheric at sea level (91,500 Pa (a)) and the walls where all the components of velocity were set to zero (this wall conditions are mimicking the testing wind tunnel walls). The fluid and structural meshes were deliberately refined in the FSI contact region for surprising in more detail the phenomena which may occur in this region. The fluid is considered Air with its standard parameters in SI.

We used Fluid142 element to model our transient fluid system involving both fluid and solid regions. The conservation equations for viscous fluid flow and energy are solved in the fluid region, while only the energy equation is solved in the non-fluid region. For this kind of elements, the velocities are obtained from the conservation of momentum principle, and the pressure is obtained from the conservation of mass principle. A segregated sequential solver algorithm is used; that is, the matrix system derived from the finite element discretization of the governing equation for each degree of freedom is solved separately. The flow problem is nonlinear and the governing equations are coupled together.

On the other hand, for the solid domain we used the Shell 181 type of element due to the fact it can model the multilayered composite orthotropic elastic materials as MMC for missile nose and fins, and also the isotropic elastic materials as Inconell X-750 for the cylindrical body of the missile.

Shell 181 element type is suitable for analyzing thin to moderately-thick shell structures. It is a 4-node element with six degrees of freedom at each node: translations in the x, y, and z directions, and rotations about the x, y, and z-axes. Shell 181 is well-suited for linear, large rotation, and/or large strain nonlinear applications. Change in shell thickness is accounted for in nonlinear analyses. In the element domain, both full and reduced integration schemes are supported. Shell 181 accounts for follower (load stiffness) effects of distributed pressures. It may be used for layered applications for modeling laminated composite shells or sandwich construction. The accuracy in modeling composite shells is governed by the first order shear deformation theory (usually referred to as Mindlin-Reissner shell theory).

Since the main problem is the FSI, the fluid-solid interaction solver was selected in simulation, it successfully solving the equations for the fluid and solid domains independently of each other. It transfers fluid forces and heat fluxes and solid displacements, velocities, and temperatures across the fluid-solid interface. The algorithm continues to loop through the solid and fluid analyses until convergence is reached for that time step (or until the maximum number of stagger iterations is reached). Convergence in the stagger loop is based on the quantities being transferred at the fluid-solid interface. In order to function properly, a FSI interface was established between the elements of fluid-solid domains.

3.2. FSI simulation of the initial model

With the so obtained model and having defined the geometry, the fluid-solid mesh domains, the FSI interface, the boundary and symmetry conditions, the materials properties for fluid, for MMC and Inconel X-750, the loads as inlet velocities and outlet pressures, is good to have a complete FSI analysis of the model. This is useful in order to check if the model is working and to have a departing point to judge the optimization outcome and the improvement capability of optimization process for missile structure and aerodynamics.

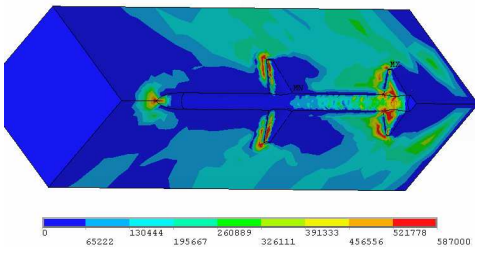

Fig.5. Pressure distribution for initial model

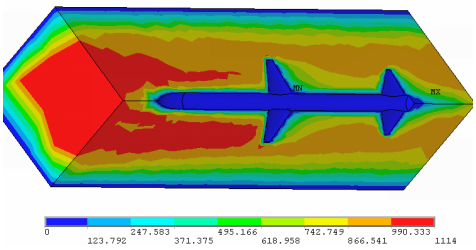

Fig.6. Fluid velocity distribution for initial model

The pressure distribution exerted by fluid on the missile structure already tells a lot about the loads on which the structure is subjected. It was almost the common sense to say that the nose, the attack edge of the fins and the rear portion of the missile to be subjected to the biggest pressure, 587e3Pa.

On the Figure 6 is presented the fluid velocity distribution around the model. The influence of walls where the velocity was imposed to be null is slowing down the fluid in its immediate vicinity and the model is determining the specific hypersonic flow separation,

wake and swirls all around the structure. The maximum achievable velocity inside the fluid domain is 1114 m/sec.

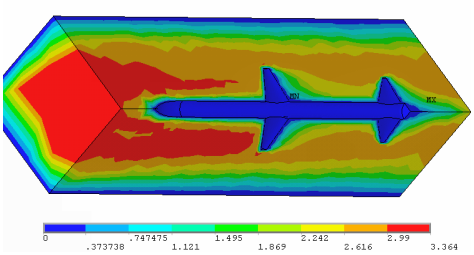

Fig.7. Mach number distribution for initial model

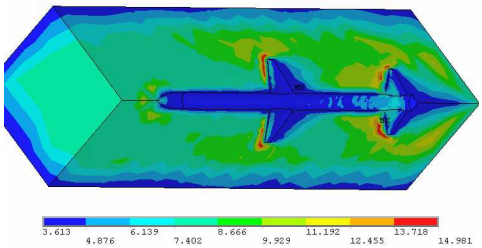

Fig.8. Fluid density distribution for initial model

The Mach number distribution inside the fluid domain (Figure7), as expected, is closely following the distribution of fluid velocities, reaching a maximum of Mach 3.36 in the very front of the missile.

The fluid density distribution (Figure 8) is somehow similar to the pressure distribution, in the fluid compressibility hypothesis; the air is “smashed” in the regions with bigger pressure fields.

The pressure exercised by fluid upon the missile’s structure will result in structural strain of the missile. The maximum strain of course will occur where the maximum fluid pressure is developing, namely on the missile fins and rear portion. The maximum strain will be 0.14% on the Inconel rear back of missile (Figure 9).

The missile structure as above stated, remaining well within the elastic region of its structural behavior, the von Mises equivalent stresses distribution will closely follow the one of strain distribution, registering a maximum of 162e6 Pa in the rear region of the missile. This is once more an assurance for the Structural Engineer that the initial model which is serving as optimization starting point is feasible in terms of structural and geometric stability (Figure 10).

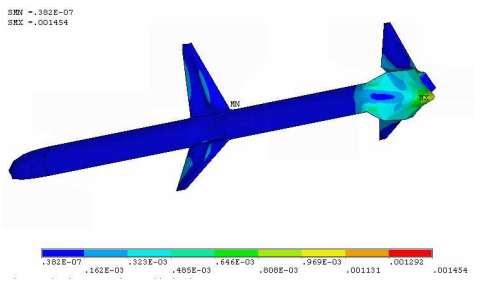

Fig.9. Von Mises equivalent strain distribution for initial model

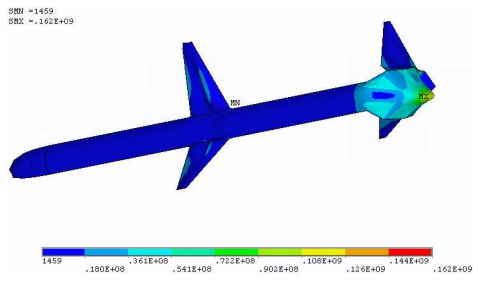

Fig.10. Von Mises equivalent stress distribution for initial model

For this study, there were established two optimization scenarios (many such scenarios may be conceived so they are not a “receipt”):

Optimization Scenario 1 - from the Structural Design Engineer point of view which may be pleased if the computed von Mises Equivalent Stresses are minimized, therefore this quantity will play the role of Objective Variable. The Optimisation Scenario no.1 represents

the Structural Engineer point of view, which always will search for that structural arrangement that provides the lower stress condition inside the structure for a given geometry/aerodynamic design/state variables.

3.3. Optimization Scenario 2

The Optimisation Scenario no.2 is represented by the Aerodynamics Design Engineer point of view, that always will search for a structural arrangement to ensure the best aerodynamic behavior for a given geometry/aerodynamic design/state variables.

In this scenario the maximum achievable von Mises equivalent stress is 170e6Pa, value almost equal to the initial model which was 162e6 Pa. In terms of structural behavior the increased aerodynamics does not it affect too much.

To be noticed the “elongation” of the missile nose, with almost 100 mm (20% bigger) which seems to impact heavily on the aerodynamic behavior of the missile. The height of fins is bigger that that of Scenario 1 but, still, smaller than the initial values.

L22 Design variable is the height of Fins set no.2, at the rear end of the missile. By studying the given graphs (Figures11, 12, 13), the overall conclusion is that the biggest values of this parameter tend to increase the stress condition in the structure. The optimum value of the parameter is 0.25633 m where the maximum velocity (Figure11 a) reaches 2400 m/sec and the “dummy” objective variable Optimvelocity (Figure11 b) has its minimum value of 3009 m/sec signaling the maximum inlet velocity of 1990 m/sec which is the best optimum in aerodynamic point of view.

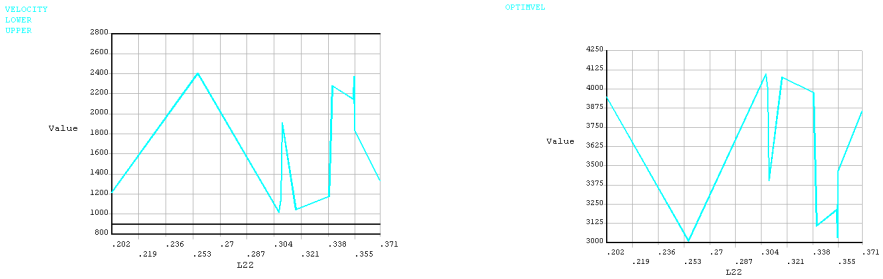

(a) ***(b)***

Fig.11. L22 Design variable impact over maximum fluid velocity and the Dummy objective function

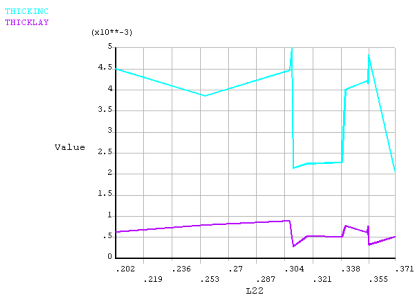

Fig.12. L22 Design variable impact over maximum structure thickness

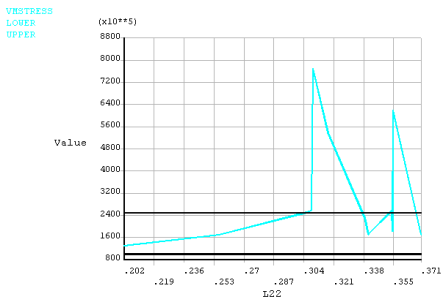

Fig.13. L22 Design variable impact over maximum von Mises stress

L31 which is the distance between the two sets of fins, determines an local maximum of velocity inside the fluid domain and a minimum for the dummy" objective variable Optimvelocity, for a value of 1.2036 m, and the worst impact should be registered for values from right side (maximum) of variation interval (see Figures14, 15, 16).

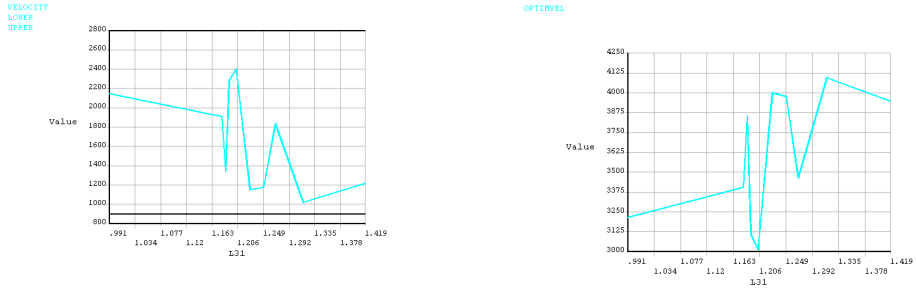

(a) ***(b)***

Fig.14. L31 Design variable impact over maximum fluid velocity and the Dummy objective function

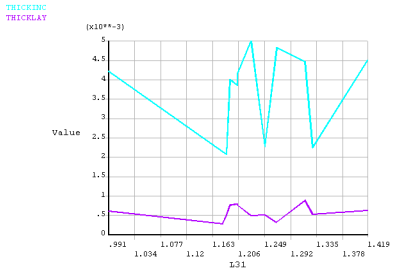

Fig.15. L31 Design variable impact over maximum structure thickness

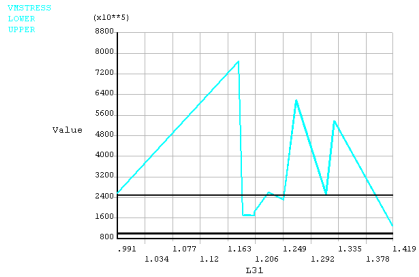

Fig.16. L31 Design variable impact over maximum von Mises stress

L23 which is the height of missile fins set 1 (Figures 17, 18, 19) determine a local maximum for velocity and a local minimum for Optimvelocity at 0.36988 m. But this local maximum/minimum is so close to a local maximum/minimum for both mentioned parameters, that this value should be a little bit decreased, 0.355 m seems to be more reasonable.

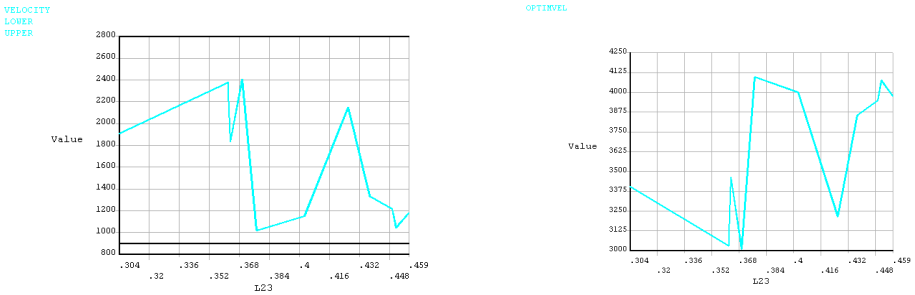

(a) ***(b)***

Fig.17. L23 Design variable impact over maximum fluid velocity and the Dummy objective function

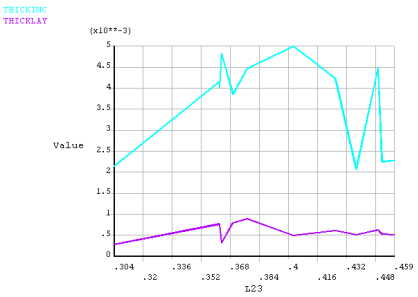

Fig.18. L23 Design variable impact over maximum structure thickness

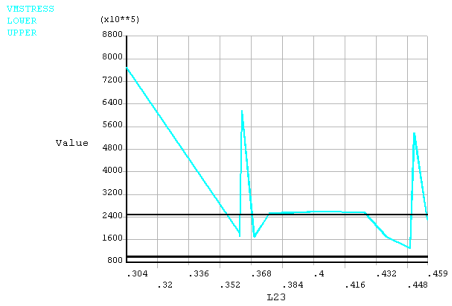

Fig.19. L23 Design variable impact over maximum von Mises stress

For more details, the following Figures are given after FSI simulation of the optimal design in Scenario 2 perspective.

The pressure distribution exerted by fluid on the missile structure is similar to that of the initial model. The nose, the attack edge of the fins and the rear portion of the missile are to be subjected to the biggest pressure, 616e3Pa.

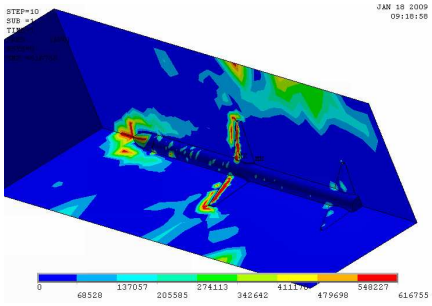

Fig.20. Pressure distribution for Optimal -Scenario 2

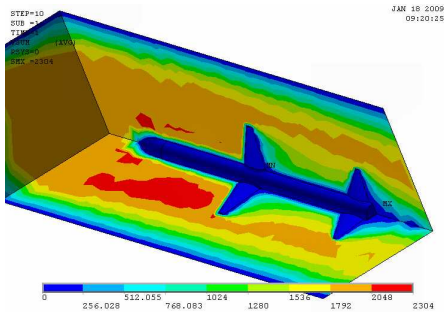

Fig.21. Fluid velocity distribution for Optimal-Scenario 2

On the Figure 21 is presented the fluid velocity distribution around the optimum model for Scenario 2. The maximum achievable velocity inside the fluid domain is 2304 m/sec, much bigger that the one computed for the initial model.

The Mach number distribution inside the fluid domain, as expected, is closely following the distribution of fluid velocities, reaching a maximum of 6.9 in the very front of the missile.

The fluid density distribution is somehow similar to the pressure distribution.

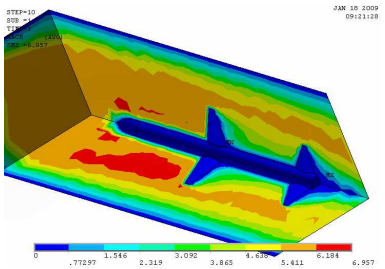

Fig.22. Mach number distribution for Optimal-Scenario 2

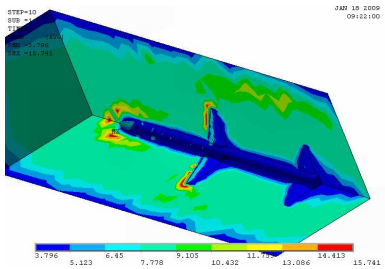

Fig.23. Fluid density distribution for Optimal-Scenario 2

The fluid turbulent energy dissipation zones are also highlighting that zones which are characterized by intense turbulent regimes, as in the rear edges of fins and missile.

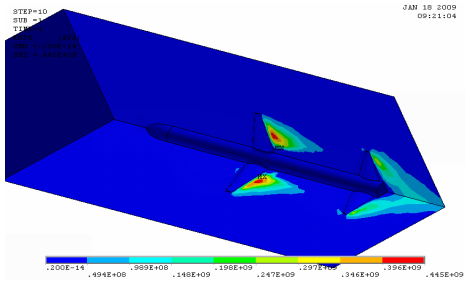

Fig.24. Fluid turbulent energy dissipation distribution for Optimal-Scenario 2

The maximum strain of course will occur where the maximum fluid pressure is developing, namely on the missile first set of fins (Figure 25). The maximum value of it is 0.08%.

The von Mises equivalent stresses distribution will closely follow the one of strain distribution, being computed a maximum of 0.17021E+09 Pa in the first set of fins of the missile (Figure 26).

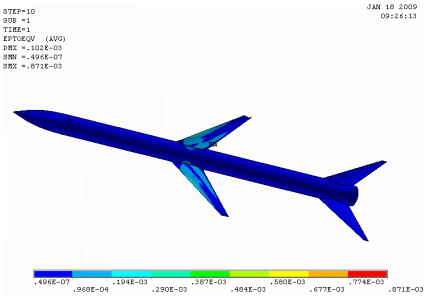

Fig.25. Von Mises equivalent strain distribution for Optimal-Scenario2

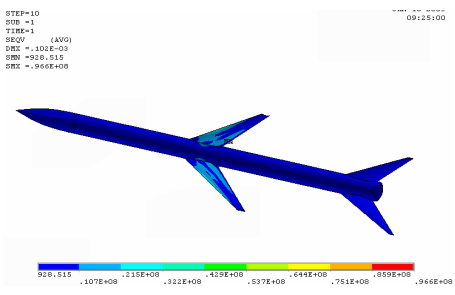

Fig.26. Von Mises equivalent stress distribution for Optimal-Scenario 2

4. CONCLUSIONS

The numeric model presented in this paper, provides consistent and reasonable results for missiles structural-aerodynamic analysis and optimization. Its results are comparable with other approaches but the optimization must be evaluated on a case-by-case basis, meaning that what is good for a certain missile structure may very well be not applicable for another. Furthermore, even the optimization is thought to minimize or diminish the designer flair in decisions making, apparently in every step of this process the designer ought to have decisive interventions. Optimization is just a tool and should be used as it is: a tool.

The results obtained from the optimization numeric simulation, may be used to define a certain structure-shape of a missile prior any attempt to in depth analyzing and testing it, this shortening the needed time for design and testing programs.

REFERENCES

[1]. Anderson D., Tannehill J., and Pletcher R.- ***Computational Fluid Mechanics and Heat Transfer***, McGraw-Hill Book Company, New York, 1984.
[2]. Cheney W. and Kincaid D.- ***Numerical Mathematics and Computing***, Brooks/Cole Publishing Company, 1999
[3]. Chin S. S.- ***Missile Configuration Design***, McGraw Hill Book Company, 1961.
[4]. Cornelisse J. W., Schoyer H. F. R., Wakker K. F.- ***Rocket Propulsion and Spaceflight Dynamics***, Pitman Publishing Limited, 1979
[5]. Felippa, C. A. and Geers T. L.- ***Partitioned analysis of coupled mechanical systems***, Engrg.Comput. , 5, 123–133, 1988.
[6]. Fleeman Eugene L.- ***Tactical Missile Design***, 2nd edition, AIAA Education Series, 2006.
[7]. Hemsch Micheal J., Nielsen Jack N.- ***Tactical Missile Aerodynamics***, ***Progress in Astronautics and Aeronautics***; V.124, American Institute of Aeronautics and Astronautics, Inc, 1992
[8]. Hirsch C.- ***Numerical Computation of Internal and External Flows***, volume 1,2. John Wiley & Sons, New York, 1988.
[9]. Kjellström G.- ***Useful Monte Carlo optimization***, Journal of Optimization Theory and Applications, Volume 69, Number 1 /April, 1991.
[10]. Kvasnov N. F.- ***Aerodynamics I, II***, 1980
[11]. Lesieutre D., Love John F., Dillenius Marnix F. E.- ***Prediction of the Nonlinear Aerodynamic Characteristics of Tandem-Control and Rolling-Tail Missiles***, AIAA 2002-4511, August,2002.
[12]. Motoda T.- ***Simplified Approach to Identifying Influential Uncertainties in Monte Carlo Analysis***, Journal of Spacecraft and Missiles, Vol. 41, No. 1, pp.1071-1074, November, 2004.
[13]. Roshanian J., Keshavarz Z.- ***Effect of Variable Selection on Multidisciplinary Design Optimization a Flight Vehicle Example***, Chinese Journal of Aeronautics, pp.86-96, 2006.
[14]. Siouris George M.- ***Missile Guidance and Control Systems***,New York, Springer, 2004.
[15]. Sooy Thomas J., Schmidt Rebecca Z.- ***Aerodynamic Predictions, Comparison and Validatind Using Missile DATCOM (97) and Aeroprediction 98 (AP98***). Journal of Spacecraft and Missiles, Vol. 42, No. 2, pp.257-265, March, 2005.
[16]. USAF DATCOM, 1970.

ANALYSIS OF THE CRACK LENGTH AND TEMPERATURE OF A CANNON BARREL USING THE J INTEGRAL

[1]CALIMANESCU IOAN, [2]STAN LIVIU-CONSTANTIN

[1,2]*Constanta Maritime University, Romania*

Perhaps the most accurate and elegant method for computing the energy release rate is to calculated the *J* integral by converting the line integral into a domain integral which can easily be calculated using the known finite element shape functions.The problem illustrates the case of a crack in a cannon barrel, together with the relevant geometry against crack length defined from the bore of the cannon. This crack geometry is the most dangerous integrity case for the cannon barrel. In this research, 155 mm cannon barrel with one crack with lengths of 4 mm, 8 mm and 12 mm on inner surface is firstly structurally analyzed at room temperature, and subsequently coupled thermo-structurally analyzed considering 4 scenarios, where the crack length was deemed to be 4 mm, the temperature of the inner surface was 100^0C, 125^0C, 150^0C, 200^0C. The numeric model presented in this paper, provides consistent and reasonable results for the dependency of stress intensity factor to the crack length and temperature of a cannon barrel using the *J* integral. The temperature fields inside the cannon barrel (and, generalizing, inside any circular structure with thick walls) tends to ameliorate the stress fields existing on the crack tip and pushing the calculated K_I downward and thus improving the crack behavior.

***Keywords**:* Cannon barrel, Stress Intensity Factor, Crack, J Integral, Coupled Thermal-Structural FEA

1. INTRODUCTION

For centuries [Burton, 2004], cannon barrel designers have focused their efforts on the development and use of steels that possess higher strength and toughness. Good mechanical properties are required to withstand the high interior ballistic (explosive) loads to which these pressure 'vessels' are subjected. In addition to high internal pressure, the cannon bore (internal surface of the cannon cylinder) is exposed to very high temperatures, as the propellant ignites and begins the evolution of hot gases to provide the propulsive force for the projectile. With the advent of ever more robust propellants, bore surface erosion has become increasingly problematic. This has forced barrel designers to implement various means that include coatings and alternate material liners to combat the phenomena. The desire for longer lasting tubes has been a major motivator for research of new and more robust materials for cannon design. Likewise, cannon barrel manufacturers have committed significant effort to developing processes that result in high quality cannons capable of withstanding these erosive environments.

In the 20th century, variations in the chemistries of Chromium-Molybdenum-Vanadium (Cr-Mo-V) steels have been introduced that allowed for moderate increases in strength,

toughness and fatigue properties. Most of these improvements come from superior processing and techniques that produce higher-quality steels (less contaminants and defects). The last major advancement in armament steels occurred in the 1970's with the introduction of ASTM A723 steel, which has yield strength more than five times that of the steel produced by Rodman more than a century earlier. It replaced the 4335-V modified steel that had been in use since before World War II.

The A723 steel is processed through either vacuum arc re-melt (VAR) or electro-slag re-melt (ESR). Both processes significantly reduce the amount of sulphur and phosphorus and, combined with an increase in the nickel content, make A723 steel an excellent candidate for "modern" armament applications. More recently, the armament community has pushed for materials with even higher strength and toughness due to more aggressive environments and higher cannon firing pressures.

Cannon-wear [Lawton, 2001] remains, to this day, one of the main factors limiting cannon's muzzle velocity and range. It normally occurs as an increase in bore diameter at the commencement of rifling and from here it spreads down the barrel towards the muzzle. As a measure of wear it is conventional to quote the increase in bore diameter measured at 25 mm from the commencement of rifling. The increase in diameter that can be tolerated before a barrel is condemned depends on the accuracy that is required. For tank cannons, which need to be very accurate in order to hit a target at the first attempt, the permissible wear is about 0.5–1% of the bore diameter. For indirect fire weapons, such as howitzers, the allowable wear may be as much as 5% or even 8% of the bore diameter. Gas leakage between the projectile and the worn barrel reduces the pressure and the projectile's muzzle velocity, range, and accuracy, gradually reduces as wear increases. Typical wear rates vary between 0.1 and 200 μm per round and usually exceed the fatigue crack propagation rate. As a rule the cannon designer arranges for the fatigue life of a barrel to exceed its wear life because fatigue failure is usually catastrophic and endangers the cannon crew, whereas barrel wear simply reduces the accuracy of the projectile without putting the crew in danger.

Typically, the bore temperature reaches 600–1200^{0}C at this place within a few milliseconds of exposure to the hot propellant gases. Heat transfer may be 500MW/m2, and the propellant gas pressure may reach 600MPa. Wear has always been related to the intense thermal conditions experienced at this point and as early as 1911, Jones [8] derived an empirical equation based on this assumption. Other early work of note includes Shulyer [21] and Kent [9]. Thornhill's work [22] is particularly interesting in that he looked for a linear correlation between wear per round and the maximum temperature at the bore, and many of the ideas he originated have found application here.

Fig. 1 (top) shows the unworn section of rifled cannon that may be compared to the eroded section at the commencement of rifling of the same cannon (middle). This is normal wear.

The bore diameter increases uniformly around the barrel at the commencement of rifling and spreads along the barrel towards the muzzle. Occasionally, oval wear occurs, that is, wear is perhaps 20% greater in the vertical plane than in the horizontal plane. This type of wear occurs at temperatures between 900 and 1400 K, which is well below the melting point of cannon steel. Gas wash past a faulty driving band can cause local melt erosion (Fig. 1 (bottom)), and such erosion is many times faster than normal erosion.

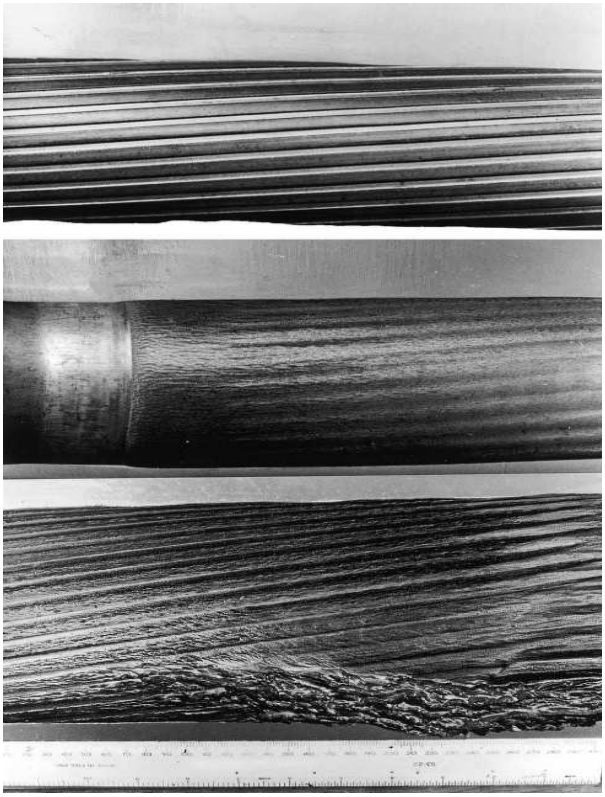

Fig. 1. Cannon barrel erosion

A photomicrograph showing the sub-surface of cannon steel, after firing 10 rounds, is shown in Fig. 2. Three layers are apparent, marked A, B and C. The layer marked A is the original structure. The layer marked B extends perhaps 200 μm from the surface and is called the heat-affected zone. In this region, the cannon steel had been subjected to a large temperature fluctuation each time the cannon was fired. The temperature fluctuation may be 1000^0C at the surface but 1mm from the surface it is only about 100^0C, and the period of the fluctuation may be 5–50 ms. The microstructure of the heat-affected zone changes towards the surface and the steel becomes harder and more brittle. The layer marked C is called the chemically-affected zone. At high temperatures, chemical species from the propellant gas diffuse into the crystal lattice altering its chemical composition. These species include the main products of propellant combustion (CO, CO_2, H_2, H_2O and N_2) and a small quantity of dissociated atomic species. This further reduces the strength and increases the brittleness of the surface layers. Hardness increases from about 250 HV in region A, to 500 HV in region B, and 1000 HV in region C. Micro-cracks form in region C, some normal to the surface and some parallel with the surface. The shear stress caused by high velocity gas flow, and the contact stress generated by the driving band, are sufficient to remove a portion of the cracked and brittle layer. The amount of wear depends on the depth to which the chemically-affected zone has penetrated which, in turn, depends on the chemical composition of the propellant and on the bore surface temperature.

A single crack [Zywicz, 1993] 30 mm or deeper which is 75 mm long is sufficient to fracture a typical 155 mm cannon barrel with a pressure at or above two-thirds (206 MPa) of the maximum operating pressure (310 MPa). Longer and deeper flaws reduce the critical

pressure required to initiate fracture. For the monolithic barrel design the postulated 30 mm deep by 75 mm long crack should propagate through the entire wall and, depending upon the new “fractured” geometry, may propagate axially down the cannon barrel.

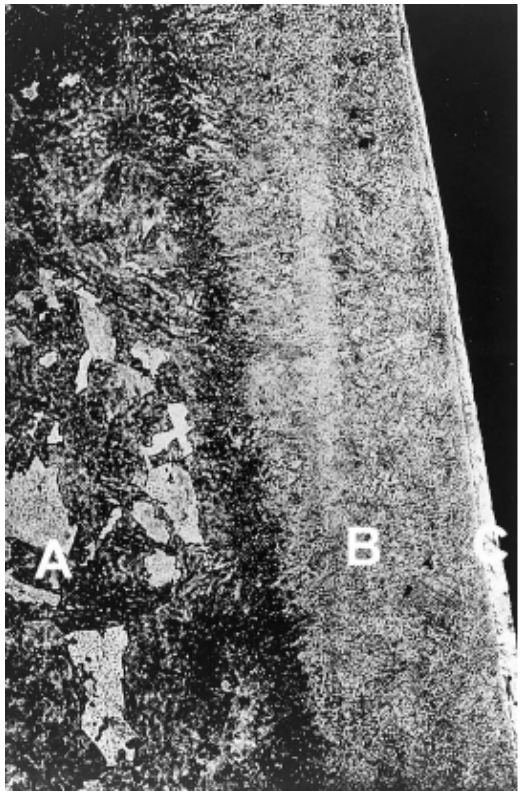

Fig. 2. Photomicrograph showing the sub-surface of cannon steel

Numerical analyses conducted [Zywicz, 1993] with straight through-thickness crack fronts propagated axially at pressures below the maximum operating pressure while those with curved crack fronts required pressures in excess of the working pressures to extend axially. In either case, a through-thickness “hole” will be formed in the barrel’s side and a reduction in firing pressure should result. Finally, debris deposited within the barrel can greatly assist the fracture process, especially at lower operating pressures.

2. SOME THEORETICAL CONSIDERATIONS

For a crack under tensile, or Mode-I loading for linear-elastic materials:

$$G = J = \frac{K_I^2}{E'} \Rightarrow K_I = \sqrt{\frac{JE}{1-\nu^2}}$$
$$E' = \frac{E}{1-\nu^2} \_ Plain - Strain \tag{1}$$

where *G* is Energy Release Rate, *E* is Young modulus and *υ* is Poisson constant, K_I is the stress intensity factor, *J* is the *J* integral.

Perhaps the most accurate and elegant method for computing the energy release rate is to calculated the *J* integral by converting the line integral into a domain integral which can easily be calculated using the known finite element shape functions.

Consider the closed contour *C* with outward unit normal vector *m* as shown in Figure 3:

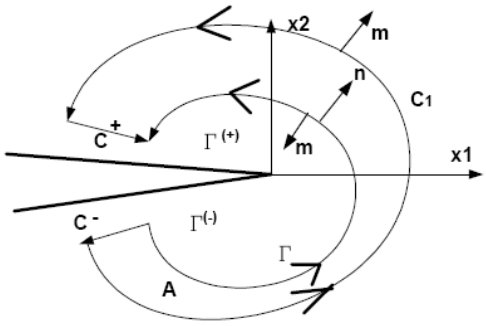

Fig. 3. Contours for derivation of domain integral calculation of J integral

The contour *C* is defined by $C = C_1 + C^+ + C^- - \Gamma$. The area enclosed by *C* is *A*. Define a function $q(x_1, x_2)$ such that q=1 on Γ and q=0 on C.

For a crack that grows straight ahead:

$$G = J = \int_\Gamma \left(Wn_1 - t_i \frac{\partial u_i}{\partial x_1} \right) d\Gamma \tag{2}$$

where Γ is a contour that starts and stops on the crack line and n is the outward unit normal to Γ.

Replacing **n** with **−m** on Γ and noting that q = 0 on C_1:

$$J = -\int_C \left(Wm_1 - \sigma_{ij} m_j \frac{\partial u_i}{\partial x_1} \right) q dC - \underbrace{\int_{C^+ + C^-} \left(\sigma_{ij} m_j u_{i,1} \right) q dC}_{0} \tag{3}$$

The second integral equals zero since on the crack faces: $\vec{m} = \pm m_2 \vec{e}_2 \Rightarrow \sigma_{ij} m_j = \pm \sigma_{i2} = 0$.

Thus *J* has been converted into an integral over a closed contour. The divergence theorem can now be used to convert *J* into an area integral:

$$\left.\begin{aligned} J &= \int_A \left[\left(\sigma_{ij} u_{i,1} q\right)_{,j} - \left(Wq\right)_{,1} \right] dA = \\ &= \int_A \left[\left(\sigma_{ij} u_{i,j} q + \sigma_{ij} u_i q_{,j}\right) - \left(W_{,1} q + W\, q_{,1}\right) \right] dA \\ \sigma_{ij,j} &= 0 \\ W_{,1} &= \sigma_{ij} u_{i,1} \end{aligned}\right\} \Rightarrow J = \int_A \left[\left(\sigma_{ij} u_{i,1} q_{,j}\right) - \left(Wq_{,1}\right) \right] dA \quad (4)$$

Typically the function q is expressed using the same shape functions that interpolate displacement, i.e. $q = \sum_{i=1}^{n} N_i q_i$ where N_i are the shape functions, qi are the nodal values of q at nodes i = 1, n.

Thus *J* may be calculated as an area integral over any annular region surrounding the crack tip.

The domain integral approach is generally very accurate even with modest mesh refinement since it does not rely on capturing the exact crack tip singular stress field, rather on correctly computing the strain energy in the region surrounding the crack tip.

The method for computing stress intensity factors rely on the accurate calculation of the stress, displacement and energy fields. Since all of the methods use information from a small distance away from the crack tip they are somewhat forgiving of errors induced by not capturing the exact crack tip singular stress field. However, more accurate results could be obtained by capturing the crack tip singular stress field. Since we know that in elastic materials the crack tip stresses are singular as $1/\sqrt{r}$ this singularity can be built into the finite element calculation from the start.

A number of methods to produce singular crack tip stresses have been developed, some of which require special elements and some of which can be used with standard elements. The natural triangle quarter-point element has constant and $1/\sqrt{r}$ strain terms, reproducing the first two terms of the Williams crack tip solution. The quarter-point finite element will be used in this study. In fact the strategy of solving the following problems is calculating via Finite Elements Analysis the *J* integral on contours around the crack tip populated with quarter-point elements, and by using the relation (1) to calculate K_I is the stress intensity factor to be compared with the Fracture toughness of the material K_{IC}.

3. NUMERICAL INVESTIGATION

3.1. Problem definition

The problem illustrates the case of a crack in a cannon barrel, together with the relevant geometry against crack length defined from the bore of the cannon. This crack geometry is the most dangerous integrity case for the cannon barrel. The stress intensity calibration includes both hoop stress and internal pressure contributions. The barrel of the FEA modeled cannon has an inner radius of 85 mm and an outer radius of 160 mm, and it operates at a firing pressure of 380 MPa. It is made from 4340 grade steel with yield strength of 1.131 GPa, a tensile strength of 1.232 GPa and a plane strain fracture toughness value of 125.8 $MPa\sqrt{m}$ In this research, 155 mm cannon barrel with one crack with lengths of 4 mm, 8 mm and 12 mm on inner surface is analyzed. Half of the cross section of the cracked cannon pipe is shown in Figure 4.

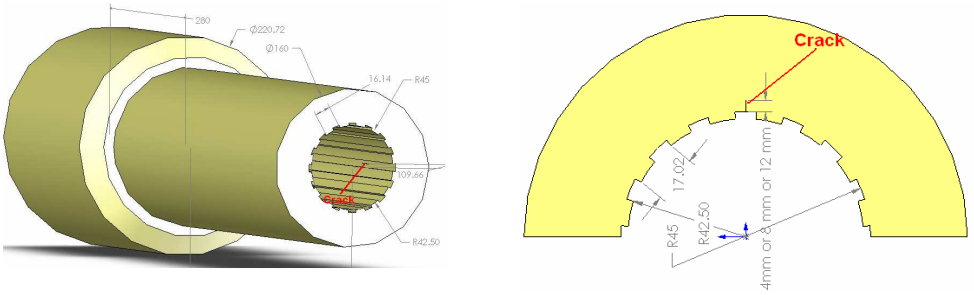

Fig. 4. Geometry of the cannon barrel and crack position and dimensions

For the thermal influence of the barrel temperature there were considered 4 scenarios, where the crack length was deemed to be 4 mm, the temperature of the inner surface was 100^0C, 125^0C, 150^0C, 200^0C, the thermal conductivity of the steel 60.5 W/m^{0}C, thermal expansion coefficient 1.2 e-5 $^0C^{-1}$ and the stagnant air convection coefficient at 20^0C around the barrel was considered 5 W/m^2 ^{0}C.

3.2 Finite Elements Model

For the first half of the problem, a structural analysis was conducted in the view of determining the stress and strain fields at the tip of the crack on a 2D model using the software ANSYS. In the figure 5 is given the FEA model comprising 3316 Plane 82 type of element with the crack tip surrounded by quarter-point elements collapsed in order to catch the details of the stress-strain fields, as seen below:

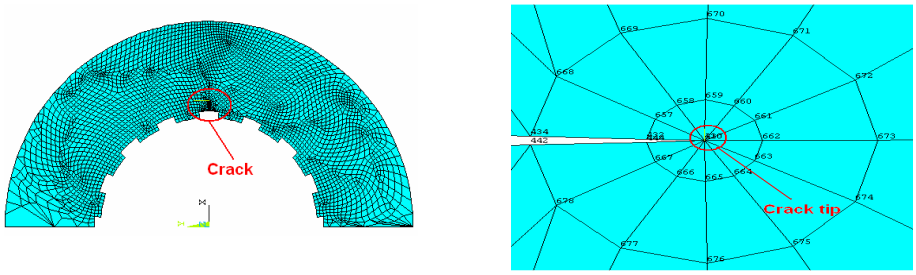

Fig. 5. FEA Model and crack tip area

For the second half of the problem, namely the coupled thermal-structural analysis, it will be deployed a sequentially coupled physics analysis which is by definition the combination of analyses from different engineering disciplines which interact to solve a global engineering problem. For convenience, the solutions and procedures associated with a particular engineering discipline will be referred to as a physics analysis. When the input of one physics analysis depends on the results from another analysis, the analyses are coupled.

Thus, each different physics environment must be constructed separately so they can be used to determine the coupled physics solution. However, it is important to note that a single set of elements/nodes will exist for the entire model. By creating the geometry in the first physical environment, and using it with any following coupled environments, the geometry is kept constant. For our case, we will create the geometry in the Thermal Environment, where the thermal effects will be applied. Although the geometry must remain constant, the element

types can change. For instance, thermal elements are required for a thermal analysis while structural elements are required to determine the stress. It is important to note, however that only certain combinations of elements can be used for a coupled physics analysis. The process requires the user to create all the necessary environments, which are basically the pre-processing portions for each environment, and write them to memory. Then in the solution phase they can be combined to solve the coupled analysis.

Therefore, for the Physical thermal environment, it will be used the same FEA spatial net of 3316 elements but with Plane 77 elements type instead, and after processing the thermal module we will migrate to the Structural Physical environment with Plane 82 elements and importing the thermal solutions we will process the structural problem having included the thermal effects.

3.3 The study of the dependency of K to the crack length

As mentioned above, 3 scenarios were simulated in 2D, with cracks of 4 mm, 8 mm and 12 mm on the inner surface in linear-elastic fracture analysis hypothesis. The frontier conditions imposed to the model were the symmetry displacement condition to the lines bordering the half of the analyzed model (see Fig.5) and on all the inner lines including the crack faces the 380 MPa pressure was imposed.

Below there will be presented the results in the crack tip area, for 4 mm crack length, for the rest a graph will be raised.

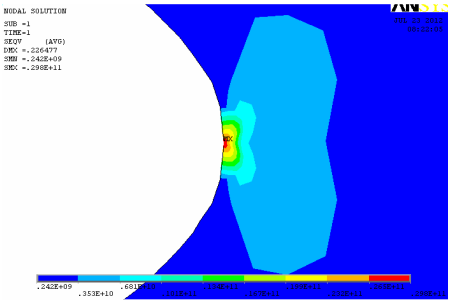

Fig.6. von Mises stress field at the crack tip for 4 mm crack length

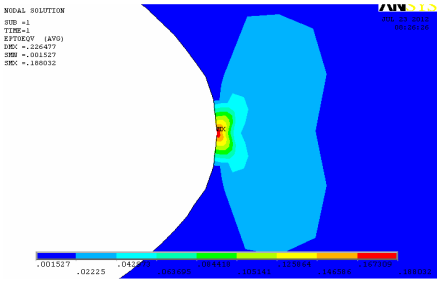

Fig.7.Von Mises strain field at the crack tip for 4 mm crack length

As it can be seen in the figures above, the maximum stress-strain field is located at the crack tip having a value of 2.98e10 Pa (the stress) and 0.188 (the strain).

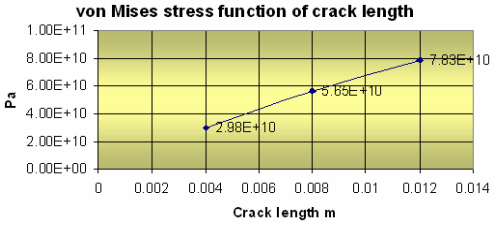

Fig.8. von Mises stress field at the crack tip for 4 mm, 8 mm and 12 mm crack length

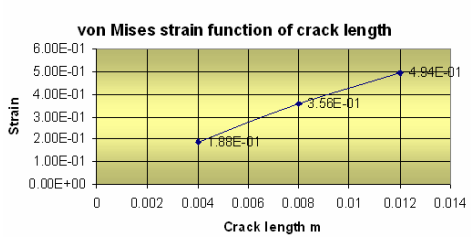

Fig.9. von Mises strain field at the crack tip for 4 mm, 8 mm and 12 mm crack length

As it can be seen above, the stress-strain fields on the crack tip are increasing almost linearly with the progress of the crack. All the stresses are in any case bigger than the yield strength of 0.1131 e10 Pa.

The next step was to calculate the *J*-Integral around the tip of the cracks and the following graph was raised:

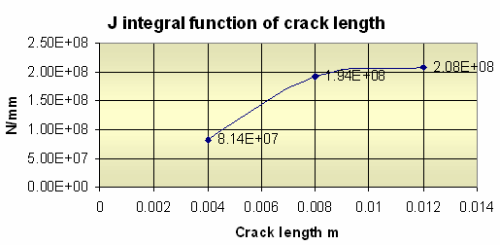

Fig.10. J integral at the crack tip for 4 mm, 8 mm and 12 mm crack length

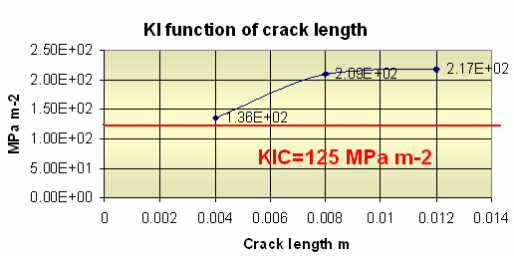

Fig.11. Stress intensity factor at the crack tip for 4 mm, 8 mm and 12 mm crack length

After calculating K_I with the relation (1) the graph in figure 11 was raised showing the both *J*-Integral (Fig.10) and the stress intensity factors are increasing with the crack length, firstly sloped until 8 mm crack length and mildly after.

First remark should be that for 4 mm crack length $K_I = 135.7MPa\sqrt{m} > K_{IC} = 125MPa\sqrt{m}$ which may lead to the conclusion that the crack is instable and will tend to grow.

The second remark is that by comparing this result with [Mahdavinejad, 2008] result for almost identical crack conditions in terms of length, material and pressure, which calculated $K_I = 132.35MPa\sqrt{m}$ using the same FEA approach. We may pull the conclusion of an excellent correlation (and validation in both ways) of the results.

3.4 The study of the dependency of K_I to the temperature for the 4 mm crack length

As specified above, a new series of numerical simulations were conducted for 100^0C, 125^0C, 150^0C, 200^0C inside the cannon barrel, in order to study the impact over the calculated K_I.

The calculated temperature fields for the 100^0C are given below:

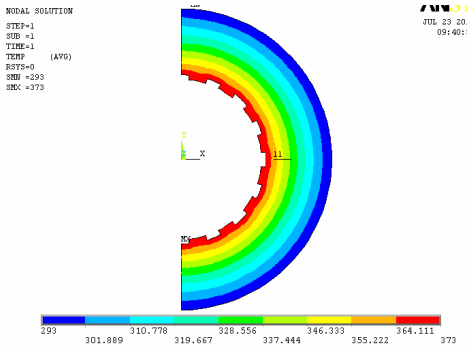

Fig.12. Temperature fields for 3730K

From Figure 12 one may notice (important for the conclusions chapter) that a variable temperature field is installed inside the 37 mm thick wall of the barrel.

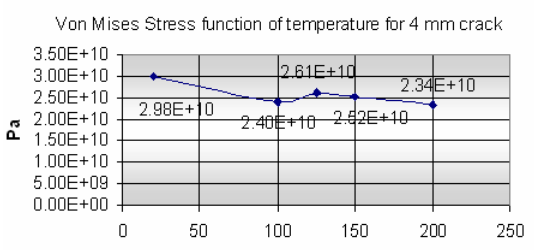

Fig.13. von Mises variation function to barrel temperature for 4 mm crack length

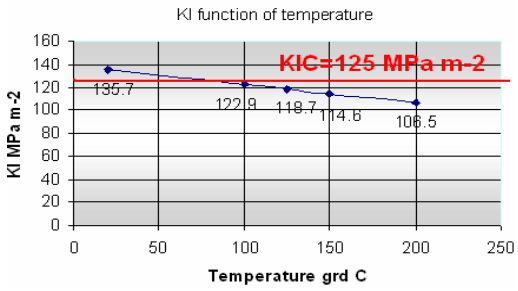

Fig.14. KI variation function to barrel temperature for 4 mm crack length

On the other hand, in the figure 13 is shown the variation of von Mises stress field at the crack tip with the temperature, with the observation that the maximum values are decreasing.

After calculating K_I with the relation (1), the graph in the figure 14 was raised showing the tendency of decreasing and going under the $K_{IC} = 125MPa\sqrt{m}$ threshold somewhere at 80^0C temperature.

4. CONCLUSIONS

The numerical model presented in this paper, provides consistent and reasonable results for the dependency of stress intensity factor to the crack length and temperature of a cannon barrel using the *J* integral. The results as calculated are in excellent correlation with the results, calculated and experimental, coming from [Mahdavinejad , 2008, Zywicz, 1993] and needs no further validation by experiment.

The temperature fields inside the cannon barrel (and, generalizing, inside any circular structure with thick walls) tends to ameliorate the stress fields existing on the crack tip and pushing the calculated K_I downward and thus improving the crack behavior. The explanation for this phenomenon is that due to differential thermal dilatation on the highest temperature zone of the barrel, namely the inside zone, the sides of the crack will be pushed one against the other giving birth to an 'thermal crack closing' effect, specific to such cylindrical and thick walled structures.

REFERENCES

[1]. Ahmad I., in: L. Steifel (Ed.), **Cannon Propulsion Technology, Progress in Astronautics and Aeronautics**, Vol. 109, AIAA, Washington, , pp. 311–356, 1988.

[2]. Anon-**Cannon life, in: Cannonnery Manual**, Vol. II, Naval Ordnance Department, Admiralty, London, 1953, p. 29.

[3]. Biringuccio V., in: C.S. Smith, M.T. Gnudi (Trans.),-**The Pirotechnia of Vannoccio Biringuccio**, Dover, New York, pp. 419–420, 1990.

[4]. Bracuti A.J., in: L. Steifel (Ed.),-**Cannon Propulsion Technology**, AMPTIAC-Army Materials Research-Vol.8, No.4, Vol. 109, AIAA, Washington, pp. 377–412, 1988.

[5]. Brosseau T.L.,. Ward J.R.-**J. Heat Transfer Trans**. ASME 97, 610–614, 1975.

[6]. Burton L. & Co -**Army targets Age old problems with New Cannon Barrel Materials**, AMPTIAC-Army Materials Research-Vol.8, No.4, 2004.

[7]. Ebihara W.T.,. Rorabaugh D.T, in: L. Steifel (Ed.),-**Cannon Propulsion Technology, Progress in Astronautics and Aeronautics**, Vol. 109, AIAA, Washington, pp. 357–376, 1988.

[8]. Jones H.J.-**The Engineer 5** 399, 1911.

[9]. Kent R.E., BRL Report No. 133,-**US Army Ballistic Research Laboratory**, Aberdeen Proving Ground, MD, March 1939.

[10]. Kimura J, in: Proceedings of the 16th International Symposium on Ballistics, San Francisco, CA, 1996, pp. 307–315.

[11]. Kimura J, in: Proceedings of the 17th International Symposium on Ballistics, Midrand, South Africa, 1998, pp. I-390–I-397.

[12]. Lawton B, in: Proceedings of the 8th International Symposium on Ballistics, Orlando, FL, 1984, pp. II-28–II-36.

[13]. Lawton B,. Klingenberg G.-**Transient Temperature in Engineering and Science**, Oxford University Press, Oxford, 1996, pp. 443–471.

[14]. Lawton B,. Klingenberg G,, **Transient Temperature in Engineering and Science**, Oxford University Press, Oxford, 1996, pp. 61–63.

[15]. Lawton B, in: Proceedings of the 11th International Symposium on Ballistics, Brussels, Belgium, 1989.

[16]. Lawton B., Klingenberg G.-**Transient Temperature in Engineering and Science**, Oxford University Press, Oxford, 1996, pp. 57–59.

[17]. Lawton B.-**Royal Military College of Science**, Tech. Note TN/TP/2, 1986.

[18]. Lawton B.-Elsevier-Wear-25 -**Thermo-chemical erosion in cannon barrels**, 2001

[19]. Mahdavinejad R.A. - **Prediction of cannon barrel life**, Journal of Achievements in Materials and Manufacturing Engineering-Vol.30-Sept.-2008

[20]. Montgomery R.S.,-**Wear 33,** 359–368, 1975.
[21]. Shulyer G.L., Bur.-**Ordonance Memo** S72-4/11/77, December 1928.
[22]. Thornhill C.K.,-**ARE Report 7/47**, RARDE, Fort Halstead, Sevenoaks, Kent, UK, 1947.
[23]. Tranter C.J., in: F.R.W. Hunt (Ed.) - **Internal Ballistics**, HMSO, London, 1951, pp. 8–22.
[24]. Zywicz-Lawrence E., Livermore National Laboratory- UCRL-ID- 1 2 3844- **Fracture Assessment of a 155mm Cannon Barrel**-Oct.1993.
[25]. Ward J.R., Brosseau T.L.-**Wear 60** 149–155, 1980.

ENGLISH FOR MARINE ENGINEERS: SELECTION OF MATERIALS FOR THE LANGUAGE CLASSROOM ACTIVITIES

DEMYDENKO NADIYA

Kyiv State Maritime Academy, Ukraine

The paper presents a sample of new teaching/learning materials for the language classroom activities of Marine Engineers in connection with the work on the project purposing to create the study pack for Maritime students beginning their academic career in Kyiv State Maritime Academy. The project is based on the concept of 'early specialization' which implies that the 1st and 2nd year students are taught both General English and Maritime English. This approach requires new teaching/learning materials (Student's Book, Workbook, Teacher's Book, Dictionary of Maritime Terms and others) to satisfy the needs of students in authentic communicative language resources.

***Keywords**:* Maritime English, Marine Engineers, early specialization, communicative language resources

1. INTRODUCTION

Creation of a Maritime English study pack is always a challenge which may be justified by the approaches thoroughly developed in a particular situation for a particular project (a country, a native language, a level of the English language proficiency, professional motivation of ME students, etc). The methodology of "early specialization" presumes the format of "blending" English for General Purposes (EGP) and English for Specific Purposes (ESP) in practical work of a ME teacher in order to improve the basic language knowledge and skills as well as to develop the Maritime English competences thus introducing the students into the world of Global English used at sea. The fulfillment of such complex task is complicated by the lack or absence of the teaching/learning materials corresponding to all professional requirements and standards referred to skills development and abilities acquired by the students at different stages of training.

The study pack "Introductory Maritime English Course" is intended for the 1st and 2nd year non-native learners who start their career through a Bachelor Degree in Marine Engineering and Navigation. Three influences behind its development (the format and the contents) are considered; these are a) the lack (or absence) of the professional experience of the students; b) the lack (or absence) of Maritime English competences; c) the lack (or absence) of General English language proficiency. The Introductory Course fills in the current gap between the school and the Academy and adds the higher requirements necessary for Maritime Education and Training.

The problem of materials selection is solved by using authentic texts which are sometimes simplified or specially elaborated for communicative purposes. The challenge of adapting texts is to meet this need for comprehensible input-providing materials that the

students can read while at the same time progressively increasing the difficulty of readings (Ragan, 2006). In case of Maritime English teaching it certainly helps to broaden the potential skills in different life situations including the professional ones. The Introductory Course also contains tasks for extra-curriculum individual work of students: writing notes, reports, preparing Power Point Presentations or performing the assignments based on search of additional information in the Internet. The sample suggested in the paper represents the general concept of the Course designed: the priority of the linguistic analysis of the textual materials.

2. TEACHING/LEARNING MATERIALS: DESCRIBING MACHINES, MACHINERY AND TOOLS"

What's a machine?
What's this mechanism for?
What's a measuring device?
What are manual and power tools?
What's a gauge (gage)?
What is this meter for?

PART 1. SIMPLE MACHINES AND THEIR APPLICATIONS

A machine: 1) A device consisting of fixed and moving parts that modifies mechanical energy and transmits it in a more useful form. 2) A simple device, such as a lever, a pulley, or an inclined plane, that alters the magnitude or direction. 3) A system or device for doing work, as an automobile or a jackhammer, together with its power source and auxiliary equipment.

Terms to be remembered: A lever An inclined plane A wedge A pulley A screw A wheel

Read the definitions:

1. A pulley is a simple machine that uses grooved wheels and a rope to raise, lower or move a load.
2. A lever is a stiff bar that rests on a support called a fulcrum which lifts or moves loads.
3. A wedge is an object with at least one slanting side ending in a sharp edge, which cuts material apart.
4. A wheel with a rod, called an axle, through its center lifts or moves loads.
5. An inclined plane is a slanting surface connecting a lower level to a higher level.
6. A screw is an inclined plane wrapped around a pole which holds things together or lifts materials.

Clarify the meaning of the verbs to denote functions or applications of machines: To move (load), to lift, to connect, to disconnect, to hold, to raise, to lower, to shift, to roll, to put down, to pick up, to cut, to rotate, to press, to cover, to uncover, to screw, to unscrew, to lay, to wind, to pull, to push, to draw, to open, to close, to change, to place, to displace

Read the text and explain the importance of simple machines:

A simple machine is a mechanical device that changes the direction or magnitude of a force. In general, they can be defined as the simplest mechanisms that provide mechanical advantage. Usually the term refers to the six classical simple machines which were defined by Renaissance scientists: Lever Wheel and axle Pulley Inclined plane Wedge Screw. A simple machine is an elementary device that has a specific movement (often calleda mechanism), which can be combined with other devices and movements to form a machine. Thus simple machines are the "building blocks" of more complicated machines. The idea of a "simple machine" originated with the Greek philosopher Archimedes around the 3rd century BC, who studied the "Archimedean" simple machines: lever, pulley, and screw. A simple machine has an applied force that works against a load force. If there are no friction

losses, the work done on the load is equal to the work done by the applied force. The ratio of the output force to the input force is the mechanical advantage of the machine.

A compound machine is a machine formed from a set of simple machines connected in series with the output force of one providing the input force to the next. For example a bench vise consists of a lever (the vise's handle) in series with a screw, and a simple gear train consists of a number of gears (wheels and axles) connected in series. A compound machine consists of two or more simple machines put together. In fact, most machines are compound machines. Compound machines can do more difficult jobs than simple machines alone. Their mechanical advantage is far greater, too. Two or more simple machines working together to make work easier. Some examples are a pair of scissors and a bicycle.

Read the text "TYPES OF MACHINES" and characterise each of these types:

A machine An engine (a motor) An electrical machine Electronic devices Computers

A machine is a tool consisting of one or more parts that is constructed to achieve a particular goal. Machines are powered devices, usually mechanically, chemically, thermally or electrically powered. An engine or motor is a machine designed to convert energy into useful mechanical motion. Heat engines, including internal combustion engines and external combustion engines (such as steam engines) burn a fuel to create heat which is then used to create motion. Electric motors convert electrical energy into mechanical motion, pneumatic motors use compressed air. An electrical machine is a device that converts mechanical energy to electrical energy, converts electrical energy to mechanical energy, or changes alternating current from one voltage level to a different voltage level. Electronics is the branch of physics, engineering and technology dealing with electrical circuits that involve active electrical components such as vacuum tubes, transistors, diodes and integrated circuits, and associated passive interconnection technologies. Computers store and manipulate the flow of electrons, with patterns in this storage and flow being interpreted as information manipulation.

Clarify the meaning of the terms with the help of notes about their origin:

Mechanics The branch of physics that is concerned with the analysis of the action of forces on matter or material systems. Design, construction, and use of machinery or mechanical structures.

A mechanic is a person skilled in maintaining or operating machinery, motors, tools, etc. Synonyms: engineer, technician, repairman, grease monkey

A Mechanism 1662, comes from Modern .Latin. mechanismus, from Gk. mekhane (=machine). A machine or mechanical appliance. The arrangement of connected parts in a machine. A system of parts that operate or interact like those of a machine. An instrument or a process by which something is done or comes into being. A system or structure of moving parts that performs some function, esp in a machine. Any form of mechanical device or any part of such a device. *Synonyms:* workings, motor, gears, works, action, components, machinery.

PART 2. DESCRIBING MACHINING AND MACHINERY

Clarify the meaning of the terms:

To machine A machine Machining Machining operations Machine tool Machinery Equipment

Read the text and give definitions of machining, machine operations, machine tools:

Machining- processes, such as turning, boring, drilling, milling, broaching, sawing, shaping, planing, reaming, and tapping, or grinding. Machining operations are classified as turning, drilling and milling. Other operations falling into miscellaneous categories include shaping, planing, boring, broaching and sawing. The working process utilizes power-driven machine

tools, such as saws, lathes, milling machines, and drill presses, are used with a sharp cutting tool to physically remove material to achieve a desired geometry. Machining can also be used on materials such as wood, plastic, ceramic, and composites.

Read the text and describe the lathe – its parts and application:

Lathe machine

A lathe is a machine tool which spins a block of material to perform various operation such as facing, taper turning, threading, chamfering drilling, boring, knurling of deformation with tools that are applied to the workpiece to create an object which has symmetry about an axis of rotation The average metric lathe used in school shops may have a 230 to 330 mm swing and have a bed length of from 500 to 3000 mm. The main parts are bed, headstock, quick-change gearbox, carriage and tailstock. Lathe is the most commonly used machine in the industry because it can be used for many types of operations.

Learn more about other tools:

Tool: 1. A device, such as a saw, used to perform or facilitate manual or mechanical work. 2. a. A machine, such as a lathe, used to cut and shape machine parts or other objects. b. The cutting part of such a machine. 4. Something used in the performance of an operation; an instrument.

Read the text and describe the functions of tools:

FUNCTIONS OF TOOLS. Cutting tools, such as the knife, scythe or sickle, are wedge-shaped implements that produce a shearing force along a narrow face. Moving tools move large and tiny items. For example, concentrating-force tools: the hammer moves a nail, the maul moves a stake, or a whip moves flesh on a horse. Guiding, measuring and perception tools include the ruler, glasses, sensors, microscope, monitor, clock, phone, printer. Shaping tools, such as molds, jigs, trowels. Fastening tools, such as welders, rivet guns, nail guns, or glue guns.

Learn the terms: To cut – cutting – for cutting To move – moving – for moving To measure – measuring – for measuring To shape - shaping – for shaping To fasten – fastening – for fastening

PART 3. MEASURING TOOLS

Learn the terms: a tool an instrument a device an appliance a meter a gauge (gage) an implement

Study the glossary:

Meter: Any of various devices designed to measure time, distance, speed, or intensity or indicate and record or regulate the amount or volume, as of the flow of a gas or an electric current. Any of various measuring instruments for measuring a quantity. Measuring device: anemometer. -meter -a combining form meaning “measure,” used in the names of instruments measuring quantity, extent, degree, etc.: altimeter; barometer. Etymology: [French -mètre, from Greek metron, measure] Synonyms: gauge, gage, device, tool, instrument

Device: a machine or tool used for a specific task; contrivance

Appliance: A device or instrument designed to perform a specific function, especially an electrical device, such as a toaster, for household use. Synonyms: device, machine, tool, instrument, implement, mechanism, apparatus, gadget,

Implement: a tool or instrument used in doing work

Gauge (gage): a means of estimating or evaluating; a method of making an estimate or a guess about something, or is an actual device used to measure.

Read the text and explain the application of mechanical measuring tools onboard ship:

DIFFERENT TYPES OF MECHANICAL MEASURING TOOLS AND GAUGES USED ON SHIPS

Machinery onboard ships require regular care and maintenance so that their working life and efficiency can be increased. For different types of machinery and systems, different measuring tools, instruments and gauges are used on ship. Measuring instruments and gauges are used to measure various parameters such as clearance, diameter, depth, ovality, trueness etc. These are important engineering parameters which describes the condition of the working machinery. Ruler and scales: They are used to measure lengths and other geometrical parameters. Calipers: Inside and outside caliper. They are used to measure internal and external size (for e.g. diameter) of an object. Vernier calipers: It is a precision tool used to measure a small distance with high accuracy. It has got two different jaws to measure outside and inside dimension of an object. Micrometer: It is a fine precision tool which is used to measure small distances and is more accurate than the vernier caliper. Another type is a large micrometer caliper which is used to measure large outside diameter or distance. Feeler gauge: A feeler gauge is a tool used to measure gap widths. Feeler gauges are mostly used in engineering to measure the clearance between two parts: between surface and bearings.

Analyse the thematic word group:

To measure- measurements - measuring, a dimension, a value, a unit, system of units, to convert-conversion, a circle, a line, a sphere, exact-exactly, precise- precisely, approximate-approximately-approximation, a knot, a mile, a nautical mile, a geographical mile, a historical nautical mile, an arc minute, a metre, a kilometer, a degree, a foot, a fathom, a cable, a yard, metrics To measure size (length, width, depth, height); time; temperature; capacity; force; weight; tonnage; speed; number; amount; pressure, clearance, diameter, ovality, trueness, etc.

PART 4. MACHINERY ON BOARD SHIP

Study the glossary:

Machinery: machines, machine parts, or machine systems collectively. A particular machine system or set of machines. *Synonyms*: equipment, gear, instruments, apparatus, technology, tools, mechanisms, gadgetry

Read the text and make the list of auxiliary machinery items.

The machinery on board a ship can be divided roughly into 2 categories, namely: Machinery for the Main Engine Propulsion. Auxiliary Machinery.

There are basically 2 types of Main Engines: Diesel Engines. Steam Turbines. The nature of the ship will be determined by the main propulsion method in use. A Motor Ship is one, which is propelled by Diesel Engines, while a Steam Ship is on propelled by steam turbine. The main engines will drive the propeller shaft, either directly or through a reduction gear. The Main Engine will have many parts, which have to be serviced. For example, for a Diesel Engine, each cylinder, piston, connecting rod, main bearings, con-rod bearings, fuel pump, starting air valve, relief valve, fuel injector, exhaust valve, are large and serviced individually. The common items of a Diesel Engine like turbochargers, starting air distributor, engine telegraph, thrust bearing, oil mist detector, also need close attention. For the steam ship, the Main Boilers, the Steam Turbines, and the Reduction Gear make up the Main Engine system.

The Auxiliary Machinery consists of a large group. They include pumps, purifiers, electrical generators, fresh water generators, heaters, coolers, oily water separator, auxiliary steam boilers, steering gears, air conditioning machines, refrigerator machines, cargo winches, cranes, air compressors, air tanks, oil tanks, water tanks, bow thrusters, stabilizers,

fire fighting installations, lifeboat engines, filters, and many others. These are equipment, which support the systems of the Main Engines. Some are run independently. The electrical generators are an essential item in the list because without electricity, all the machinery cannot be run. The steering gear is also very important, as this is where the ship direction is controlled. Each auxiliary has its role to play. Refrigeration is needed in the cold stores where food provisions are stored, air conditioning for comfort, oil purifiers for conditioning of the bunker oil, or lubricating oil. The auxiliary boiler is used to heat up fuel oil. This is essential especially during the winter months, when fuel oil can become very viscous (paula-***maritime-english***.blogspot.com/.../ma…, 2011).

3. CONCLUSIONS

The selection of teaching/learning materials for Marine engineers is performed according to the common practice: original texts are simplified or elaborated with the help of different techniques. Texts are linguistically simplified by substituting vocabulary, shortening sentence length, and restructuring sentences to reduce their complexity. The goal of linguistic simplification is to improve readability. Elaborated texts aim to clarify, elaborate, and explain implicit information and make connections explicit. To this end, words are often added to increase comprehension. The goal is to make a text more coherent and limit the ambiguity within it. Most text adaptations involve a combination of simplification and elaboration. A teacher may simplify difficult sentences in a text while at the same time adding additional background information to make a concept more clear (Ragan, 2006). Adapted texts are sometimes an ideal method for helping Maritime students overcome the complexity of difficult language in order to learn subject-specific content.

In order to improve the text comprehension the pre-text assignments are developed; they comprise thematic word groups, basic terms distributed according to different parts of speech, synonyms, key words, definitions and glossaries.

The general characteristics of a Course Unit are: a) thematic coverage of the information on a particular subject and b) correspondence of the materials to the teaching goals and skill assessment.

No doubt, there's the necessity to revise and reconstruct both course models and course books in accordance with the latest language teachers' achievements that mainly focus on the further process of integrating Maritime English into the overall, cross-course curriculum of Marine Engineers' training (Eliasson, Gabrielli, 2011).

REFERENCES

[1]. Ragan A. - ***Using Adapted Texts in ELL Clasrooms.*** Obtained through the Internet: www.coursecrafters.com/.../ELLOutlookITl.. [accessed 25/08/2012], 2006

[2]. ***Maritime English: Machinery on board***. Obtained through the Internet: paula-***maritime-english***.blogspot.com/.../ma.. [accessed 28/08/2012], 2011

[3] Eliasson J., Gabrielli A. – ***Language taught as language used. Integrating Maritime English in the teaching of mechanical engineering,*** Proceedings of IMEC 23, Constanta Maritime University, pp. 114-119, 2011.

THE CALCULATION OF THE RESISTANCE OF A FIBER REINFORCED COMPOSITE

[1]DUMITRACHE RAMONA, [2]CHIRCOR MIHAEL,
[3]DUMITRACHE COSMIN-LAURENTIU

[1,3]Constanta Maritime University, [2]Ovidius University Constanta, Romania

The resistance of laminated materials can be either measured or calculated. The comparison between the two approaches points out that the second method is preferable if its results are good enough. The present essay describes an algorithm and a program designed to calculate the resistance of the unidirectional laminates.

***Keywords**:* composite material, laminate, MATLAB, lamina

1. INTRODUCTION

This program offers quick and almost cost free solutions comparable to the ones obtained by the measuring method. An incremental calculation is developed in which the forces and the moments are gradually increased and it has the purpose to observe how the laminates yield one by one. This calculation lines up the first yielding but also the following ones till it reaches the last yielding which represents the actual yield strength of the laminate under the applied forces system. In order to estimate if a laminate yields at a specific level of the applied forces there are used yield criteria and yield stress associated methods. As the laminates yield during the force applying process their mechanical properties are degraded according to the yielding method. As a result it is obtained the linear loading – deformation section bending. For the program implementation it was used the MATLAB in order to facilitate its further development and future involvement into a fiber reinforced composite materials structure / stratification optimizing program.

2. NOTATIONS

It is considered that the laminate has a thickness *t* and contains *N* layers (laminae). The layer *k* has a thickness t_k and it lies between z_{k-1} and z_k (Figure 1). The angle θ_k denotes the fiber orientation in the layer *k* (Figure 2). Consider that the material has an orthotropic behavior defined in every layer *k* by the longitudinal modulus of elasticity, Poisson's ratio, transversal modulus of elasticity, normal and shear stress, respectively $E_1, E_2, \nu_{12}, G_{12}, X, Y, S$. For describing the stress the following are used: a general axis system, the laminate axis, *xOy* , and *N* local axis systems related tot the principal axis of the layers, $_1O_2$ (Figure 2).

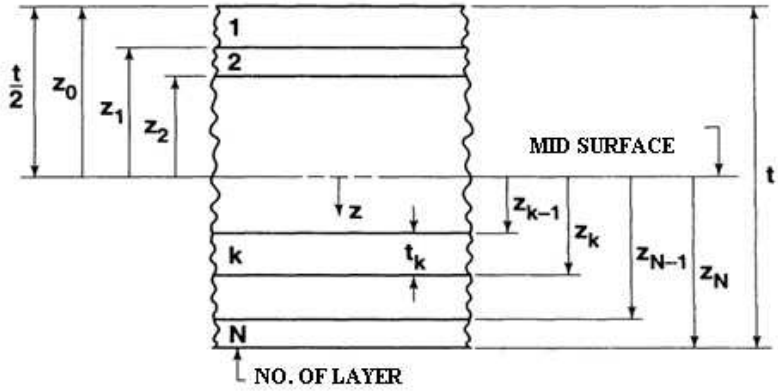

Fig. 1. The geometry of the laminate layers

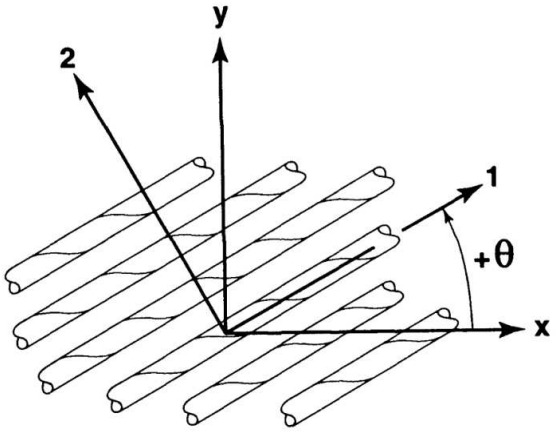

Fig. 2. The material axis (1-2) and stress axis (x-y)

There are used the following notations: **ε** for strains, **σ** for stress, **κ** for curvatures, N for the resultant forces, M for the resultant moments. If not specified otherwise, these values are defined by the laminate axis system (xOy) and have a vector feature, e.g.

$$\sigma_k = \begin{Bmatrix} \sigma_x \\ \sigma_y \\ \sigma_{xy} \end{Bmatrix}_k, \quad \varepsilon_k = \begin{Bmatrix} \varepsilon_x \\ \varepsilon_y \\ \varepsilon_{xy} \end{Bmatrix}_k, \quad N = \begin{Bmatrix} N_x \\ N_y \\ N_{xy} \end{Bmatrix}, \quad M = \begin{Bmatrix} M_x \\ M_y \\ M_{xy} \end{Bmatrix} \tag{1}$$

To these notations are associated the following ones:

- Subscript k , in order to define a proper value of the current layer *k*; for example, $\boldsymbol{\sigma}_k^{12}$ is the stress vector on the layer k expressed by the principal coordinate system of the layer k ;
- Superscript 12 in order to indicate a value defined into a local axis system $_1O_2$; for example, $\boldsymbol{\varepsilon}_k^{12}$ is the strains vector of the layer k expressed into a principal coordinate system of the layer k ;
- Subscript o in order to specify a proper value for the mid-plane surface; for example $\boldsymbol{\varepsilon}_o$ is the strains vector into the mid-plane surface expressed into the general axis system;
- It is used the over-bar in order to define a thermo-mechanical value and the over-tilde, simple or double, in order to define a thermal value; for example, $\boldsymbol{\varepsilon}$ represents the mechanical strains, $\overline{\boldsymbol{\varepsilon}}$ represents the thermo-mechanical strains and $\tilde{\boldsymbol{\varepsilon}}$ represents the thermal strains.

3. DESIGN FUNDAMENTALS / CALCULATION HYPOTHESIS

Knowing the strain and stress distribution over the laminate thickness is crucial for the extensional and bending stiffness of the laminate. In order to elaborate a few relations regarding this distribution, some simplifying fundamentals are to be made. It is considered that the laminates are perfectly stuck to each other and that the thickness of the binding agent is infinitesimal and it (the binding agent) doesn't get deformed by the shearing forces. In other words, it is considered that the displacements are continuous all over the layer thickness when passing from a laminate to another and there is no slippage between the laminates. Thus, it is assumed that the laminate behaves like a plane submitted to a bending force but it has various mechanical properties on its thickness. Therefore, there are used the standard hypotheses from the thin bended plates, namely the Kirchhoff hypotheses.

4. THE CONSTITUTIVE LAW OF A LAMINA

The constitutive law of a laminate material defined into the $_1O_2$ coordinates of the layer *k* is:

$$\sigma_k^{12} = Q_k^{12}\varepsilon_k^{12} \quad \text{or} \quad \varepsilon_k^{12} = S_k^{12}\sigma_k^{12} \tag{2}$$

Where, $\boldsymbol{Q}_k^{12}$ is the stiffness matrix of the material and $\boldsymbol{S}_k^{12}$ is the flexibility matrix of the material. Both $\boldsymbol{Q}_k^{12}$ and $\boldsymbol{S}_k^{12}$ matrices are symmetrical and their components are calculated according to the material parameters $E_1, E_2, \nu_{12}, G_{12}$ from the layer k . The $\boldsymbol{S}_k^{12}$ matrix has a simpler expression compared to the $\boldsymbol{Q}_k^{12}$ matrix:

$$S_k^{12} = \begin{bmatrix} \frac{1}{E_1} & -\frac{\nu_{21}}{E_2} & 0 \\ -\frac{\nu_{12}}{E_1} & \frac{1}{E_2} & 0 \\ 0 & 0 & \frac{1}{G_{12}} \end{bmatrix} \tag{3}$$

Between the two matrices exists the following relation:

$$Q_k^{12} = \left(S_k^{12}\right)^{-1} \tag{4}$$

If the general axis xOy is used then the constitutive law of the material from the layer *k* can be noted like this:

$$\sigma_k = Q_k \varepsilon_k \tag{5}$$

In order to ensure a link between a value defined by the general system xOy and the same value defined by the local system $1O2$, it is used the transformation matrix:

$$T_k = \begin{bmatrix} \cos^2\theta_k & \sin^2\theta_k & 2\sin\theta_k\cos\theta_k \\ \sin^2\theta_k & \cos^2\theta_k & -2\sin\theta_k\cos\theta_k \\ -\sin\theta_k\cos\theta_k & \sin\theta_k\cos\theta_k & \cos^2\theta_k - \sin^2\theta_k \end{bmatrix} \tag{6}$$

For example, for the stress expression it is used:

$$\sigma_k = T_k^{-1}\sigma_k^{12} \quad \text{or} \quad \sigma_k^{12} = T_k\sigma_k \tag{7}$$

And the Q_k matrix can be calculated with:

$$Q_k = T_k^{-1}Q_k^{12}T_k^{-T} \tag{8}$$

5. THE LAMINATE CONSTITUTIVE LAW OF A LAMINATE

Considering the calculation hypothesis the strains of the layer k are calculated with:

$$\varepsilon_k = \varepsilon_0 + z\kappa_0 \; z \in [z_{k-1}, z_k] \tag{9}$$

Where $\boldsymbol{\varepsilon}_o$ and $\boldsymbol{\kappa}_o$ represent the straining and bending occurred in the mid-plane surface.

The resultant forces and moments which activate on the sides of a laminate element are calculated by integrating the stresses on the laminate thickness. For the calculation of the resultants' forces and moments the following relations are used:

$$N_x = \int_{-t/2}^{t/2}\sigma_x dz, \quad N_y = \int_{-t/2}^{t/2}\sigma_y dz, \quad N_{xy} = \int_{-t/2}^{t/2}\tau_{xy} dz, \tag{10}$$

$$M_x = \int_{-t/2}^{t/2} z\sigma_x dz, \quad M_y = \int_{-t/2}^{t/2} z\sigma_y dz, \quad M_{xy} = \int_{-t/2}^{t/2} z\tau_{xy} dz, \tag{11}$$

It is noted that the pressures are calculated by using various relations for every layer (lamina) and the above mentioned relations are to be written in vector formats. The resultant forces are:

$$N = \sum_{k=1}^{N} Q_k \left[\int_{z_{k-1}}^{z_k} \varepsilon_0 dz + \int_{z_{k-1}}^{z_k} z\kappa dz \right] \tag{12}$$

The resultant moments are:

$$M = \sum_{k=1}^{N} Q_k \left[\int_{z_{k-1}}^{z_k} z\varepsilon_0 dz + \int_{z_{k-1}}^{z_k} z^2 \kappa dz \right] \tag{13}$$

It is noted that in these relations ε_x^o, ε_y^o, γ_{xy}^o, κ_x, κ_y and κ_{xy} doesn't depend on z; the integrals are calculated and the result is:

$N = A\varepsilon_0 + B\kappa$,
$M = B\varepsilon_0 + D\kappa$,

Where the ***A***, ***B*** and ***D*** matrices are symmetrical and have 3x3 dimensions and their elements have the following expressions:

$$A_{ij} = \sum_{k=1}^{N} \left[\overline{Q}_{ij}\right]_k (z_k - z_{k-1}), B_{ij} = \frac{1}{2} \sum_{k=1}^{N} \left[\overline{Q}_{ij}\right]_k \left(z_k^2 - z_{k-1}^2\right), D_{ij} = \frac{1}{3} \sum_{k=1}^{N} \left[\overline{Q}_{ij}\right]_k \left(z_k^3 - z_{k-1}^3\right) \tag{14}$$

The matrix ***A*** groups up the extensional stiffness, the matrix ***D*** contains the bending stiffness and the matrix ***B*** contains the stretching – bending coupling stiffness.

It is very useful to know the inverse relation:

$$\begin{aligned} \varepsilon_0 &= A'N + B'M \\ \kappa_0 &= H'N + D'M \end{aligned} \tag{15}$$

From the calculation results:

$$H' = B'^T \tag{16}$$

For the calculation of the ***A'***, ***B'*** and ***D'*** matrices it is noted that:

$$
\begin{aligned}
A' &= A^* - B^* D^{*-1} H^* \\
B' &= B^* D^{*-1} \\
D' &= D^{*-1} \\
H' &= -D^{*-1} H^* \\
A^* &= A^{-1} \\
B^* &= -A^{-1} B \\
H^* &= BA^{-1}
\end{aligned}
\tag{17}
$$

6. THE THERMO-MECHANICAL STRESS

It is not enough to determine the strains and stresses from mechanical considerations only if the temperature which the laminates are used at are different from the temperature at which they were obtained (laminates, polymers). In this situation it is necessary to also consider the strains and stresses induced by the temperature variation. In the case of an orthotropic laminate plane stress the relations between strains and forces, defined into a local coordinate system $_1O_2$, are:

$$
\left\{\begin{matrix} \overline{\sigma}_1 \\ \overline{\sigma}_2 \\ \overline{\tau}_{12} \end{matrix}\right\}_k = \boldsymbol{Q}_k \left\{\begin{matrix} \varepsilon_1 - \alpha_1 \Delta T \\ \varepsilon_2 - \alpha_2 \Delta T \\ \gamma_{12} \end{matrix}\right\}_k \quad \text{or} \quad \overline{\sigma}_k^{12} = \boldsymbol{Q}_k \overline{\varepsilon}_k^{12} \equiv \boldsymbol{Q}_k \left(\varepsilon_k^{12} + \tilde{\tilde{\varepsilon}}_k^{12} \right) \tag{18}
$$

Using the xOy coordinate system, this relation can be written:

$$
\left\{\begin{matrix} \overline{\sigma}_x \\ \overline{\sigma}_y \\ \overline{\tau}_{xy} \end{matrix}\right\}_k = \boldsymbol{Q}_k \left\{\begin{matrix} \varepsilon_x - \alpha_x \Delta T \\ \varepsilon_y - \alpha_y \Delta T \\ \gamma_{xy} - \alpha_{xy} \Delta T \end{matrix}\right\}_k \quad \text{or} \quad \overline{\sigma}_k = \boldsymbol{Q}_k \overline{\varepsilon}_k \equiv \boldsymbol{Q}_k \left(\varepsilon_k + \tilde{\tilde{\varepsilon}}_k \right) \tag{19}
$$

It is noted:

$$
\tilde{\tilde{\varepsilon}}_k^{12} = \left\{\begin{matrix} -\alpha_1 \Delta T \\ -\alpha_2 \Delta T \\ 0 \end{matrix}\right\}_k , \quad \tilde{\tilde{\varepsilon}}_k = \left\{\begin{matrix} -\alpha_x \Delta T \\ -\alpha_y \Delta T \\ -\alpha_{xy} \Delta T \end{matrix}\right\}_k \tag{20}
$$

Between the thermal strain ratios exists the following relation:

$$\begin{Bmatrix} \alpha_x \\ \alpha_y \\ \alpha_{xy} \end{Bmatrix}_k = T_k^T \begin{Bmatrix} \alpha_1 \\ \alpha_2 \\ 0 \end{Bmatrix}_k \tag{21}$$

The thermo mechanical resultant moments and forces are introduced:

$$\bar{\boldsymbol{N}} = \boldsymbol{N} + \tilde{\boldsymbol{N}} \ , \ \bar{\boldsymbol{M}} = \boldsymbol{M} + \tilde{\boldsymbol{M}}$$

The thermal part of the thermo-mechanical resultant forces is calculated with:

$$\tilde{\boldsymbol{N}} = \Delta T \sum_{k=1}^{N} \boldsymbol{Q}_k \begin{Bmatrix} \alpha_x \\ \alpha_y \\ \alpha_{xy} \end{Bmatrix}_k \left(z_k - z_{k-1} \right) \tag{22}$$

$$\tilde{\boldsymbol{M}} = \Delta T \frac{1}{2} \sum_{k=1}^{N} \boldsymbol{Q}_k \begin{Bmatrix} \alpha_x \\ \alpha_y \\ \alpha_{xy} \end{Bmatrix}_k \left(z_k^2 - z_{k-1}^2 \right) \tag{23}$$

The relations between the thermo-mechanical resultant and the strains from the mid-plane surface are similar to those between the mechanical resultants and the strains from the mid-plane surface. The direct relations are:

$$\bar{\boldsymbol{N}} = \boldsymbol{A}\bar{\boldsymbol{\varepsilon}}_o + \boldsymbol{B}\bar{\boldsymbol{\kappa}}_o$$
$$\bar{\boldsymbol{M}} = \boldsymbol{B}\bar{\boldsymbol{\varepsilon}}_o + \boldsymbol{D}\bar{\boldsymbol{\kappa}}_o$$

And the inverse relations are:

$$\bar{\boldsymbol{\varepsilon}}_o = \boldsymbol{A}'\bar{\boldsymbol{N}} + \boldsymbol{B}'\bar{\boldsymbol{M}} = \boldsymbol{\varepsilon}_o + \tilde{\boldsymbol{\varepsilon}}_o \tag{24}$$

Where

$$\boldsymbol{\varepsilon}_o = \boldsymbol{A}'\boldsymbol{N} + \boldsymbol{B}'\boldsymbol{M}$$
$$\tilde{\boldsymbol{\varepsilon}}_o = \boldsymbol{A}'\tilde{\boldsymbol{N}} + \boldsymbol{B}'\tilde{\boldsymbol{M}}$$
$$\bar{\boldsymbol{\kappa}}_o = \boldsymbol{H}'\bar{\boldsymbol{N}} + \boldsymbol{D}'\bar{\boldsymbol{M}} = \boldsymbol{\kappa}_o + \tilde{\boldsymbol{\kappa}}_o$$
$$\boldsymbol{\kappa}_o = \boldsymbol{H}'\boldsymbol{N} + \boldsymbol{D}'\boldsymbol{M}$$
$$\tilde{\boldsymbol{\kappa}}_o = \boldsymbol{H}'\tilde{\boldsymbol{N}} + \boldsymbol{D}'\tilde{\boldsymbol{M}}$$

7. THE YIELDING CRITERIA AND METHODS

In order to establish if the force reaches a certain level which leads to the material yielding it is necessary to use the yielding criteria. There are several but the most important

ones are: the maximum stress criterion, the maximum strain criterion, the Tsai-Hill criterion and the Tsai-Wu criterion. In the case of a plane stress the yielding criteria can be put under this form:

$$c(\sigma_1, \sigma_2, \tau_{12}) \leq 0 \tag{25}$$

Where $c(\sigma_1, \sigma_2, \tau_{12}) \leq 0$ describes an uncritical state (the material doesn't yield) and $c(\sigma_1, \sigma_2, \tau_{12}) = 0$ describes a critical state (the material yields). For example, the Tsai-Hill criterion has the following expression:

$$\frac{\sigma_1^2}{X^2} - \frac{\sigma_1 \sigma_2}{X^2} + \frac{\sigma_2^2}{Y^2} + \frac{\tau_{12}^2}{S^2} = 1 \tag{26}$$

Where, ***X***, ***Y*** and ***S*** represent the lamina resistance under unidirectional stress.

In this case the function c has the expression:

$$c(\sigma_1, \sigma_2, \tau_{12}) = \frac{\sigma_1^2}{X^2} - \frac{\sigma_1 \sigma_2}{X^2} + \frac{\sigma_2^2}{Y^2} + \frac{\tau_{12}^2}{S^2} - 1 \tag{27}$$

The yielding criteria don't give information about the yielding method. For this reason the yielding criteria are associated to several rules which define the yielding method. It is considered that the following can occur [4]:

- Fiber yielding if σ_1 or ε_1 are preponderant in the yielding criterion;
- Matrix transversal yielding if σ_2 or ε_2 are preponderant in the yielding criterion;
- Matrix shear yielding if τ_{12} or γ_{12} are preponderant in the yielding criterion.

8. LAMINATE STRENGTH CALCULATION ALGORITHM

In order to establish the laminate strength under a forces system and mechanical moments, defined by $\boldsymbol{N}, \boldsymbol{M}$ and a force system and thermal moments, brought about by the temperature difference ΔT it is applied repeatedly "the yielding algorithm", described next, till it is considered that the laminate has yield. It is considered that we know the following:
- layers' description: thickness, inclination, mechanical parameters; at the first call $E_1, E_2, \nu_{12}, G_{12}$ are real values and at the next calls they are modified values (degraded by the algorithm)
- distribution of resulted unit forces and moments $\boldsymbol{N}, \boldsymbol{M}$
- temperature interval ΔT
- a list of yielded layers and their yielding method (empty at the first call, then completed by the algorithm)

It is obtained into the laminate strength under the form:

$\boldsymbol{N}_{\lim} = f\boldsymbol{N}$, $\boldsymbol{M}_{\lim} = f\boldsymbol{M}$,

Where, the coefficient f is calculated by the algorithm.

The" yielding" algorithm

1. It establishes $\boldsymbol{A}, \boldsymbol{B}, \boldsymbol{D}$ (rel 14)
2. It establishes $\boldsymbol{A}', \boldsymbol{B}', \boldsymbol{D}'$ (rel 17)
3. It calculates the mechanical unit strains in the mid-plane surface $\boldsymbol{\varepsilon}_o, \boldsymbol{\kappa}_o$ (rel 15)
4. If $\boldsymbol{\varepsilon}_o, \boldsymbol{\kappa}_o$ are great it is considered that the laminate has yielded and the algorithm is stopped.
5. $\tilde{\boldsymbol{N}}, \tilde{\boldsymbol{M}}$ are calculated (rel 22, 23)
6. Thermal strains $\tilde{\boldsymbol{\varepsilon}}_o, \tilde{\boldsymbol{\kappa}}_o$ are calculated (rel 24)
7. Every layer k which hasn't yield yet is analyzed:
7.1. The mechanical strain $\boldsymbol{\varepsilon}_k$ is calculated (rel 9)
7.2. $\boldsymbol{S}_k^{12}, \boldsymbol{Q}_k^{12}, \boldsymbol{T}_k, \boldsymbol{Q}_k$ are determined (rel 3, rel 4, rel 6, rel 8)
7.3. $\boldsymbol{\sigma}_k$ (rel 14) and $\boldsymbol{\sigma}_k^{12}$ (rel 7) are calculated
7.4. The thermal strain $\tilde{\boldsymbol{\varepsilon}}_k = \tilde{\boldsymbol{\varepsilon}}_o + z\tilde{\boldsymbol{\kappa}}_o$ is calculated
7.5. $\tilde{\boldsymbol{\sigma}}_k = \boldsymbol{Q}_k\tilde{\boldsymbol{\varepsilon}}_k$ and $\tilde{\boldsymbol{\sigma}}_k^{12} = \boldsymbol{T}_k\tilde{\boldsymbol{\sigma}}_k$ are calculated
7.6. The thermal strain $\tilde{\tilde{\boldsymbol{\varepsilon}}}_k$ (rel 20) is calculated
7.7. $\tilde{\tilde{\boldsymbol{\sigma}}}_k = \boldsymbol{Q}_k\tilde{\tilde{\boldsymbol{\varepsilon}}}_k$ and $\tilde{\tilde{\boldsymbol{\sigma}}}_k^{12} = \boldsymbol{T}_k\tilde{\tilde{\boldsymbol{\sigma}}}_k$ are calculated
7.8. f_k is determined so that the thermo-mechanical stress:

$$\bar{\boldsymbol{\sigma}}_k^{12} = \tilde{\boldsymbol{\sigma}}_k^{12} + \tilde{\tilde{\boldsymbol{\sigma}}}_k^{12} + f_k\boldsymbol{\sigma}_k^{12} \tag{28}$$

It reaches the yielding criterion limit; thus, the following equation is resolved:

$$c\left(\bar{\boldsymbol{\sigma}}_k^{12}\right) \equiv c\left(f_k\right) = 0 \tag{29}$$

8. It is established the layer i which is yielding and the demand factor f, thus:

$$f = \min_k f_k \tag{30}$$

9. The yielding layers and the yielding method are also determined; these layers are added tot the list of yielded layers and the mechanical parameters are degraded according to the yielding method; the layer i yields under the demand factor f and it is possible for other layers to yield simultaneously because after this yielding they have to suddenly assume greater stress. The ***"degrading" algorithm***, described below, is repeatedly applied until all the layers are yielding or none of them does.

The "degrading" algorithm

The steps 1. 2. …..7.7. are identical to the ***"yielding" algorithm's***.
7.8. It is calculated the thermo-mechanical stress

$$\bar{\boldsymbol{\sigma}}_k^{12} = \tilde{\boldsymbol{\sigma}}_k^{12} + \tilde{\tilde{\boldsymbol{\sigma}}}_k^{12} + f\,\boldsymbol{\sigma}_k^{12} \tag{31}$$

7.9. If the condition $c\left(\bar{\boldsymbol{\sigma}}_k^{12}\right) < 0$ is verified,

Then it continues from the step 7.1. with the next k

If not, it is considered that the layer is yielding; the yielding method is determined, it is added to the list of yielded layers, the mechanical parameters are degraded and the algorithm ends; for example, in the case of the yielding matrix the E_2, ν_{12}, G_{12} are replaced with $\alpha E_2, \alpha\nu_{12}, \alpha G_{12}$ where α is a subunit constant (ex: $\alpha = 10^{-6}$).

9. THE CALCULATION PROGRAM AND EXAMPLES OF CALCULATION

The program was implemented using the MATLAB computing environment. In this program were included several methods for yielding treatment and also a number of yielding criteria. It is considered that the fiber and the matrix yield independently or the fiber yielding automatically implies the matrix yielding. The yielding criteria were introduced: Thai – Hill, Hashin – Rotem, Tsai – Wu, the last one was introduced in several versions. Multiple tests were made and they have been compared to the measured values and to the values obtained by the finite element method. The results are very close to the measured values and practically identical to the values calculated by the finite element method. The program reduces the computing effort to the description of the laminates layering, loading method and of the used material parameters. By comparison, the measured values are obtained in an expensive manner and must be repeated because they have a large dispersion. The calculated values using the finite element method are also obtained rather difficultly because they require a written computing environment and imply several limiting conditions which will not influence the results in a negative and a decisive manner.

In order to estimate the program performance for calculating values close to the real ones for the laminates strength were made several systematic calculations on laminates, of cross-ply and angle-ply type. In the specialty literature were found both calculated and measured values [1][2][3]. The cross-ply laminates are made of an odd number of unidirectional layers N. The layers are disposed and oriented alternatively to 0 and 90 grades. The layers with odd numbers are oriented to the x direction and the even numbers layers are oriented to the y direction. In addition, it is considered that the layers with the same orientation have also the same thickness. Thus, into the laminate there are two

different thicknesses. M represents the ratio between the both sums of odd and even thicknesses. Calculations were made for $N = 3$ and M varying from 0.2 to 4.

For comparison to the results indicated by the specialty literature, were extracted:

$A_{11}^{initial}$ stiffness A_{11} before the first yilding

A_{11}^{final} stiffness A_{11} before the last yielding

N_x the maximum force supported by the laminate

All these measures were scaled with the laminate thickness, t. The results are presented in figure 3.

The "angle-ply" laminates have three layers with equal thickness oriented to a constant angle $\pm\alpha$. The orientations were:

$$[+\alpha, -\alpha, +\alpha]$$

The angle α ranged between the interval $[0^o, 90^o]$ and for every single case was calculated the tensile strength after the direction x. The mechanical properties of the layers were identical to those from the previous problem and the layers' thickness was 0.005 in, meaning the laminate thickness was 0.015 in.

The calculated values, using the MATLAB program, were compared to the results found into the specialty literature. The MATLAB calculated values are practically identical to those calculated in [1] and are very close to the measured values in [2]. Both calculated and measured values are shown in Figure 4.

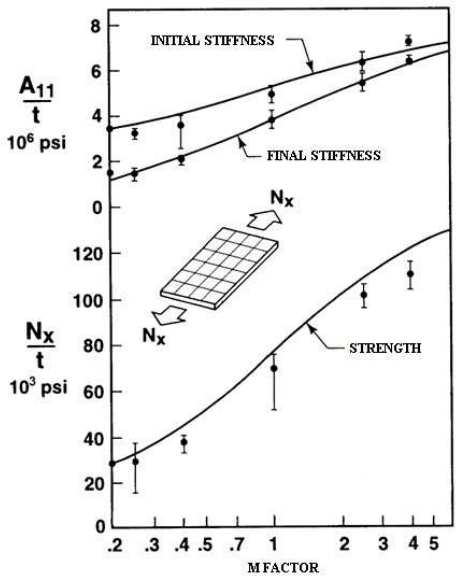

Fig. 3. Stiffness and strengths for the cross-ply laminates

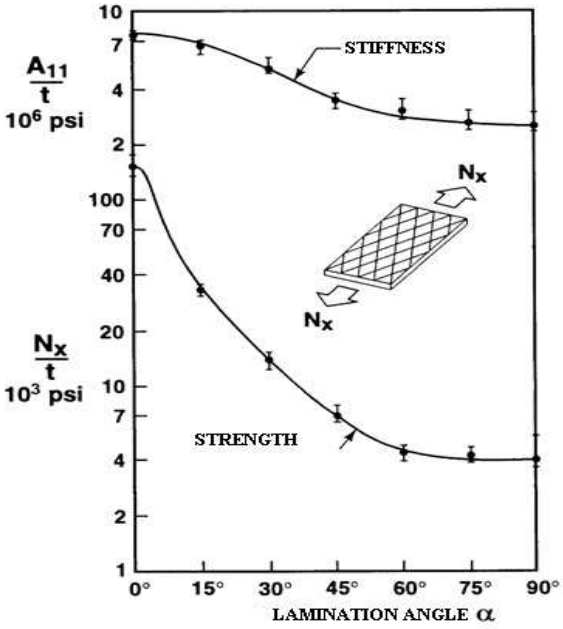

Fig. 4. Stiffness and strengths for the angle-ply laminates

10. CONCLUSIONS

The present work describes a simple algorithm and an original program for the calculation of the laminate strength. Of course, several similar programs were written but they are relatively inaccessible. For example, this type of program is used in [4] for calculating the laminate strength. In [4] it is also included the FORTRAN source code of the program but unfortunately, this source code is incorrect. The program results were compared to the results of the finite element analysis and it was observed that they were identical. It is remarkable the fact that the use of a general finite element program implies an ingenious and experimented user for the selection of the computing environment and of the limiting conditions because they can influence the calculation results in a negative manner. The program was developed during the doctoral studies and is available as an open source directly from the author.

REFERENCES

[1]. Jones, R. M. – ***Mechanics of composite materials***, Second Edition, Taylor & Francis, 1999
[2]. Sun, C.T. , Quinn, B.J., Tao, J. , Oplinger, D.W., Hughes, W. J. – ***Comparative Evaluation of Failure Analysis Methods for Composite Laminates***, U.S. Department of Transportation, Federal Aviation Administration,1996
[3]. Tsai, S. W. – ***Strength Characteristics of Composite Materials***, NASA CR-224, 1965
[4]. Tsai, S. W., Adams, D. F., Doner, D. R. – ***Analysis of Composite Structures***, NASA CR-620, 1966
[5]. Morais, A.B. – ***Prediction of the longitudinal tensile strength of polymer matrix composites***, Composites Science and Technology 66, 2006

A PERFORMANCE IMPROVING OF A TYPICAL TRANSCRITICAL CO_2 REFRIGERATION CYCLE

MEMET FEIZA

Constanta Maritime University, Romania

Together with the care for our environment, the natural refrigerant CO_2 is seen as an attractive solution due to its excellent advantages in refrigeration application. In some cases transcritical vapor compression cycles are used instead of the conventional vapor compression cycles (air conditioning). Transcritical CO_2 refrigeration cycles present low efficiencies because of losses encountered during expansion processes.
In this paper, an ejector expansion transcritical CO_2 refrigeration cycle is used to improve the performance of a typical transcritical CO_2 cycle since a constant pressure mixing zone ejector is used instead of the expansion device from the basic transcritical CO_2 refrigeration cycle.

***Keywords**:* transcritical, ejector, influence, performance.

1. INTRODUCTION

Two centuries ago, carbon dioxide was spreaded in refrigeration. But in 1930s, hydrochlorofluorocarbons displaced this refrigerant since lower system pressures were available. The care for the ozone layer led in 1987 to the Montreal Protocol which has restricted the use of hydrochlorofluorocarbons as refrigerants. It was the moment for the introduction of a new family of refrigerants, hydrofluorocarbons, which are synthetic refrigerants. These new refrigerants have no ozone depletion Potential (ODP=0), but their global warming potential (GWP) is even higher than that of the natural refrigerants as ammonia or carbon dioxide. That is why several researches are oriented towards refrigeration systems working with environmentally safe natural refrigerants.

Lately, CO_2 is seen as a promising substitute of hydrofluorocarbons due to its zero global warming potential, nul ozone depletion potential and acceptable cost level.

CO_2 refrigeration systems often work under transcritical conditions. Recently, many studies focused on the transcritical carbon dioxide refrigeration cycle due to the excellent properties of CO_2 as a refrigerant.

2. BACKGROUND

A basic transcritical carbon dioxide refrigeration cycle includes a compressor, a gas cooler, an expansion device (throttling valve or an expander) and an evaporator, as depicted in Figure 1.

The working fluid enters in the compressor with state 1, and leaves this component with state 2 as high pressure vapor. The process 2–3 is the cooling of the CO_2 refrigerant, the cooled CO_2 (state 3) being expaned in the expansion device to the evaporator pressure (P_4). In the evaporator, the refrigerant extracts heat from the cold space and after that, with state 1, enters in the compressor.

Throttling loss in the expansion device is one of the important thermodynamic losses in these systems. During the isenthalpic process taking place in the expansion device, the kinetic energy, developed as the pressure of the refrigerant is diminishing, is dissipated to the refrigerant as friction heat. Because of the isenthalpic feature of the process, the refrigerating effect of the cycle is reduced. This is why the reduction of losses during expansion is a modality to improve the efficiency of this cycle.

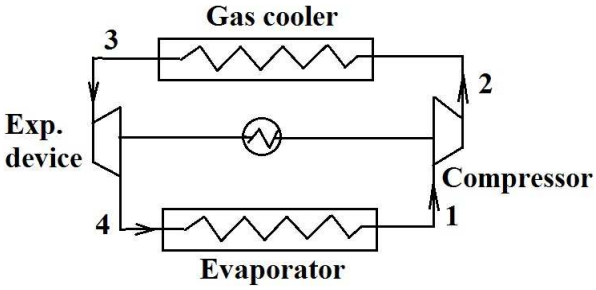

Fig. 1. Schematic representation of a typical transcritical CO_2 refrigeration cycle

Several studies revealed the fact that by using an ejector instead of the expansion device it is possible to recover a part of the kinetic energy of the expansion process. The benefit of the ejector is seen in a higher compressor suction pressure in comparison with the typical cycle, leading to a less compression work and finally to a better system efficiency.

In this work, an ejector is placed instead of the throttling valve from the conventional transcritical CO_2 cycle, resulting a transcritical CO_2 refrigeration cycle with an ejector expansion device (ejector expansion transcritical CO_2 refrigeration cycle). Its specific chart and diagram are presented in Figures 2 and 3.

High pressure vapors (primary fluid) enter in the ejector and are accelerated in the nozzle resulting a decrement of pressure allowing the admission of vapors produced by the evaporator (secondary fluid). These two fluids are mixed in the mixing chamber of the ejector, before entering in its diffuzor. Here the mixture is decelerated and the pressure increases again. In the particular case of refrigeration, the two fluids are the same.

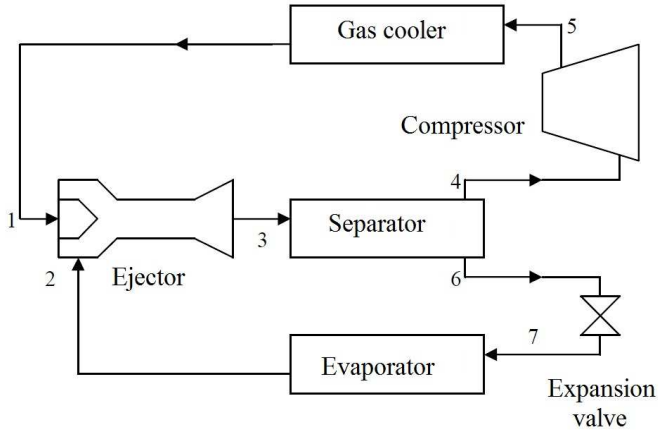

Fig. 2. Schematic view of the ejector expansion refrigeration cycle

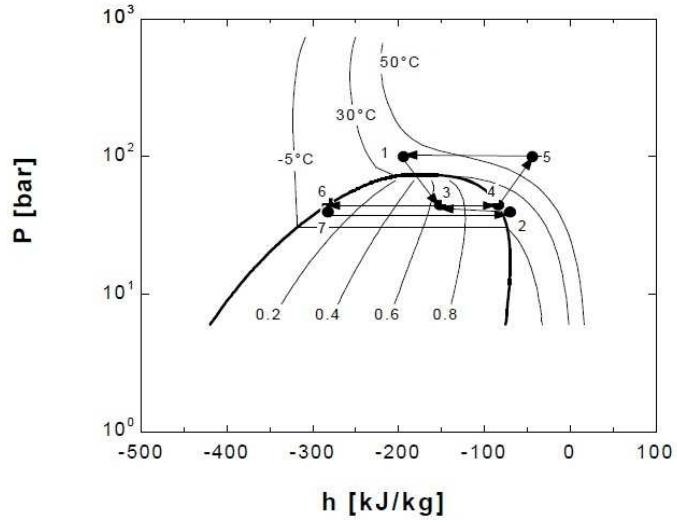

Fig. 3. Ejector expansion transcritical CO_2 refrigeration cycle in (pressure–enthalpy) diagram

In the following it will be used a constant pressure mixing model for the ejector in order to study from thermodynamic point of view the ejector expansion refrigeration cycle.

In order to simplify the study of this model are introduced the following assumptions:

- are neglected frictions at the walls, the pressure drop in the gas cooler, in evaporator and also in connection tubes;
- there are no heat losses to the environment due to the thermal insulation, except the heat rejection in the gas cooler;
- vapor stream from the separator (4) is saturated vapor and the liquid stream from the separator (6) is saturated liquid;
- the process taking place in the expansion device is isenthalpic;
- the compressor presents a constant isentropic efficiency which is not depending on the compression ratio or the compressor speed;

- from the evaporator leaves either saturated vapor or superheated vapor; temperature at the gas cooler exit is given by the temperature of the environment;
- the flow in the ejector is considered to be one dimensional homogeneous equilibrium flow;
- the primary stream and the secondary stream reach the same pressure at the entrance of the constant area mixing section of the ejector;
- the two streams do not mix before the inlet of the constant area mixing section;
- are neglected the inlet velocities of the primary and secondary flows;
- homogenous equilibrium flow conditions are considered at the nozzle outlet in the primary flow;
- the isentropic expansion efficiencies of the primary stream and secondary stream are taken as constant and the ejector diffuzer has a constant isentropic efficiency.

The comparison factor between, F, between the typical transcritical cycle and the ejector one is defined by:

$$F = \frac{COP_{ej}}{COP_t} \tag{1}$$

The coefficient of performance of the typical cycle (COP_t) depends on the gas cooler pressure and is the ratio between the specific refrigeration effect (q) and the specific compression work (l):

$$COP_t = \frac{q}{l} \tag{2}$$

The coefficient of performance of the ejector expansion cycle (COP_{ej}) depends on the high pressure of the cycle and the pressure drop, ΔP – the difference between the expanded flow and the low pressure side ejector inlet flow.

The entraiment ratio of the ejector, w, is the amount of the motive flow required to entrain and compress a given amount of suction flow. Together with the compression ratio (β), they are key parameters of the ejector

$$\beta = \frac{P_3}{P_2} \tag{3}$$

3. RESULTS AND DISCUSSIONS

The results are obtained for the following input data: the gas cooler exit temperature is 308 K, evaporation temperature is 275 K and the superheat at the evaporator exit is 5 K; efficiencies are given by: the nozzle efficiency and the secondary stream expansion efficiency are both 0,85, while the diffuser efficiency is 0,75 and the isentropic compression efficiency is 0,8.

In Figure 4 are given the influences of the pressure drop on the ejector compression ratio and on the comparison factor of the ejector transcritical CO_2 cycle.

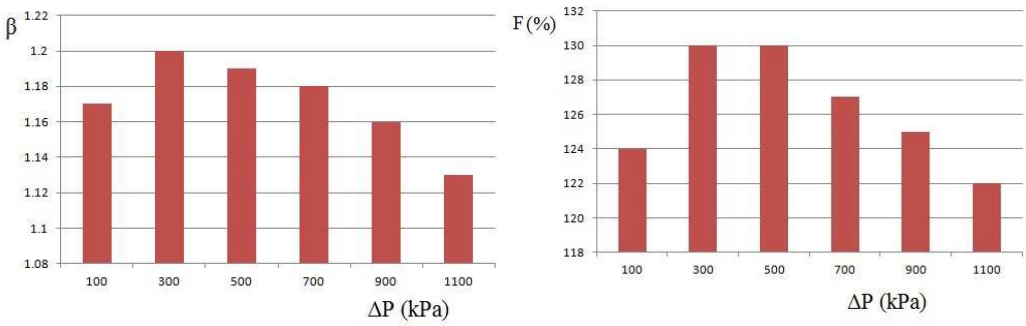

Fig. 4. Influence of pressure drop on the ejector compression ratio and on the comparison factor

It is seen that together with the increment of the pressure drop the comparison factor register also an increment followed by a decrement. The factor F presents a maximum value (130%) for a pressure drop between 300 kPa and 500 kPa.

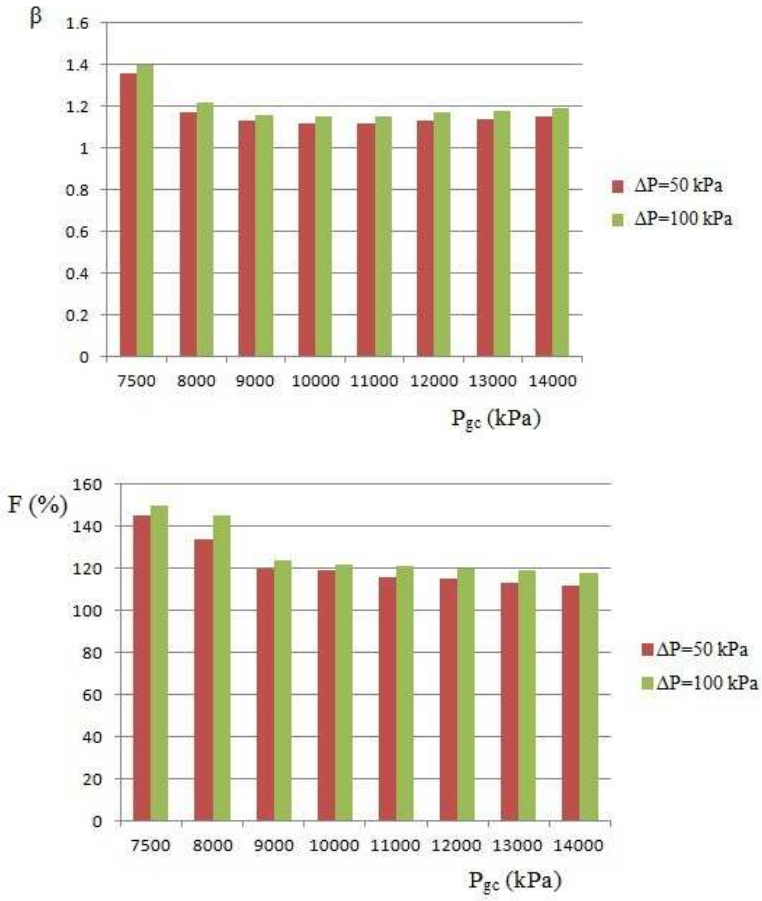

Fig. 5. Influence of the gas cooler pressure on the ejector compression ratio and on the comparison factor

It is seen that for a higher value for the pressure drop results higher values for the ejector compression ratio and for the comparison factor, for the same values of the gas cooler pressure. Together with the increase of the gas cooler pressure, the ejector compression ratio is decreasing and also the comparison factor. For a gas cooler pressure values higher than 1100 kPa, it is seen a slight increment for β values. The factor F presents its best values for gas cooler pressures between 7500 and 8000 kPa.

In Figure 6 it is given the consequence of the gas cooler pressure variation on the entrainment ratio, while in Figure 7 it is presented the dependency gas cooler pressure–coefficient of performance of the ejector expansion cycle (COP_{ej}). Are considered also two values for the pressure drop.

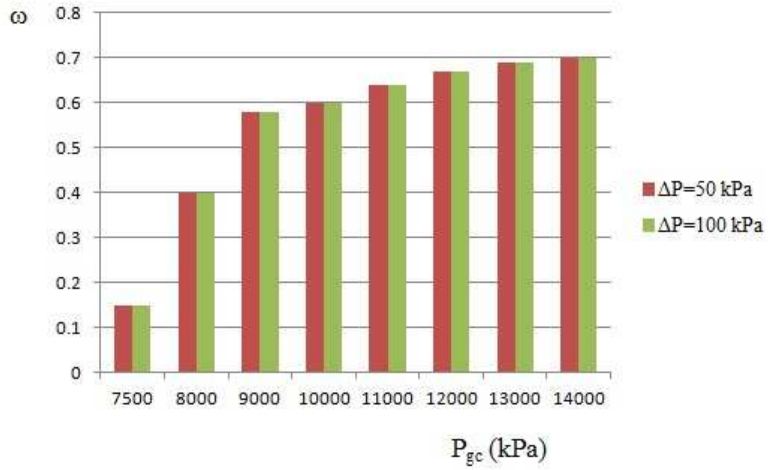

Fig. 6. Effect of the gas cooler pressure on the entrainment ratio

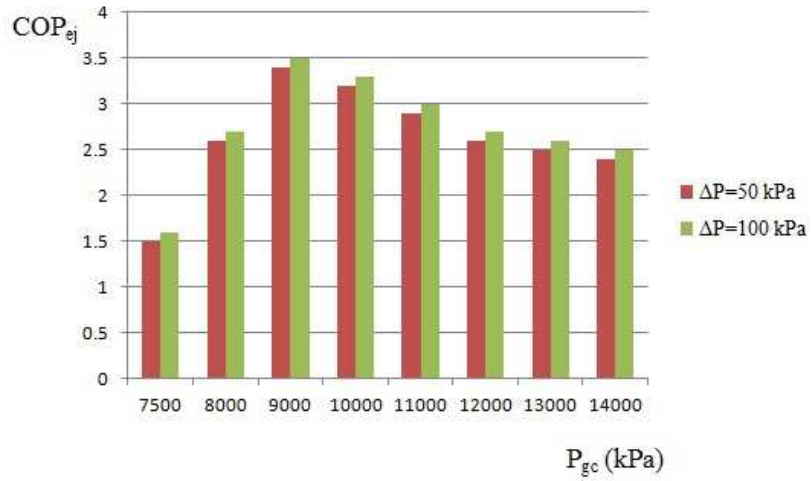

Fig.7. Effect of the gas cooler pressure on the coefficient of performance of the ejector expansion cycle

The entrainment ratio increases together with the gas cooler pressure. For the interval (7500-9000) kPa, values of ω increase suddenly, for the following pressure interval the

increment of the ω values being slight. For the maximum gas cooler pressure considered (1400 kPa), it is obtained the maximum value for ω: 0,7 – for the same levels of the pressure drop.

Increasing the gas cooler pressure are obtained better values for COP_{ej}. Best COP_{ej} values are obtained for P_{gc}=9000 kPa. Arising the gas cooler pressure over 9000 kPa, COP_{ej} is decreasing.

In Figure 8 it is shown the relationship between the ejector compression ratio and respectively the comparison factor of the ejector transcritical CO_2 cycle and the gas cooler outlet temperature.

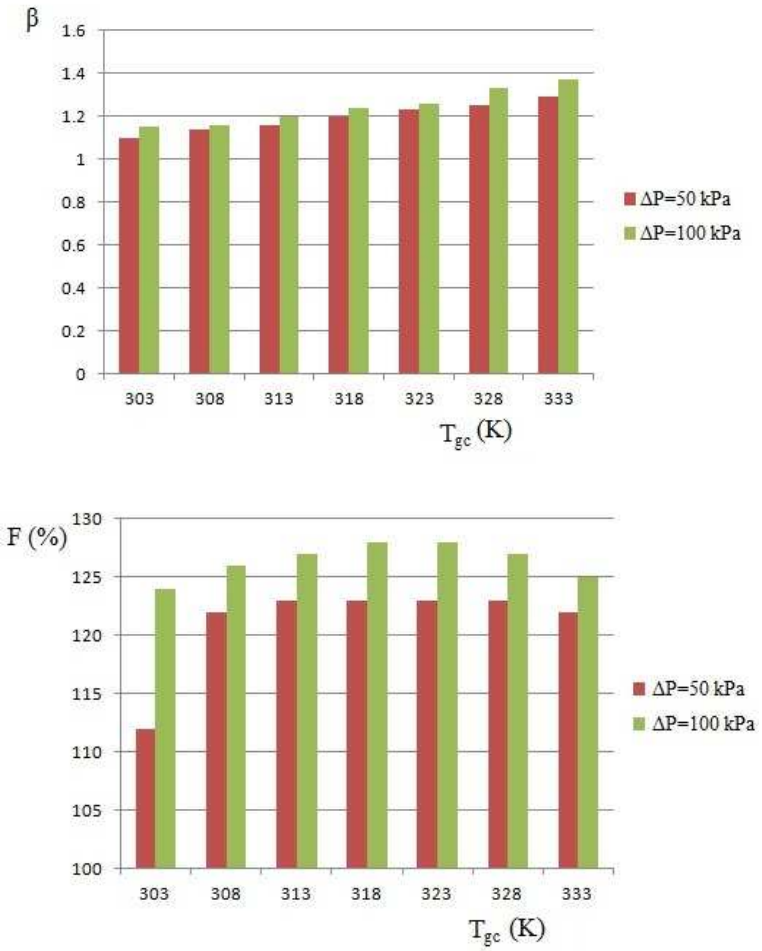

Fig. 8. Relationship between ejector compression ratio and comparison factor – gas cooler outlet temperatur

The ejector compression ratio visibly grows in gas cooler outlet temperature od, while the comparison factor arises slightly till T_{gc}=318 K and after that decreases slightly. A higher pressure drop reveals higher values for F (F_{max}=123% for ΔP=50 kPa, while F_{max}=128% for ΔP=100 kPa).

In Figure 9 it is revealed the influence of the evaporation temperature, T_0, on β and F of the ejector transcritical CO_2 cycle.

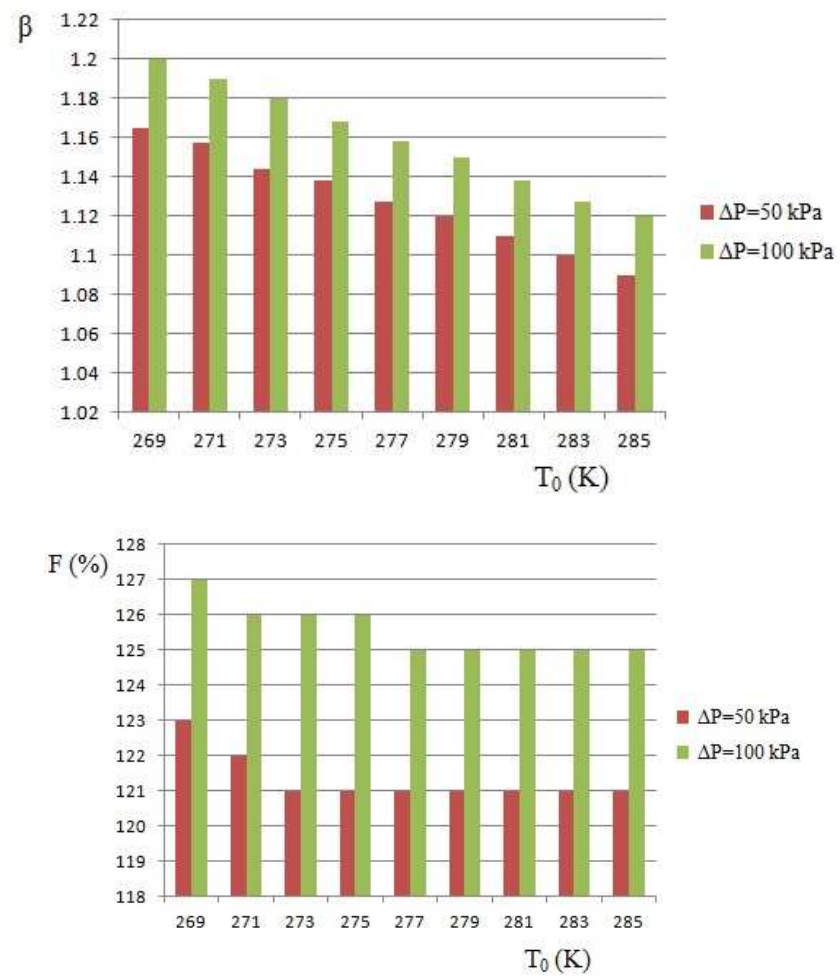

Fig. 9. Influence of the evaporation temperature on the ejector compression factor and on the comparison factor

Increasing the evaporation temperature, the ejector comparison factor is decreasing while F values remain almost constant. β and F present higher values for higher values of the pressure drop. For the analysed range, F has a maximum (127%) for T_0=269 K.

The effect of the superheat at the evaporator exit, TS, on F and ω can be seen in Figure 10.

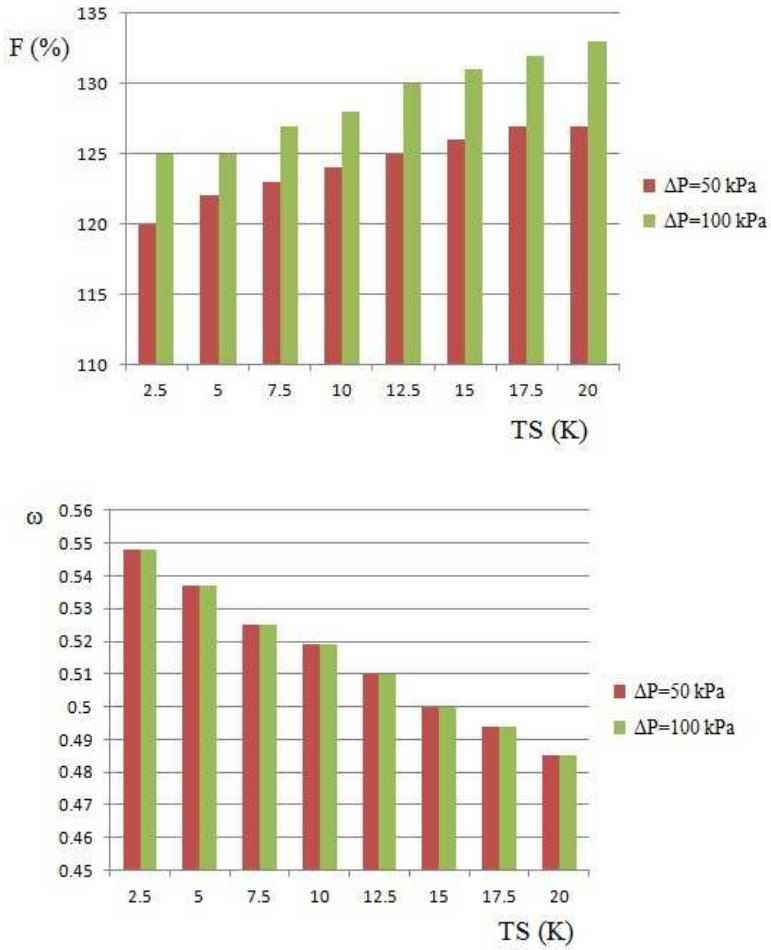

Fig. 10. Influence of the evaporator exit superheat on the comparison factor and on the entrainment ratio

The comparison factor increases slightly with the superheat increase, while the entrainment factor is decreasing. Moreover, ω values are not influenced in a significant way by the increment of the pressure drop. F values increase with the increment of the pressure drop: F_{max}=133% for TS=20 K and ΔP=100 kPa. The superheat affects more the performance of the conventional cycle than the ejector one. In the conventional cycle, the compressor suction is superheated, while in the ejector cycle the suction is in saturated vapor and the secondary stream is superheated; this fact affects the entrainment ratio because of the mixture quality increment.

4. CONCLUSIONS

The performance of a basic transcritical carbon dioxide refrigeration cycle can be improved by the use of an ejector as an expansion device resulting thus a decrement in expansion process losses.

Assuming a constant pressure mixing zone model for the ejector, was analised the influence of the pressure drop, gas cooler pressure, gas cooler outlet temperature, evaporation temperature and evaporator exit superheat variation on the ejector compression ratio, comparison factor and entrainment ratio.

The increment of pressure drop values till 300 kPa improves the ejector cycle performance as also the decrease of the gas cooler pressure (7500 kPa); the best performance of the ejector expansion cycle is found for P_{gc}=9000 kPa (COP_{ej} = 3,5 for ΔP=100 kPa). Values of the entrainment ratio suddenly rise, but it is seen that values of the entrainment ratio are independent of the pressure drop.

The increment of gas cooler outlet temperature visibly influences the ejector compression factor, but has a less influence on the comparison factor.

The decrement of the evaporation temperature influences in a more visible way the ejector compression factor, but less the comparison factor. Higher values of the comparison factor are found for low values of the evaporation temperature.

The increment of the evaporator exit superheat makes the comparison factor to increase and the entrainment factor to decrease.

REFERENCES

[1]. Cabello R., Sanchez D., Llopis R & Torella E. – ***Experimental evaluation of the energy efficiency of a CO_2 refrigeration plant working in transcritical conditions,*** Applied Thermal Engineering, vol 28, pp.1596-1604, 2008

[2]. Danfoss Ltd. – ***Transcritical refrigeration systems with CO_2,*** Danfoss, Refrigeration and Air-Conditioning Division, www.danfoss.com., 2008

[3]. Kauf F. – ***Determination of the optimum high pressure for transcritical CO_2 refrigeration cycles,*** International Journal of Refrigeration, vol 38, pp.325-330, 1999

[4]. Li D., Groll E.A. – ***Transcritical CO_2 refrigeration cycle with an ejector expansion device,*** International Journal of Refrigeration, vol 28, pp.766-773, 2005

[5]. Tao Y.B., He Y.L., Tao W.Q., Wu Z.G. – ***Experimental study on the performance of CO_2 residential air-conditioning system with an internal heat exchanger,*** Energy Conversion and Management, vol 51, pp.64-70, 2010

[6]. Yang J.L., Ma Y.T., Li M.X., Guan H.Q. – ***Exergy analysis of transcritical carbon dioxide refrigeration cycle with an expander,*** Energy, vol.30, pp.1162-1175, 2005

TRENDS AND PERSPECTIVES ON THE EFFICIENCY ROMANIAN PORTS

MIHAILOVICI CRISTINA-STELIANA

Universitat Politècnica de Catalunya, Spain

This article discusses predictions on the ports efficiency in the actual Romanian ports, in the short and medium term. We are looking for answering some questions related to measures leading to development of the Romanian Ports and their management.

***Keywords**:* perspectives, efficiency, analysis, DEA, factors.

1. INTRODUCTION

In the last years maritime transport showed an extraordinary evolution both in terms of goods transported and, especially, in the structural change of the industry obtained via mergers and acquisitions which confirms and strengthens the oligopolistic setup of the market. In parallel to the rapid development of maritime transport, ports enhanced their activity levels.

The Black Sea area was always well known for its developed trade relations and contacts, in fact is the region of the Black Sea offers the best possibility for efficient south-east and east west transport, provided that its capacity will be strengthen, upgrading its ports system and its multi-modal links towards central and western Europe.

Romania has 30 inland waterway ports with a combined handling capacity of 52 million tonnes per annum. The largest ports are Braila, Galati, Tulcea and Sulina (in total 34 million tonnes capacity) which are part of the TEN-T network. The inland ports have 48.5 km of quayside, of which 85% is in poor physical condition due to their age and lack of maintenance.

Freight traffic on the Romanian inland water transport routes is very low; it has accounted for only 15,000 tonnes (4.3 million tonne kms) in recent years. Total traffic in the ports amounted to 71,700 tonnes, but only 31,000 tonnes related to inland water traffic. Almost all traffic is carried on private vessels.

Maritime transport is provided by the direct access to the Black Sea through the three maritime ports of Constanta, Mangallia and Midia.

The port of Constanta is by far the largest of the three and among the largest ports on the Black Sea, with a traffic capacity of 105 million tonnes per year. It has nearly 30 km of quays with up to 19 m water depth.

It can accommodate vessels with a maximum capacity of 165,000 dwt for bulk carriers and 250,000 dwt for tankers. The condition of the infrastructure is deteriorating, due to its old age and prolonged use over 40 years.

2. DEA (Data Envelopment Analysis) METHODOLOGY

For the analysis of the expected Romanian Port efficiency, we could apply the DEA methodology with tolerances. Figure 1 illustrates the single input-single output DEA production possibility frontier.

The feasibility assumption, displayed by the piecewise linearity, implies that the efciency of C, for instance, is not only ranked against the real performers A and D, called the peers of C in the literature, but also evaluated with a virtual decision maker, V , which employs a weighted collection of A and D inputs to yield a virtual output. DMU C is lying below the variable returns to scale (VRS, further defned below) efciency frontier, XADF, by DEA ranking. The input-oriented technical efciency of C is defned by TE = Y V=Y C.

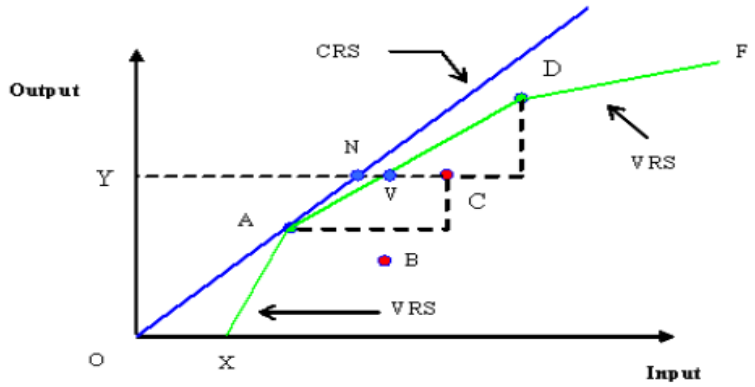

Fig. 1. DEA production possibility frontier

If constant returns to scale (CRS) characterize the production set, the frontier may be represented by a ray extending from the origin through the efficient DMU (ray OA). By this standard, only A would be rated eficient. The important feature of the XADF frontier is that this frontier reects variable returns to scale. The segment XA reects locally increasing returns to scale (IRS), that is, an increase in the inputs results in a greater than proportionate increase in output. Segments AD and DF reect decreasing returns to scale. It is worth noticing that constant returns to scale technical efficiency (CRSTE) is equal to the product of variable returns to scale technical efficiency (VRSTE) and scale efficiency (SE). Accordingly, DMU D is technically efficient but scale inefficient, while DMU C is neither technically efficient nor scale efficient. The scale efficiency of C is calculated as Y N=Y V .

The shipping business and port services are characterized by scale economies, as the cost of mobilizing a 40-foot container is more or less the same as mobilizing a 20-foot one.

For those ports that are inefficient, the adjustment path towards the efficiency frontier will depend on their location with respect to the increasing returns to scale (IRS) or decreasing returns to scale (DRS) portions of the efficiency frontier.

3. THE EFFICIENCY FACTORS OF THE ROMANIAN PORTS

Some ports more than others benefited from the growth trends thanks not only to their structural and location characteristics but also to the fact of being chosen by powerful shipping companies able to make the fortune or the misfortune of a port.

Poor port efciency will increase import prices and reduce the competitiveness of the country's exports in world markets. Port efciency is a critical link between the domestic economy and the rest of the world. Lowering transport costs will, presumably, increase trade volume and, consequently, enhance the productivity of domestic factors of production, leading to higher growth rates.

We believe that the major factors that will impact on the marine sector in the Romanian ports over the period to 2012 are: the political and economic change, the globalization, the population growth & demographic change, the energy supply and demand, and prices.

Globalization will continue to be driven by the lower costs of the developing countries and the ageing of populations in the developed world. This will result in an increasing demand for commodity feedstock, and for energy – particularly oil and liquid fuels for transportation, perhaps increasingly derived from gas.

The sustainable intermodal freight transportation solution will require coordinated efforts among industry, government, and academia, along with improved understanding by the general public about how their food, clothing, housing, and other material needs are delivered.

As these efforts proceed, the maritime transport industry will continue to involve technologies (including environmental control technologies for air emissions, ballast water, hull coatings, etc.), energy systems.

In the Romanian Ports System exist an important player - the Romanian Naval Authority's which mission is to ensure a customer’s satisfaction, ensuring greater safety and security in shipping, by providing better customer services as this area of activity and continuous improvement of service quality in terms of efficiency , flexibility and cost optimization.

4. CONCLUSIONS

The key points of the development are the privatization of port activities and emergence of some figures of the terminal operator, the services that have been restructured in an entrepreneurial key required by the ship and by the commodity, to engrave acceleration to the realization of a surplus of ability of the infrastructure of Romanian ports.

In terms of port efficiency, ports across the world have improved their efficiency over time based on three distinctive sources: improvement in management of capital inputs, production scale adjustment, and technological progress.

The influences from external environments still play an important role in shaping port efficiency.

The roles of efficient capital management and capital investment supported by institutional restructuring are not minimal but substantial for the operation of ports over the medium-to-long term. Given the current globalized shipping market and scopes of port activities, the strategies to combine institutional restructuring and capital investment can suggest the potential to partly overcome the limitations of the external conditions, as can be found from examples like the Port of Dubai and the Port of Singapore. However, a strategy focusing only on aggressive capital investment in technological progress has limitations in that it is relatively easier for other ports to replicate. As a result, it could lack the potential to increase relative competitiveness.

Ports’ patterns of efficiency change can be different, based on how the different sources of efficiency act in improving ports’ overall total factor productivity and compensate for the deterioration of other sources of efficiency. These characteristics of efficiency change are influenced not only by market advantages and hinterland conditions, but also from strategic efforts to combat or to reap the benefits of these conditions.

We propose some measures that we think that will help the maritime transport, the development of the Romanian ports and the ports management.

- eliminate unnecessary taxes and implement a system of payment that will be facilitating the development of the maritime traffic in the Romanian ports;
- analyzing always the market transparency;
- encourage the development of transport projects and the investments. The implementation of TEN-T networks should be carried out with due consideration of likely social and environmental impacts;
- create the favorable conditions to attract cargo and passengers, especially for commercial shipping where the focus is on upgrading the ports to multimodal logistics centers or hubs which will result in a significant increase in container handling;
- attracting private capital investment for ports and granting access permits with transparent procedures.

The Romanian Ports offers numerous opportunities for the economical development of the maritime commerce and regional cooperation.

We have the obligation for our future generations to contributing at the development of the maritime transport in this region, to encourage the cooperation, the transparency and the investment and ignore the global crisis that affect all the world.

REFERENCES

[1] ANDERSEN P. y PETERSEN, N.C.,- ***A procedure for ranking efficient units in data envelopment analysis, Management Science,*** 1993, vol. 39, p. 1261–1264.

[2] BOSCA, J. E.; MARTÍNEZ, A.; LIERN, V. y SALA, R., - ***Ranking decision making units by means of soft computing DEA models***, International Journal of Uncertainty, Fuzziness and Knowledge- Based Systems, 2011, vol. 19, n.1, p. 115-134.

[3] CHARNES, A.; COOPER, W. W. y RHODES, E., - ***Measuring the inefficiency of decision making units***, European Journal of Operational Research, 1978, vol. 2, p. 429-444.

[4] GONZÁLEZ, M. M. y TRUJILLO, L., - ***Efficiency measurement in the Port industry: a survey of the empirical evidence,*** Journal of Transport Economics and Policy, 2009, vol. 43, n. 2, p. 157–192.

[5] TONGZON, J., - ***Port choice and freight forwarders, Transportation Research*****,** Part E: Logistic and Transportation Review, 2009, vol. 45, p. 186-195.

[6] TSOUA, Ch. y HUANGB D., - ***On some methods for performance ranking and correspondence analysis in the DEA context,*** European Journal of Operational Research, 2010, vol. 203, p. 771- 783.

EFFICIENCY ANALISYS OF WAVES ENERGY CONVERSION SYSTEM WITH FLOATING CYLINDERS

[1] NEDELCU DRAGOS-IULIAN, [2] SAJIN TUDOR
[1,2] *"Vasile Alecsandri" University of Bacau, Romania*

Starting from the particularities of offshore surface waves, the paper propose the analysis of a new system with floating bodies articulated, connect between them with levers, designed for potential waves energy and for its conversion. From the analysis of technical stage was chosen the cylindrical shape for which the waves energy absorption efficiency is higher than in a vertical plate case. It was established that the efficiency of capture system with floating cylinders in function by their diameters and by the ratio of lever length connection at wavelength of wave.

***Keywords**:* waves, conversion, potential energy, floating body, cylinder.

1. INTRODUCTION

In the case of theoretical analysis of wave energy conversion systems in electrical power, start with a simplifying assumptions of the surface waves in deep water (Agheev V.A., 2004):

- the waves are indestructible, having a sinusoidal form with length, phase and incidence direction irregular;
- the movement of each particle of liquid is circular;
- the amplitude of liquid particles movement decrease with depth water;
- the wave amplitude is independent by length λ, by speed of propagation C and by the period T, this depends only by the character of previous interaction of the wind with sea surface.

The equations (1) and (2) describe the gravitational waves having as classic example the waves in emerging (Diviyinzuk M.M. et al., 2010):

$$\nabla\left(\frac{\partial\varphi}{\partial t}+\frac{p}{\rho_C}+\frac{v^2}{2}+gz\right)=0 \tag{1}$$

$$\sigma^2\varphi=0 \tag{2}$$

where: φ – the gradient of a scalar function of the potential speed;; p – the pressure that leads to the wave appearance, [N/m^2]; v – the speed of elementary volume, [m/s]; z – vertical coordinate; σ – the ratio between force and surface, [N/m^2].

2. THE DEPENDENCE OF ABSORPTION EFFICIENCY OF WAVES ENERGY BY FORM OF FLOATING BODY

The efficiency of a conversion system is defined by the ratio between the available power per width unit of the incident wave what is extracted by floating body. The relationship will depend clearly by the details of interaction between body and the fluid.

According to studies made by (Evans D.V., 1976), the available power per length power for one sinusoidal progressive bidimensional wave is the average of energy flux per length unit intersecting the vertical normal plane in wave direction, resulting that $R_{C1}\overline{R}_{C1}\left(T_{C1}\overline{T}_{C1}\right)$ it measure the quota of power in reflected wave (transmitted). Follows that, the efficiency of system η, is given by relation:

$$\eta = 1 - R_{C1}\overline{R}_{C1} - T_{C1}\overline{T}_{C1} \tag{3}$$

where R_C is the complex coefficient of reflection for dissipation problem, and T_C is the complex coefficient of transmission for dissipation energy problem.

If cylinder is fixed so that the displacement on coordinate axes ξ_i=0, substituting in the above relation, is obtained:

$$\eta = 1 - R\overline{R} - T\overline{T} = 0 \tag{4}$$

showing that, in this case the flux of wave energy is conserved.

Was developed the mathematical model of wave energy absorption by (Evans D.V., 1976), by which was determinate the maximum efficiency of absorption for available power by floating body in function by its shape (semi-submerged cylinder, vertical rolling plate) by level of submergence and by wave number. It has been established that the most efficient is the body with cylindrical shape, in according with figure below.

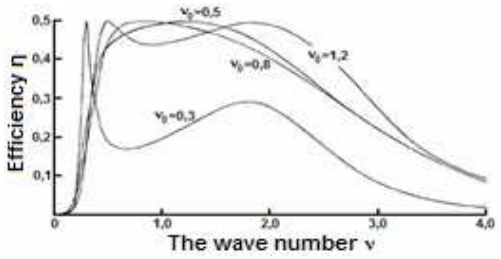

Fig. 1. The absorption efficiency of power η for a vertical rolling plate in function by dimensionless wave number ν for different values (ν_0=0,3; 0,5; 0,8; 1,2)

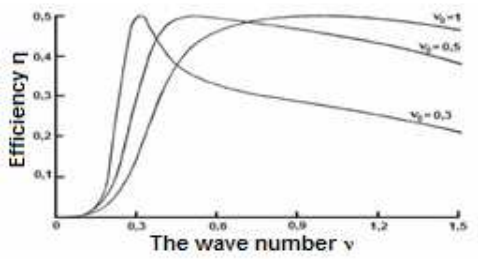

Fig. 2. The absorption efficiency of power η for a semi-submerged cylinder in function by dimensionless wave number ν for different values (ν_0=0,3; 0,5; 1)

3. THE MODEL OF POTENTIAL ENERGY EXTRACTION BY SYSTEM WITH FLOATING BODIES

In patent application (Nedelcu D.-I., 2009) is given a new concept of wave energy capture system, which include a set of more floating cylinders articulated linked between them with levers.

The elementary scheme of calculation of the potential energy conversion system (Nedelcu D.-I., 2011), include three floating bodies: central one, which is the floating body considered, and two peripherals, which interacts through the levers with length *l* the central floating body. In case of the systems with a higher number of floating cylinders, the model can be symmetrical extrapolated with the elementary calculation scheme.

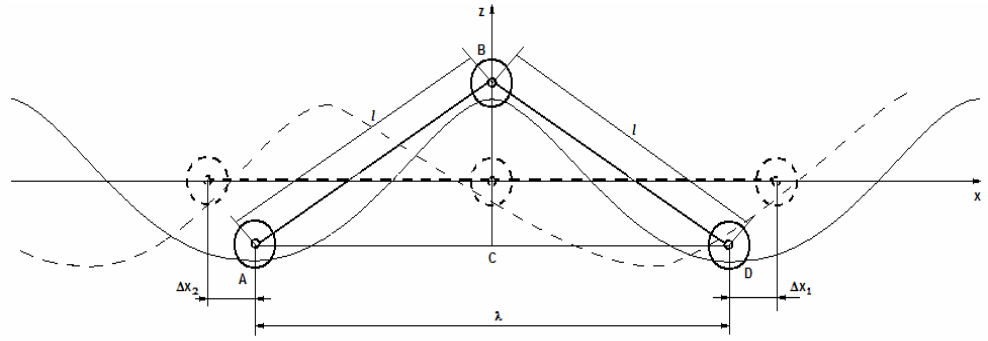

Fig. 3. Scheme for calculating the dynamics of motion of an element of wave

Are known the waves parameters: wavelength λ and the oscillations period T, with which is calculated: the wave amplitude $a = \lambda/2\pi$; oscillation frequency (angular speed), $\Omega = 2\pi/T$ and the phase speed $C = \lambda/T$.

We also know the constructive characteristics for the capture device: diameter for the floating cylinders D, length of the floating cylinders L, the length of the connection rods between the floating cylinders l, thickness of the floating cylinder wall δ, weight of the constructive elements (transmissions, electric generator, arresters, bearings, etc.) compared to the weight of the floating cylinder m_0.

The differential equation for the oscillation of the central floating cylinder on the Z axis can be written as:

$$m\frac{d^2z}{dt^2} = -kz - c\frac{dz}{dt} + F_0\cos\Omega t \quad \text{or} \quad \frac{d^2z}{dt^2} + 2b_a\frac{dz}{dt} + \omega^2 z = \frac{1}{m}F_0 c\,, \tag{5}$$

where k is the elastic constant, [kg/s^2]; c – water resistance coefficient, [kg/s]; b_a – damp coefficient, [s^{-1}]; ω_p – frequency of own oscillations for floating cylinder without damping, [s^{-1}]; F_0 – excitation periodic force amplitude, [N]; Ω – wave oscillation frequency, [s^{-1}]; t – time, [s]. The following relations exist between these values:

$$\omega_p^2 = \frac{k}{m}; b_a = \frac{c}{2m}; \tag{6}$$

$$m = m_0 \cdot L\left[\left(L + \frac{D+\delta}{4}\right)\cdot \pi\delta(D+\delta)\cdot\frac{1}{V_{mc}} + 1\right]; \tag{7}$$

$$F_0 = \left[\frac{\pi D^2}{4}(L-2\delta) - V_{mc}\right]\cdot\rho g - mg\ . \tag{8}$$

The values of m_0 and V_{mc} are chosen in a way that they satisfy the relation:

$$mg = \left[\frac{\pi D^2}{4}(L-2\delta) - V_{mc}\right]\cdot\rho g\ , \tag{9}$$

in which states that the amplitude of the excitation force on the oscillation period remains constant and at a value equal to half of the Archimedes force.

The mechanical power extracted by the device to capture wave energy is determined using the formula:

$$P(t) = F_1(t)\cdot v_1(t) + F_2(t)\cdot v_2(t)\,. \tag{10}$$

The available power for the wave on the length L of the floating cylinders is given by the relation:

$$P = \frac{1}{2}\cdot\frac{\rho g a^2\cdot L\cdot\lambda}{T}\quad . \tag{11}$$

The useful power $P_{ut}(t)$ is considered to be the positive part of the expression (10).

Using the values of the powers (42) and (43) we can calculate the efficiency for the device to convert the wave energy, at a given moment:

$$\eta(t) = \frac{P_{ut}(t)}{P}\cdot 100 \tag{12}$$

and the average value for the wave period,

$$\eta_m = \frac{\int_0^T P_{ut}(t)dt}{\frac{1}{2}\rho g a^2\cdot L\cdot\lambda} \tag{13}$$

In according with performed simulations with help of Mathcad 14, the software on floating cylinders system, showed that the forces between the peripheral cylinders and the rods have different variations, but they coincide at the beginning, the middle and the end of the wave period (fig. 4). There are time frames when both forces have the same orientation (the most benefic case for the wave conversion process) and there are time frames when the

forces have opposite orientation. In the latter case, where the modules of the forces are equal the device will not produce energy.

The useful mechanical power extracted has an oscillating period equal to half the wave period, and it's maximum value is reached at the beginning and at half the period *T* and it's minimal value is reached at 0.3·*T* and 0.8·*T* (fig. 5).

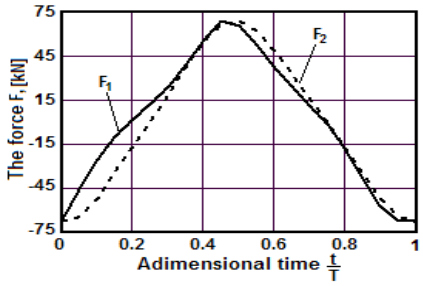

Fig. 4. Variation of the forces between the peripheral cylinders and the rods during one wave period

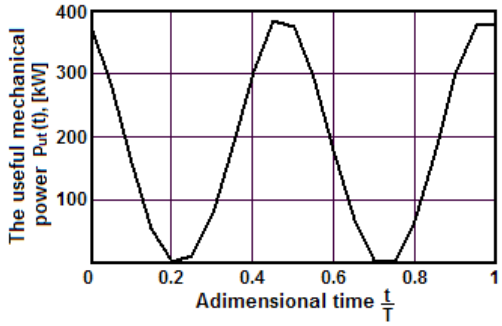

Fig. 5. Chart of the useful mechanical power extracted by the cylinders

Given that the efficiency is calculated with relations (12) and (13), the character of chart will be similar with character as the chart for the mechanical torque.

The variation of the average efficiency during the wave period reaches maximum value for *l/λ<0.5*, (fig. 6).

According to properties of the material of which is made the ensemble, (steel with density ρ=7850 kg/m^3), the average efficiency increases with the increase of the diameter of the cylinders and has a tendency to stay level at values for *D* >1.8 *m* (figure 7).

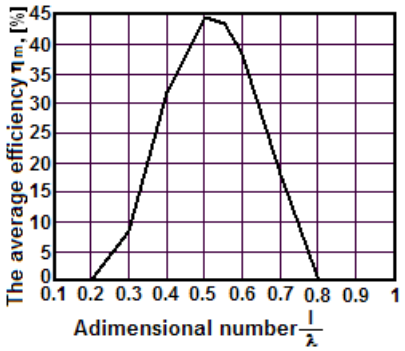

Fig. 6. Chart for average efficiency depending on the wave length

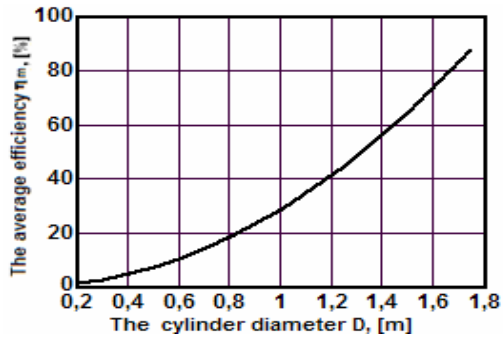

Fig. 7. Chart for average efficiency depending on the cylinder diameter

4. CONCLUSIONS

1. From the analysis of actual stage were presented the equations that describe the movement of gravitational waves of deep water, starting at a few simplifying assumptions and was chosen the cylindrical shape for floating body, being more efficient from point of view of wave energy absorption efficiency in comparison with floating body like as vertical plate.

2. Was formulated and simulated the mathematical model of potential wave energy capture, where the base is the elementary calculation scheme with three floating cylinders linked between them with levers.

3. The useful power becomes maxim when the linear speeds and the forces have the same phase, but is zero when they oscillate in counter-phase.

4. The device efficiency has the same variation degree as the useful power.

5. The average absorption efficiency for potential wave energy increases for ratio of lever length connection at wavelength of wave $l/\lambda = 0,5$, and with the rise in diameter D of the cylinders and the efficiency tends to have the same values for $D > 1,8$ m.

REFERENCES

[1] Agheev, V.A. – ***Netradiționâe i vozobnovleaemâe istocinichi energhii***, Institut Mehanichi i Energhetichi Moscovscogo Gosuniversiteta, 2004.

[2] Diviyinzuk, M.M., Tretyakova, L.V., Pleskacheva, I.A., Shramkova, E.A. – ***Matematicheskie zakonomernosti formirovaniya morskih voln, opredelyayushchih akusticheskie i antropogennâe svoistva pripoverhnostnogo sloya vod,*** 2010.

[3] Evans, D.V. (1976). ***A theory for wave-power absorption by oscillating bodies***, Journal Fluid Mech., vol. 77, part 1, Great Britain, p. 1-25, 1976

[4] Nedelcu, I., Sajin, T., Vernica, S., Aniței, F., Marian, M., Bîrsan, C., Ostahie, N. (2009). ***Instalație pentru conversia energiei valurilor***, Pattent application nr. A/00136, 12.02.2009.

[5] Nedelcu D.-I. – ***Contribuții la studiul proceselor de conversie a energiei valurilor***, Teza de doctorat, 2011

THE STUDY OF WAVES ENERGY CAPTURE PROCESS BY MECHANICAL AND ELECTRICAL ANALOGY

[1]SAJIN TUDOR, [2]NEDELCU DRAGOS-IULIAN

[1,2]*"Vasile Alecsandri" University of Bacau, Romania*

Starting from the concept of an device for waves energy conversion, constituted by floating cylinder structure, the paper intends to carry out a comparative analysis between mechanical and electrical analogy, for a more precisely determination of parameters that have a influence on oscillating system for waves energy capture.

Keywords*:* waves, conversion, potential energy, mechanical analogy, electrical analogy.

1. INTRODUCTION

The researches into waves energy domain have spread on last 4 decades, stimulated on one side by big energy resources on the oceans and, on the other part, by the depletion of fossil fuels resources. The World Ocean presents a big surface of water currents, which is in permanent motion and cover approximately 71% of the planet surface. The intensive use of the fossil fuels that in the second half of twentieth century was added and nuclear fuel, has led to more negative consequences: pollution of aquatic and aerial basins, acid rains, soil degradations, draining of the natural resources and danger of the radioactive pollution (Ambros T et al., 1999).

Following the analysis of actual study, (Bostan I., 2007), the waves energy conversion systems are divided in two categories:

- shoreline and near/shore wave energy collecting installations;
- offshore wave energy collecting installations.

Wave energy conversion installations can be characterized by:

- taking over the wave energy, realized through: the air oscillating column formed by the sea water; floating objects of different shapes and sizes; oscillating panels; the accumulation of water rised by waves into a reservoir;
- the acting of turbines which can be realized with the aid of: air; sea water; hydraulic oils in a closed circuit;
- the acting of electrical generators with the aid of: air turbines; hydraulic turbines;
- mechanical machines having floating objects as an action element.

One of the installation with a good efficiency compared with other offshore installations is Pelamis (fig.1), which is composed from multiple large size tubes, interconnected with the

help of joints, which, due to angular inclination created by waves, act some oil pumps in closed circuit. At their turn, the pumps act the hydraulic turbines that are connected to electric generators.

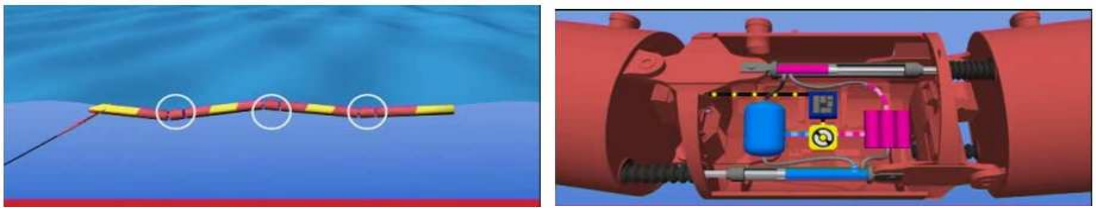

Fig. 1 Pelamis installation scheme

2. WAVE ENERGY CONVERSION SYSTEM

The patent of this installation (Nedelcu et al., 2009) has the prototype the Pelamis system (Yemm R., et. al., 2001). The installation for wave energy conversion (fig. 2) consists from a floating cylinders structure 1, which is anchored in the symmetry centre to the bottom of the sea.

The floating cylinders 1 are mounted in such a way that they have the possibility to rotate on their longitudinal axis 2 and have on both ends connecting rods 3 perpendicular to the longitudinal axle 2. This way, one end of the connecting rod 3 is rigidly connected to the end of a floating cylinder 1 and the other end of the connecting rod 3 is rigidly connected to the longitudinal axle 2 of the neighbor floating cylinder 1.

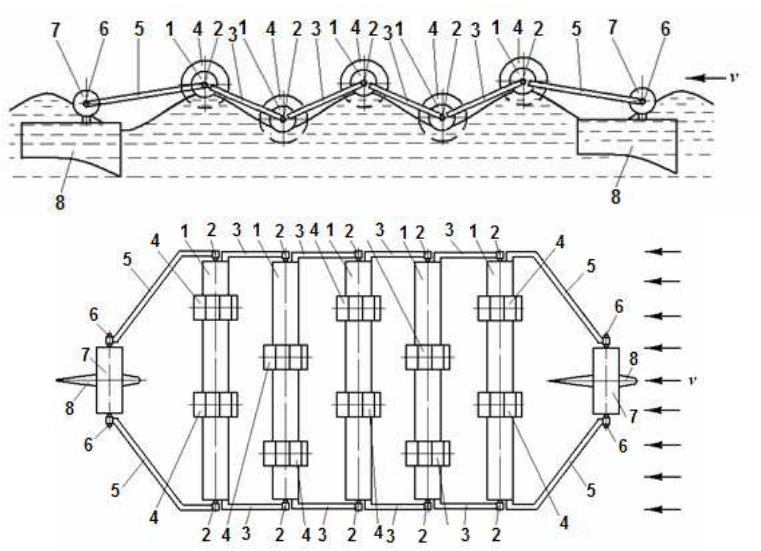

Fig. 2. Wave energy conversion installation
1 – floating cylinders; 2 – longitudinal axis; 3 – connecting roads; 4 – water wheels; 5 –cross beams; 6 – additional longitudinal axis; 7 –additional floating cylinders; 8 – rudders

In comparison with the system (Yemm R., et. al., 2001), the installation (Nedelcu et al., 2009) has the advantage to capture a potential and kinetic components of mechanical energy from waves at high efficiency.

3. CONCEIVING OF EXPERIMENTAL STANDS FOR DETERMINATION OF POTENTIAL WAVE ENERGY CONVERSION

According to (Nedelcu I., 2011), it was proposed a mathematical model of wave energy extraction process, which has been adapted for oscillation process a mechanical laboratory with two articulated cylinders.

For the study of conversion of the potential wave component, is desired implementation of some stands using the method of mechanical and electrical analogies, given the low cost of components and the location in space as compact.

The installation for study of determination of potential wave energy conversion through mechanical analogy is presented in figure 3 and contain inertia, elastic, dissipative and disturbing elements (Nedelcu I., 2011).

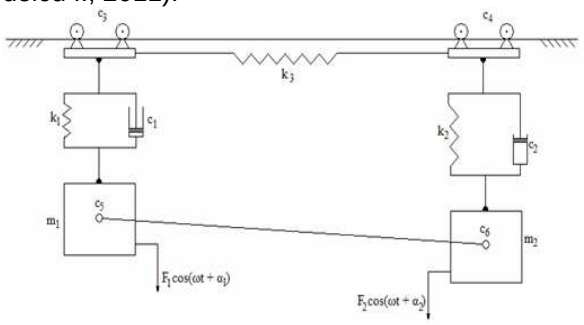

Fig. 3. Analogical scheme of experimental model study for wave energy conversion m_1, m_2 – inertia elements; k_1,k_2, k_3 – elastic elements; c_1,c_2,c_3, c_4,c_5,c_6 – dissipative elements; $F_1\cos(\omega t + \alpha_1)$ and $F_2\cos(\omega t + \alpha_2)$ – disturbing elements

The stand, (figure 4), is composed by a crankshaft 1 with bearing fixed in a metallic frame 2

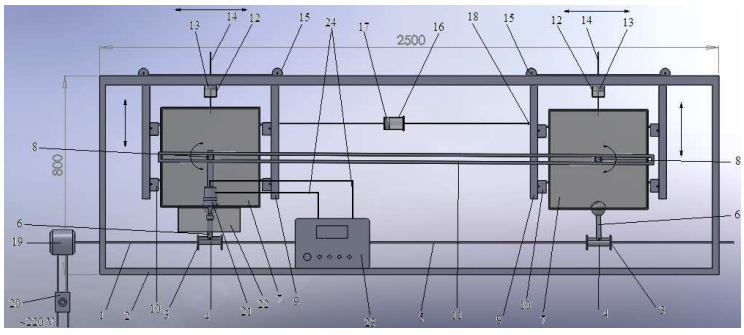

Fig. 4. Stand for simulating of potential energy by the method of mechanical analogy: 1 – crankshaft; 2 – metallic frame; 3 – discs for changing of waves parameters; 4 – fixing element; 5 – the transmission shaft; 6 – rod balls; 7 – bodies; 8 – the conversion shaft; 9 – the rolling path; 10 – a guiding wheels; 11 – the connecting rod; 12–springs; 13,16,17 – cylinder with piston; 14,18 – adjustement bolt cylinder; 15 – rolling panel;

19 – electric motor; 20 – potentiometer; 21 – electrical generator; 22 – rolling plate of rotor of the electrical generator; 23 – oscillograph; 24 – electrical cables connection

and kinematic coupled to an electric motor, which has the role of disturbing elements. With the help of discs 3, of fixed elements 4 and rod with balls 6, the crankshaft 1 is kinematic joined with bodies 7 which simulates the floating cylinders and acts as inertia elements of hydro-mechanical analogy model.

Experimental installation simulates the waves energy conversion process trough the mechanical analogy and allows the experimental determination of elongations, deviation angle, angular and linear speeds, the forces that are acting in oscillating bodies joints with lever, a extracted useful power and the efficiency in normal conditions of function and in near of resonance.

For the determination of waves energy potential energy efficiency are following the next steps:

1) adjusting of the parameters of waves simulations;
2) measuring of the dynamic parameters of the system elements;
3) calculating the relative errors that occur in measurements.

Since in the perform measurements by mechanical analogy occur the perturbations in the measurement process due to friction, a clearance of articulated elements of installation, it follows achievement of a stand for making of measurements through electrical analogy, starting from mechanical scheme of a conversion element, according with fig. 3.

In this system, the deformation speed of the spring *k*, as elastic element, and the damper *c,* at dissipative element, at the same and have the speed motion values *V* of the weight *m*. In electrical scheme from fig. 5, to this condition correspond the connection in series of inductance, capacity and the resistance.

Returning at the installation of the fig. 3, the scheme of the circuit developed by electrical analogy, will be made from two RLC circuits (fig. 5) with the possibility of changing the phase shift between the voltage of the two current sources, the graphic determinations are being made with the aid of a oscilloscope.

The testing of analogical models was made on example of elongation of sinusoidal oscillation analysis during a period, this varying in the interval $-a \leq z(t) \leq a$, where a is amplitude of elongation.

In this case, the elongations $z_1(t)$ and $z_2(t)$ will depend by phase shift of oscillation between the two bodies.

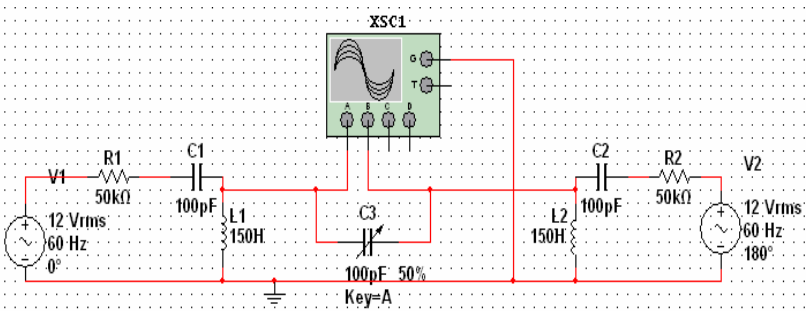

Fig. 5. Analogical electric scheme of the experimental model for study of waves energy conversion

Is obvious that for $\alpha = 0$ and $\alpha = 2\pi$ (fig. 6) elongations coincide, ie $z_1(t) = z_2(t)$. Therefore, at zero or 2π phase shift, it won't be an angular deviation of the bar that connect the axis of oscillating bodies and the installation will not absorb the useful power.

With increasing of phase shift in the $0 \leq \alpha \leq \pi$ interval, the variation of difference $z_1(t) - z_2(t)$ will be held in a interval as higher as is α, this interval becoming the maxim for $\alpha = \pi$, when the bodies oscillate in opposite phase. Therefore and the useful extracted power will be maximum for $\alpha = \pi$.

Further increasing of phase shift in interval $\pi \leq \alpha \leq 2\pi$ leads to reduction at zero for the variation difference interval $z_1(t) - z_2(t)$.

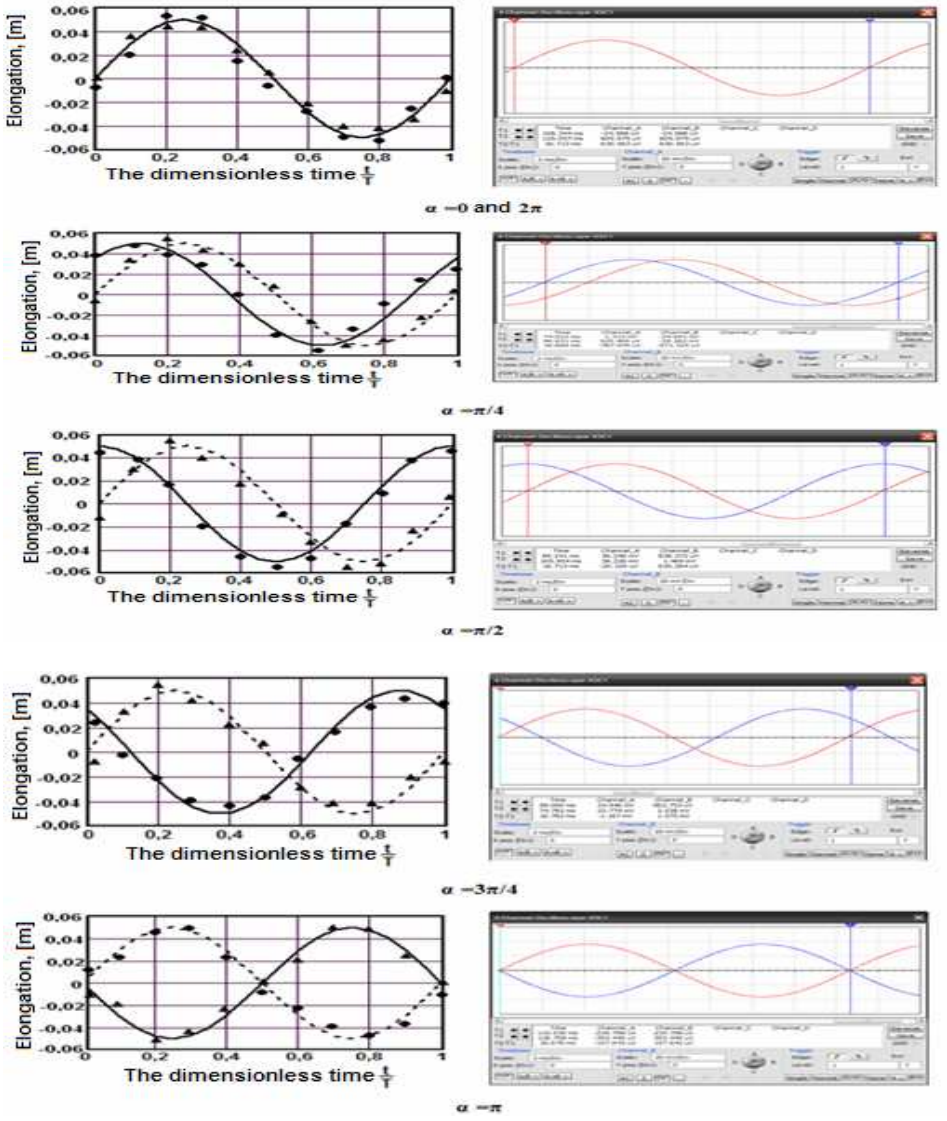

Fig. 6. The variations of elongation of oscillating bodies on the period of oscillation determined by hydro-mechanical and hydro-electrical analogy

4. CONCLUSIONS

Making a comparative analysis of existing installations for waves energy conversion, they were classified according to the location, as well by action mode of electric generators, which determines that each country what have a coastline or ocean to choose the type of suitable installation in function by waves parameters.

Was designed a new installation for mechanical capture of waves energy and conversion of this in electricity. The installation is composed by floating bodies series, kinematic connected with the help of rods. Therefore the elongation of cylinder oscillations is transformed in angular movement which through a multiplier is transmitted at the shaft of electric generator. The installation also contains water wheels for kinetic conversion of waves energy.

Starting at mechanical analogy of waves interaction with conversion elements of installation, it was realized also an electrical analogy with the help of RLC circuits, which allow elimination of the disturbing factors from the measurement process and have a low cost of the equipments that where used.

The testing of analogical installations was made on example of variation of elongations bodies oscillating in the period of oscillation in function by oscillation phase shift of this.

REFERENCES

[1] Ambros T. et al. – ***Surse regenerabile de energie***, Editura „Tehnica-Info", Chişinău, 1999
[2] Bostan, I., et al. – ***Sisteme de conversie a energiilor regenerabile***, Ed. Tehnica-Info Chişinău, 2007
[3] Nedelcu I. – ***Contribuții la studiul proceselor de conversie a energiei valurilor***, Teza de doctorat, 2011
[4] Nedelcu I., et. al. – ***Instalație pentru conversia energiei valurilor***, Cerere de brevet de invenție nr. A/00136, depozit12.02.2009
[5] Yemm R., et. al. – ***Floating apparatus and method for extracting power from sea waves***, US patent no. 6476511, priority data 30.05.2001

THE ACADEMICIAN PROFILES OF MARITIME HIGHER EDUCATION INSTITUTIONS IN TURKEY*

[1]SELCUK NAS, [2]BURCU CELIK

[1]Dokuz Eylül University, Izmir, Turkey, [2]RTE University, Rize, Turkey

One of the most important missions of maritime educational institutions is to educate the qualified labor force meeting the international maritime manpower market needs. For that purpose in Turkey, the number of educational institutions providing manpower to the maritime industry has been rapidly increased in the last decade. Concordantly, there have been a lot of investments in laboratories, classrooms and simulators in order to enable sufficient training. Despite of all these aforesaid developments, the most important issue, instructor or academicians with maritime background, was neglected. Now, Academicians have become the most important human capital. This capital cannot be created immediately yet it can be brought into existence within a long period of time. Without this capital is not possible to train qualified seafarers, to survive in the maritime industry.
The aim of this study is to determine the profiles of the maritime higher education institutions in Turkey, their capacities and profiles of the academicians with maritime background employed in such institutions. During the study, structured interview questions have been used. Data collected was obtained through official sources. Maritime higher education institutions providing education at the undergraduate level with fulltime employed academicians (with maritime background) have been evaluated via the data obtained using the methods of statistical analysis.

Keywords: Academician, Maritime Higher Education, Student

*****This paper was presented in Congress of IMLA 20 "International Maritime Lecturer Association" conducted in 02-05 July 2012, in Terschelling-The Netherlands.

1. INTRODUCTION

Last twenty years, when trouble is taken all over the world about the qualified officer, the academicians with maritime background who was needed to train qualified seafarer was behind the scenes. To train a skilled officer, first the necessity of qualified instructors who have experienced on the sea service, have been expressed on all platforms. Nevertheless, about transforming qualified officers into academicians, the situation of not been created attractive opportunities is also known. In this study, analysis of the profile information of academician with maritime background who is employed as fulltime staff in maritime education institutions at the bachelor level in Turkey has been made.

2. THE BRIEF HISTORY OF MARITIME EDUCATION IN TURKEY

The maritime education in Turkey dates to Ottoman Empire. The first school, named Merchant Navy Boarding School (Leyli Tüccar Kaptan Mektebi), was establish in 15th December 1884 at Heybeliada Istanbul [6].

In 1909, Merchant Navy Boarding School was closed and National Merchant Marine School (Milli ve Hususi Ticaret-i Bahriye Kaptan ve Çarkçı Mektebi) was established (National Council, 2000).

In 1928, National Merchant Marine School (Milli Ticaret-i Kaptan Mektebi) was closed and Merchant Marine School (Ticaret-i Bahriye Mekteb-i Alisi) was opened by the state. According to the regulation of the school, becholar degree was given to the graduates. After 1934, the school was named as Merchant Marine School (Yüksek Deniz Ticaret Mektebi).

From 1946 till 1981 name of school was called as Merchant Marine Academy (Yüksek Denizcilik Okulu). After the military intervention in 1980 the Academy was given under responsibility of the Navy and the moved to Tuzla (Karakaya, 2011).

From 1981 till 1988 school name was called Maritime High School and Commander of Training Center (National Council, 2000). In 1988, the school was re-established as a Maritime Faculty and tied to the Istanbul Technical University [1]. At the same year, School of Maritime Business and Management of Dokuz Eylul University was established in Izmir. The following years respectively, Istanbul University (1991), Karadeniz Technical University (1996) and Near East University (1996) were established maritime education and training institutions [7].

As of 2012, the number of universities providing maritime training at the bachelor degree is 11. Granting institutions of higher education in Turkey, divided into two groups as the bachelor's and associate's degree programs according to the duration of education. The numbers of university offering associate degree in maritime education is 8. In the Table 1, as of 2011, numbers of institution providing maritime training and education at officer level, degrees of education, capacities of deck and Engine departments and total capacities in Turkey are shown.

Table 1: Student Capacity of Maritime Education Institutions in Turkey in 2011

	Level of Education -STCW-	Number of Institutions	Capacity of Student (Deck)	Capacity of Student (Engine)	Total Capacity
Faculty and School	Op.*and Man.*	11	781	459	1240
Vocational High School	Operation	8	395	355	750
Vocational School	Restricted Op.	33	1469	1268	2737
TOTAL		**52**	**2642**	**2080**	**4722**

*Op.: Operation Level; Man.: Management Level

When Table 1 is examined, annual capacity of educational institutions providing maritime training at operational and management levels, can be seen that 4722 student. Utilizing that this capacity's fullness and percentage of graduates prefer to work at the sea is excluded from the scope of this study.

In Table 2, as of 2011, analyzing about education institutions at the bachelor degree in Turkey is shown. Table was prepared utilizing the data of The Student Selection and Placement Center (OSYM). 11 of 14 educational institutions are active and 3 of them don't accept any students for now as shown in Table 2. 5 of 11 active institutions are providing both deck and engine officers training. The others are providing only one of two. Three educational institutions that is not currently active, are working to fulfill requirements of Ministry of Maritime, Transport and Communication in line with the provisions of STCW. Moreover, these institutions use Academician Trainee Programs of Council for Higher Education for supply of academician with maritime background.

Table 2: Higher Education Institutions Providing Education in Deck and Engine Officer in Turkey and Their Undergraduate Capacity in 2011

	Educational Institution's Name	Started Years	Capacity	
			DECK	ENGINE
1	ITU- Istanbul Technical University Maritime Faculty *[1]	1884	187	130
2	IU- Istanbul University Faculty of Engineering	1991	72	-
3	DEU- Dokuz Eylul University Maritime Faculty *[2]	1995	78	42
4	KTU- Karadeniz Technical University Surmene Faculty of Marine Science	1996	77	-
5	NEU- Near East University Faculty of Marine Studies	1996	70	50
6	OU- Ordu University Fatsa Faculty of Marine Science	2003	-	-
7	PRU- Piri Reis University Maritime Faculty	2008	120	120
8	YTU- Yildiz Technical Uni. Maritime Architecture and Maritime Faculty	2008	-	57
9	RTE- Recep Tayyip Erdogan University Turgut Kiran Maritime High School	2009	72	-
10	ZIRVE- Zirve University Faculty of Engineering	2010	60	60
11	GIRNE- Girne American University Marine School	2011	45	-
12	BAU-BalikesirUniversity Bandirma Maritime Faculty	**-**	**-**	**-**
13	KCU- Katip Celebi University Faculty of Shipbuilding and Marine	-	-	-
14	BTU- Bursa Technical University Maritime Faculty	**-**	**-**	**-**
	TOTAL		**781**	**459**
			1240	

*[1] Inc. joint program with US Maine Maritime Academy
*[2] Inc. program in North Cyprus Campus and joint program with US Sunny Maritime College

Source: The Student Selection and Placement Center (OSYM)

Universities in Table 2 are sorted as the years beginning of the academic education. Istanbul Technical University Maritime Faculty observed as the highest capacity. Co-operative programs have been included in this capacity. In Turkey, officer education institutions at the bachelor degree give operation and management levels of the STCW both together and in 4 years. In this respect, in Turkey, the student capacity of bachelor degree officer education in 2011 is 1240 students. The range of the overall student capacity in years is shown in Table 2.

Table 3 shows the distribution of the capacity the educational institutions providing deck officer education by the years. Table 4 shows the distribution of the capacity the educational institutions providing engine officers by the years.

Table 3: Distributions of the Universities' Capacities that Gives Education in Deck Officer in Turkey by the Years

	ITU*[1]	IU	DEU*[2]	KTU	NEU	PRU	RTEU	ZIRVE	GIRNE	TOTAL CAPACITY
1990	62									**62**
1991	62	26								**88**
1992	62	31								**93**
1993	103	31								**134**
1994	103	31								**134**
1995	101	31	31							**163**
1996	103	46	31	41	150					**371**
1997	103	46	31	26	100					**306**
1998	103	42	31	26	60					**262**
1999	103	42	31	26	44					**246**
2000	103	42	41	31	44					**261**
2001	103	53	41	31	40					**268**
2002	103	62	52	52	25					**294**
2003	128	62	52	50	25					**317**
2004	133	62	52	52	24					**323**
2005	143	62	52	52	24					**333**
2006	143	62	52	52	44					**353**
2007	143	62	52	52	53					**362**
2008	153	72	62	62	64					**413**
2009	153	72	62	62	64	84	62			**559**
2010	154	72	67	77	70	100	72	60		**672**
2011	187	72	78	77	70	120	72	60	45	**781**
2012	198	77	83	82	70	120	77	40	70	**817**

*[1] Inc. program in North Cyprus Campus and joint program with US Sunny Maritime College
*[2] Inc. joint program with US Maine Maritime Academy

Source: The Student Selection and Placement Center (OSYM)

Table 4: Distributions of the Universities' Capacities that Gives Education in Marine Engineering in Turkey by the Years

	ITU*[1]	NEU	DEU*[2]	PRU	YTU	ZIRVE	TOTAL CAPACITY
1990	41						**41**
1991	41						**41**
1992	41						**41**
1993	52						**52**
1994	52						**52**
1995	50						**50**
1996	52	150					**202**
1997	52	100					**152**
1998	52	60					**112**
1999	52	44					**96**
2000	52	44					**96**
2001	52	40					**92**
2002	52	25					**77**
2003	77	25					**102**
2004	82	5					**87**
2005	77	10					**87**
2006	16	25	87				**128**
2007	21	25	87				**133**
2008	87	43	26				**156**
2009	97	43	26	90	52		**308**
2010	97	50	31	100	57	60	**395**

2011	130	50	42	120	57	60	**459**
2012	142	50	47	120	62	40	**461**

*[1] Inc. program in North Cyprus Campus and joint program with US Sunny Maritime College
*[2] Inc. joint program with US Maine Maritime Academy

In Figure 1, it was visualized the capacities of the institutions that provides Deck and Engine Officer Education. One interesting point is the fact that there was dramatically an increase in the capacities after the years of 1996 and 2009.

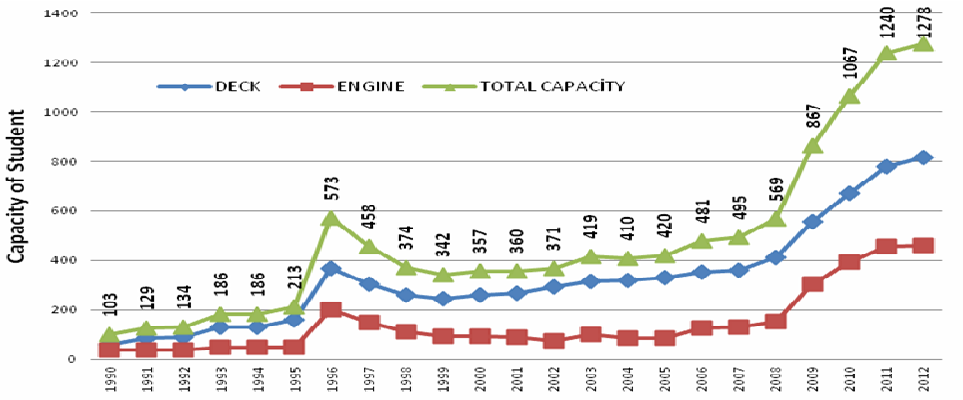

Fig. 1 Total Capacities of Student with Bachelor Degree, by the Years

The rapid increase in the number of institutions that provides education to students requires a parallel increase in the number of academicians that provides education with the same rate. But, the increasing rate of the academicians with maritime background has been well below the increasing number of institutions. The most important question is: *Is it sufficient to increase the number and capacity of the educational institutions in order to meet the qualified seafarer needs of maritime industry*?

The number of educational institutions providing manpower to the maritime industry has rapidly increased in the last decade. Moreover, there have been a lot of investments in laboratories, classrooms and simulators in order to enable sufficient training. Still everybody can see that the most important factor is an investment in 'human capital'. In other words, highly educated, skilled trainers who create added value by educating seafarers are the most valuable resource for the maritime industry (Nas, 2011). Sag (2010), provides some kind of solutions to handle this asymmetrical increase in the academician numbers. In the long run, universities, such as ITU, YTO, DEU, KTU, PRU and IU should open Deck and Engine departments' doctorate programs in the five years. In this special field of area, academicians with maritime background must be educated.

3. METHODOLOGY

In order to collect the profile data related to Academicians with Maritime Background, the structured interview form was prepared. In this interviews, genders, age, marital status, certification as officer, duration of employment, type of employment, and the titles of the participants was asked. The structured interview form was sent to the head of the departments, university managers and academicians with the legal permission letter for the

application of this study. The return of the data was provided by e-mails, telephones via postal services. In data was collected until the end of January, 2012.

4. SAMPLING

Target population of the study is constituted as academicians who service on maritime education at the level of undergraduate engaged to the HEC (Higher Education Council). In this study, institutions at the undergraduate level are limited to the deck and engine officers. The scope of “Academician with maritime background” concept is limited to graduated from Naval Academy, who has a unlimited watchkeeping officer/ engineer based maritime education at undergraduate level and who has title the Maritime Transportation Engineer. If the scope of “Academician” concept is limited to human resources who are employed as fulltime staff “with maritime background” at universities.

In this study, 111 academicians with maritime background who are employed at the associate’s and undergraduate degree maritime institution in Turkey have been identified. Yet, scope of the study focused academician who is employed maritime institutions at undergraduate degree. Therefore sample size was 89 academicians.

When evaluating data from the study observed that the academic staff employed in several institutions at the same time. To avoid misleading numbers, only academicians who are employed full-time were evaluated. Data concerning 89 Academician with maritime background who is employed at faculty and school is gathered. Academicians under the “Academician Trainee Programs” were evaluated in the universities where the main fulltime staff.

5. THE FINDINGS OF THE ANALYSIS AND STUDY

The findings obtained in the study have been analyzed with SPSS 20. Table 5, as a result, shows the average sea service, gender distribution and the age range of the academicians providing maritime education in Turkey. In Turkey, the number of academicians at the undergraduate maritime institutions is 89. Their average sea service period is 4, 99 years. The academicians with the most experience on sea service at the private foundation universities.

The age range of the academicians with maritime background varies between 24 and 66. The average age is 37, 24. The institution with the highest average age is Piri Reis University (54, 33).

The number of female academicians at the undergraduate institutions providing maritime education is 11. The proportion of the female academicians to the whole academicians in the maritime institutions is 12%. Istanbul University has the highest number of female academicians. It is followed by Istanbul Technical University (3), RTE University (2). In addition to that, there are no female academicians employed on maritime higher institutions at the Yildiz Technical University, Ordu, Zirve, Girne, Balikesir, Bursa and Katip Celebi Universities.

Table 5: The Sea Service Period, Gender and Age Distribution of the Academicians with Maritime Background Employed at Maritime Institutions

Num.	Name of Institution	Sea Service (year)	Mean Age	Gender		Number of Academi
				F	M	
1	NEU- Near East University Faculty of Marine Studies	19,33	50,75	-	9	**9**
2	GIRNE- Girne American University Marine School	15,00	46,00	-	1	**1**
3	PRU- Piri Reis University Maritime Faculty	10,16	54,33	-	9	**9**
4	ITU- Istanbul Technical University Maritime Faculty *[2]	7,10	37,24	3	22	**25**
5	KTU- Karadeniz Technical Uni. Surmene Faculty of Marine Science	6,02	37,90	1	9	**10**
6	DEU- Dokuz Eylul University Maritime Faculty *[1]	5,70	36,00	1	13	**14**
7	ZIRVE- Zirve University Faculty of Engineering	4,00	33,00	-	1	**1**
8	RTE- Recep Tayyip Erdogan University Turgut Kiran Maritime School	1,33	27,16	2	4	**6**
9	YTU- Yildiz Technical Uni. Maritime Architecture and Maritime Faculty	0,62	33,00	-	3	**3**
10	OU- Ordu University Faculty of Marine Science	0,33	24,66	-	3	**3**
11	IU- Istanbul University Faculty of Engineering	0,26	33,40	4	1	**5**
12	BAU-BalikesirUniversity Bandirma Maritime Faculty	0,00	25,00	-	1	**1**
13	BTU- Bursa Technical University Maritime Faculty	0,00	24,00	-	1	**1**
14	KCU- Katip Celebi University Faculty of Shipbuilding and Marine	0,00	27,00	-	1	**1**
	Total/ General Average	**4,99**	**37,24**	**11**	**78**	**89**

The academicians with maritime background who started their academic career at universities continue their master's or doctoral education either at their home university or other universities. As of January 2012, Table 6 shows the standing of the academic career of the academicians with maritime background. Through analysis, it has been identified that the highest number of academicians employed at Istanbul Technical University. In terms of the academicians, ITU is followed by DEU (14) and KTU (11). PRU, which started accepting students in 2009, follows these universities. It has been identified that there are 4 professors with maritime background.

Table 6: Academic Career of the Academicians with Maritime Background

Number	Name of Institution	Total	Bachelor Degree	Master Degree	Doctorate	Asst Prof.	Assoc. Prof.	Prof. Dr.
1	ITU- Istanbul Technical University Maritime Faculty	**25**	11	4	1	7	1	-
2	DEU- Dokuz Eylul University Maritime Faculty	**14**	5	5	-	2	2	-
3	KTU- Karadeniz Technical Uni. Surmene Faculty of Marine Science	**10**	3	5	1	1	-	
4	PRU- Piri Reis University Maritime Faculty	**9**	3	-	-	3	-	3
5	NEU- Near East University Faculty of Marine Studies	**9**	7	2	-	-	-	-
6	RTE- Recep Tayyip Erdogan Uni. Turgut Kiran Maritime School	**6**	6	-	-	-	-	-
7	IU- Istanbul University Faculty of Engineering	**5**	-	-	3	2	-	-
8	YTU- Yildiz Tech. Uni. Maritime Architecture and Maritime Faculty	**3**	1	1	-	-	-	1
9	OU- Ordu University Faculty of Marine Science	**3**	3	-	-	-	-	-
10	ZIRVE- Zirve University Faculty of Engineering	**1**	1	-	-	-	-	-
11	GIRNE- Girne American University Marine School	**1**	1	-	-	-	-	-
12	BAU-BalikesirUniversity Bandirma Maritime Faculty	**1**	1	-	-	-	-	-
13	BTU- Bursa Technical University Maritime Faculty	**1**	1	-	-	-	-	-
14	KCU- Katip Celebi University Faculty of Shipbuilding and Marine	**1**	1	-	-	-	-	-
	TOTAL	**89**	**44**	**17**	**5**	**15**	**3**	**4**

Table 7 shows the relation between the capacity of the undergraduate educational institutions in Turkey and the number of the academicians with maritime background. According to that, the number of students for one academician is 13,93. This figure is a reference point for the educational institutions that are planned in the future.

As of January 2012, when total annual capacity of institutions (1240) is considered, during the four years education in undergraduate level, all educational institutions total capacity of students can be predicted approximately 4960. The average number of students per academician with maritime background can be calculated as a 26,24.

Table 7: The Numbers of Student Per Academician with Maritime Background at the Undergraduate Level.

Num	Name of Institution	Capacity of Student	Numbers of Academician	Numbers of Student Per Academician
1	ITU- Istanbul Technical University Maritime Faculty	317	25	12,68
2	PRU- Piri Reis University Maritime Faculty	240	9	26,67
3	DEU- Dokuz Eylul University Maritime Faculty	120	14	8,57
4	NEU- Near East University Faculty of Marine Studies	120	9	13,33
5	ZIRVE- Zirve University Faculty of Engineering	120	1	120,00
6	KTU- Karadeniz Technical Uni. Surmene Faculty of Marine Science	77	10	7,70
7	IU- Istanbul University Faculty of Engineering	72	5	14,40
8	RTE- Recep Tayyip Erdogan University Turgut Kiran Maritime School	72	6	12,00
9	YTU- Yildiz Tech. Uni. Maritime Architecture and Maritime Faculty	57	3	19,00
10	GIRNE- Girne American University Marine School	45	1	45,00
11	OU- Ordu University Faculty of Marine Science	-	3	-
12	BAU-BalikesirUniversity Bandirma Maritime Faculty	-	1	-
13	BTU- Bursa Technical University Maritime Faculty	-	1	-
14	KCU- Katip Celebi University Faculty of Shipbuilding and Marine	-	1	-
	TOTAL	**1240**	**89**	**Mean 13,93**

Table 8 lists the academicians with maritime background and the education institutions at which they completed their undergraduate education.

Table 8: Distribution of the Academicians with Maritime Background and the Education Institutions at Which They Completed their Undergraduate Education

Name of Institution	Numbers of Academician
ITU- Istanbul Technical University Maritime Faculty	42
IU- Istanbul University Faculty of Engineering	16
KTU- Karadeniz Technical University Surmene Faculty of Marine Science	10
Naval Academy	9
DEU- Dokuz Eylul University Maritime Faculty	6
NEU- Near East University Faculty of Marine Studies	2
YTU- Yildiz Technical University Naval Architecture and Maritime Faculty	2
Others	2
Total	**89**

Istanbul Technical University was established in 1884 and has been giving maritime education since then under different names and graduated 42 academicians. Istanbul University, starting after ITU, graduated 16 academicians. It is followed by Karadeniz Technical University (10), Naval Academy (9), Dokuz Eylul University (6), Near East University (2), and Yildiz Technical University (2).

6. CONCLUSIONS

For last two decades, number and capacity of MET Institutions have been increased by very unplanned and unscheduled in Turkey. How long will this unplanned and arbitrary increase continue to? When the total capacity of students reach to a number more than 5000 in undergraduate level, how many of them will be able to find opportunity to make their sea service on board ships? While these questions are waiting for some answers, will this - speculatively created- enormous capacity turn our country into a country that can export manpower abroad? Such question must be taken into consideration.

According to researches conducted, it is seen that, there some institutions that haven't accepted students while their aim of establishing was to accept them, and that, beacuse of its popularity, it is planned to settle a maritime education faculty in each of the cities, and that over capacities on the current branch are continuously, arbitrarly, increased. But, how much increase has been seen in the number of academicians with maritime background who expected to create value, provide training to this enormous capacity? Until 1990, only institution providing maritime education and trainee in undergraduate level ITU' s capacity was 103 student, but now all educational institutions's total capacity is 1278 (As of July, 2012).

In contrast with enormous increase 12 fold, it is necessity to question the increasing number of academician with maritime background. This study aims to make the current status more clear. In the studies to be executed from now on, it is necessary to perform a need – analysis on the number of qualified officers that are needed by our country and on the quantity of manpower to be exported, then according to the evaluated data, it is essential to determine the number of required academicians.

Another important issue is that, being an academician with maritime background has its own difficulties and hardships in our country and it requires physical and emotional self - sacrifice. Academic life, as a long and exhausting process, must be made more popular, more supported and more encouraged. "

"The Academician Trainee Programs" being organised and coordinated by Higher Education Council are well promising projects for training qualified academicians who is needed by maritime education.

REFERENCES

[1]. BIMCO/ISF***, Manpower 2010 Update,*** , Institute for Employment Research University of Warwick, Team Impression Ltd. 2010.

[2]. Karakaya, M M. ***Cumhuriyet Döneminde Ticari Denizcilik Eğitiminin Tarihsel Gelişimi (1928-1981).*** Basılmamış Yüksek Lisans Tezi. İstanbul Üniversitesi Atatürk İlke ve Inkilap Tarihi Enstitüsü. İstanbul, 2010

[3]. Nas, S. ***Transas News***, http://www.transas.com, accessed 12.05.2012, 2010

[4]. National Maritime Council, ***Eğitim Çalışma Grubu Raporu,*** 2000
[5]. Sag, O K. “Sorunlar ve Çözüm Önerileri 2”. Deniz Ticareti. Mart 2010, p. 30-36, 2010
[6]. www.maritime.itu.edu.tr accessed 01.02.2012
[7]. http://www.osym.gov.tr/dosya/1-57952/h/2011tablo4-2172011.pdf accessed 27.4.2012
[8] http://personel.yok.gov.tr/AkademikDuyuru/?sayfa=yonetmelik accessed 13.02.2012

SIMULATION BASED TRAINING ON MARITIME EDUCATION AND APPLICATION ON ICE NAVIGATION MODULE

[1]TÖZ ALİ CEMAL, [2]KÖSEOĞLU BURAK

[1,2]Dokuz Eylül University Maritime Faculty,Izmir, Turkey

From the shipping industry's point of view cold winters mean nothing else than trouble. Navigation in Arctic waters is unique compared to all other ship operations. Significant changes in climate and their impacts are visible regionally and are expected to become more pronounced in the next decades. Trade in ice covered waters continues to grow and increasingly, operators looking for future flexibility are building ships classed for operations in ice. In the future the Northwest Passage and Northern Sea Route are likely to provide alternative shipping lines for international trade. Ice navigation is probably the most difficult and challenging mode of navigation possible. Few other areas of maritime operation are exposing the ship and its crew for more dangerous situations.

The use of ship-bridge simulators is becoming an accepted method of training in the maritime education. Many simulator-based training courses were developed ad hoc, often designed to individual requirements of a shipping company or training establishment. For ice navigation module, the goal of training module is to reduce the risks of winter navigation and to ensure safe operations even in severe ice conditions.

This article aims to analyze effectiveness of maritime simulation systems on strengthening the maritime training for ice navigation module in Dokuz Eylül University Maritime Faculty.

***Keywords*:** simulation, maritime training, global warming, ice navigation.

1. INTRODUCTION

The Earth's climate has warmed by approximately 0.6 8C over the past 100 years with two main periods of warming, between 1910 and 1945 and from 1976 onwards. The rate of warming during the latter period has been approximately double that of the first and, thus, greater than at any other time during the last 1,000 years (Third Assessment Report of the Intergovernmental Panel on Climate Change - IPCC ,2001)

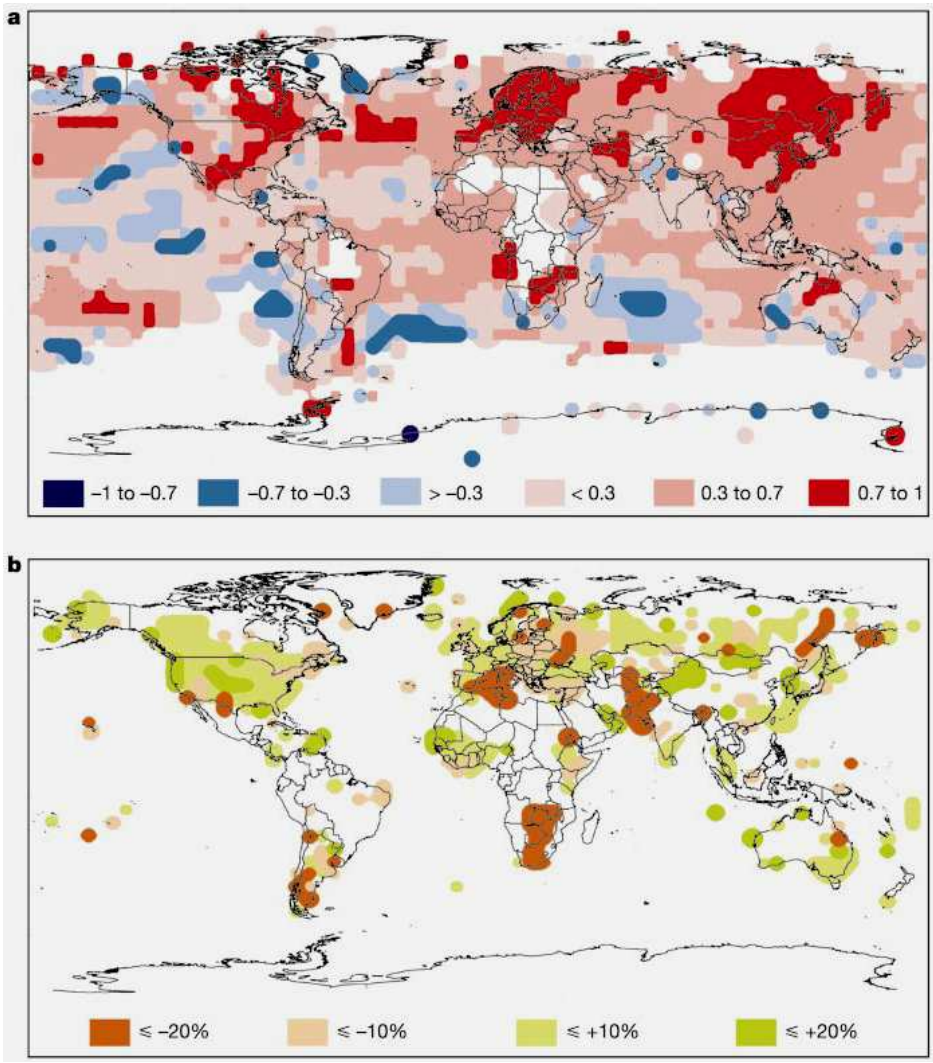

Fig. 1. Spatial variability of annual trends in temperature and precipitation since 1976 relative to 1961 to 1990 normal's (ref. 1, modified): a, Temperature (8C per decade); b, precipitation (% per decade).
Source: *Walther, et. al., 2002; 390*

2. GLOBAL WARMING AND CLIMATE CHANGE

On a global scale, there is increasing evidence that climate is changing. Increased concentrations of greenhouse gases in the atmosphere due to human activities are believed to be the underlying cause of the change in global climate.

Since 1860, mean global temperatures have risen by between 0.3℃ and 0.6℃.Warming since the mid-1970s has been particularly rapid with nine of the ten warmest years have occurred since 1990, including 1999 and 2000 despite cooling influence of the tropical Pacific La Niña which contributed to a somewhat lower global average (0.29℃ and 0.26℃ above average, respectively) (IPCC, 2001).

The fact that concentrations of carbon dioxide in the atmosphere are increasing is known to all ecologists; it is fair to describe this as the best documented global change. However, the uniqueness of the increase (at least in the past 200 000 yr), the thoroughness with which it has been documented, the level of certainty concerning its causes, and the multiple consequences of elevated carbon dioxide concentrations are not well understood by the educated public. The results display two major signals: a seasonal cycle that reflects the metabolism of terrestrial ecosystems in the northern hemisphere (Fung et al. 1987) and an accelerating increase in troposphere concentrations throughout the period of record.

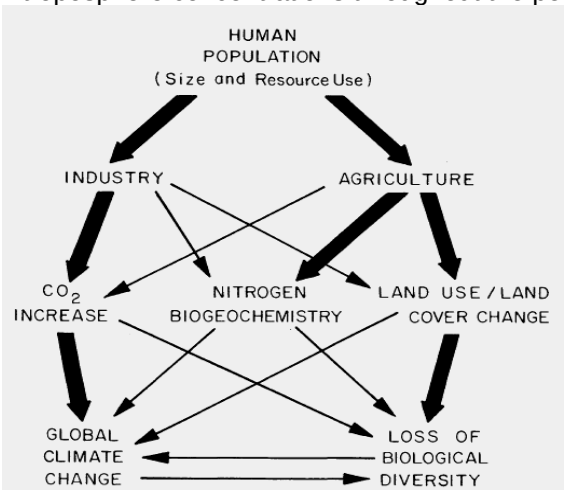

Fig. 2. The components of global environmental
Source: *Vitousek, 1994*

The warming trend is spatially widespread and is consistent with the global retreat of mountain glaciers, reduction in snow-cover extent, the accelerated rate of rise of sea level during the 20th century relative to the past few thousand years, and the increase in upper-air water vapor and rainfall rates over most regions. The ocean, which represents the largest reservoir of heat in the climate system, has warmed by about 0.05℃ averaged over the layer extending from the surface down to 10,000 feet, since the 1950s. A decline of about 10% in spring and summer continental snow cover extent over the past few decades also has been observed. (IPCC, 2001).

2.1 Observed Changes in Sea Ice Extent and Concentration

Sea ice is important because it regulates exchanges of heat, moisture and salinity in the polar oceans. It insulates the relatively warm ocean water from the cold polar atmosphere except where cracks, or leads, in the ice allow exchange of heat and water vapor from ocean to atmosphere in winter.

2.2. Climate and Ice Condition in Arctic

The Arctic region has been a central focus of many climate change studies in recent years, both because of the large amount of change seen in the Arctic (Comiso and Parkinson, 2004) and because of the expectations of an amplified climate signal in the Arctic

due to the ice-albedo and snow-albedo feedback effects associated with the high reflectivity of ice and snow (Holland and Bitz, 2003). Among the changes in the Arctic are increasing melt areas over the Greenland ice sheet, retreating glaciers, reduced sea ice coverage, permafrost thawing, and rising surface temperatures (ACIA, 2005).

One of the most remarkable of the quantified changes in the Arctic is the 9 – 10% decline per decade in the perennial sea ice cover during the SMMR/SSMI era (Comiso, 2002; Stroeve et al., 2007). Perennial ice is the ice cover that remains during minimum ice extent and consists mainly of thick multiyear ice floes. These ice floes are the mainstay of the Arctic Ocean sea ice cover. The Arctic perennial ice is accompanied through much of the year by considerable additional but much younger sea ice termed seasonal ice because of not lasting through the entire year. Together, the perennial and seasonal ice constitute the full Arctic sea ice cover. The full ice cover has also been decreasing, but until recently this has been at the more modest rate of about 3%per decade (e.g., Bjorgo et al., 1997; Parkinson et al., 1999; Parkinson and Cavalieri, 2002). We report here both that the perennial ice is showing enhanced signs of its rapid demise and that the decrease in the full ice cover has now speeded up to the point that it is experiencing the much higher retreat rates earlier reported for the perennial ice alone.

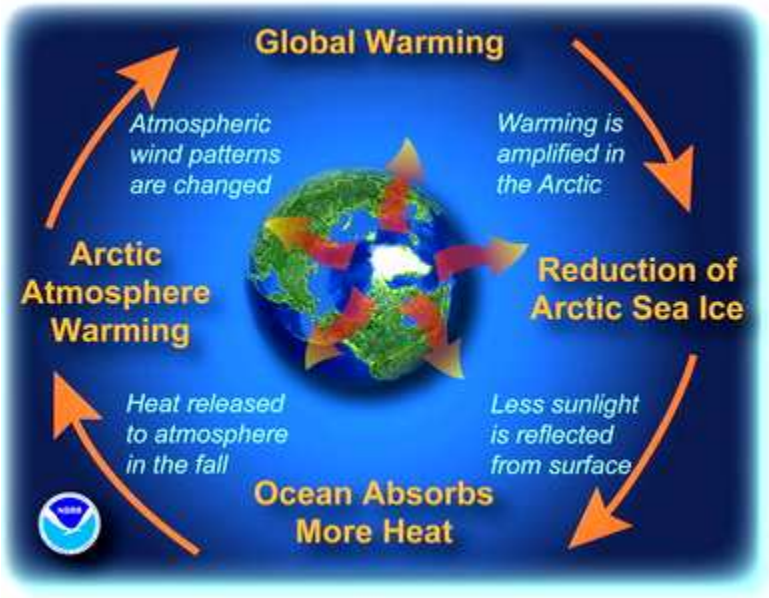

Fig. 3. The components and effects of global warming
Source: *www.noaa.org*

3. COMMERCIAL SHIPPING ON THE NORTHERN SEA ROUTE (NSR)

Nowadays the melting of the arctic ice opens the new maritime route between the markets of Northern Asia and North-Western Europe, passing through the Arctic Ocean Northern Sea Route, or also so-called North-East Passage- as a possible alternative for Royal route through the Suez Canal. The Northern Sea Route is a shipping lane from the Atlantic Ocean to the Pacific Ocean along the Russian Arctic coast from the Barents Sea, along Siberia, to the Far East. Historically the motivation to navigate the Northeast Passage was initially economic. Sea ice in Arctic Regions continues to decrease each year. Most

climate models predict an absence of perennial sea ice by the year 2030 (Chernova and Volkov, 2010).

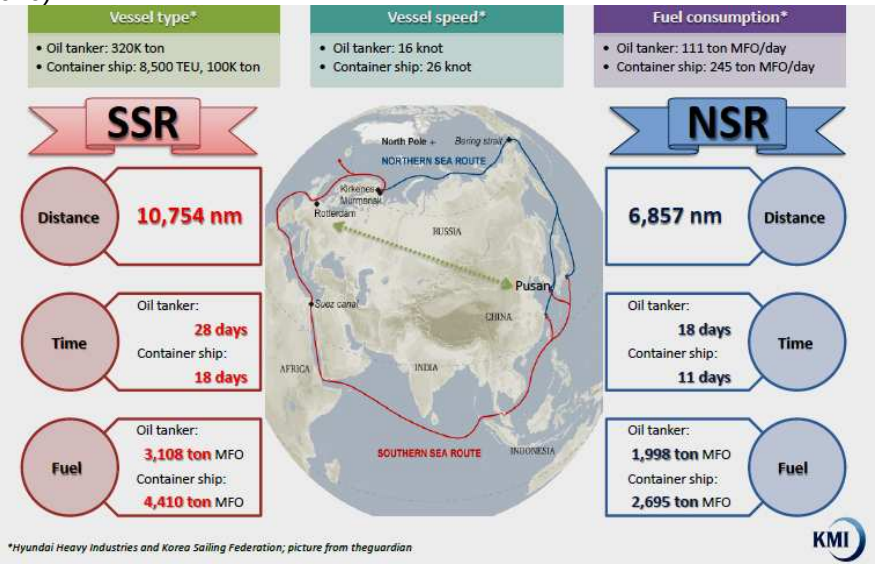

Figure 4: Comparison Northern(Arctic) Shipping Route (NSR)with Southern Shipping Route (SSR)

Source: *Cho, The Melting Arctic Changing the World: New Sea Route*

Several seaports along the NSR are ice-free all year round (Laiho, et al., 2005). They are, west to east, Murmansk on the Kola Peninsula, and on Russia's Pacific seaboard Petropavlovsk in Kamchatka, Vanino, Nakhodka, and Vladivostok (Laiho, et al, 2005). Arctic ports are generally usable July to October, or, such as Dudinka, are being served by nuclear powered icebreakers. Since its discovery the Route was mainly used by Russia, but not by other countries. Only explorers were travelling for the whole route, others were using only ice-free part of it for reaching northern part of the middle Russia. After the breakup of the Soviet Union in the early 1990s, commercial navigation in the Siberian Arctic went into decline. (Laiho, et al., 2005).

During the last ten years the interest to the Northern Sea Route is increasing. In 1998 NSR has received the status of independent Eurasian maritime transport corridor. Also Russia has published the Rules to be followed on the Northern Sea Route, signing the navigation description, ecological and safety norms. Discovery of oil fields and natural gas in the arctic has led to an increased interest in the development of ice-breaking cargo vessels and/or tankers for use in transporting these resources to refineries and consumers at remotely situated markets.

Table 1: Comparison of Distances Through Suez Canal and NSR

Shipping distance from Hamburg to				
	Vancouver	Yokohama	Hong Kong	Singapore
NSR	6635	6920	8370	9730
Suez Canal	15377	11073	9360	8377

Source: Moe and Jensen,2010

Floating markers are not practical in ice prone areas. Markers can be repositioned by shifting ice sheets or snagged by ice jams and pulled out of position. In some areas navigation markers can be removed during the worst conditions but some areas are never fully free of floating ice (www.maritime.about.com).

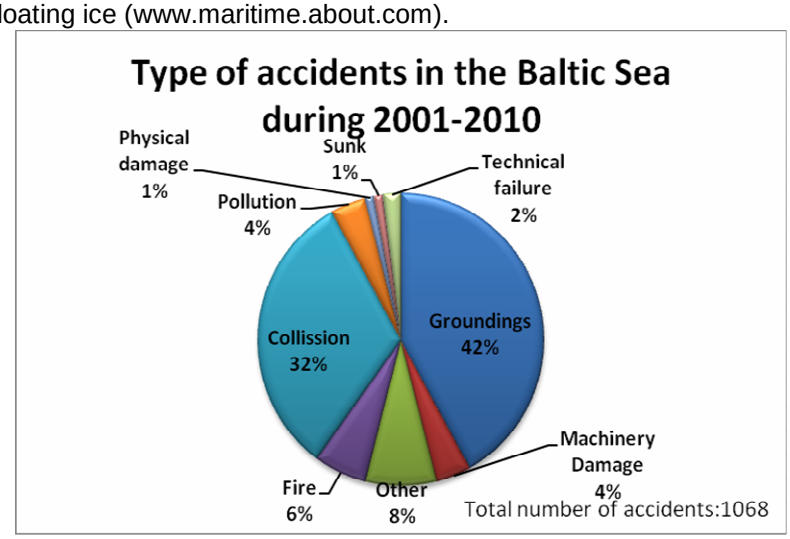

Fig. 5. Types of accidents in the Baltic Sea during 2001-2010
Source: *www.helcom.fi*

The main types of shipping accidents in Baltic Sea Area during 2001-2010 were 32% collision and 42% groundings. Fire made up 6% of the shipping accidents. In this time pollution and machinery damage were 4%. Technical failures were 2%, sunk and physical damages were 1%. Other unspecified reasons accounted for 8% of the reported shipping accidents during 2001-2010 in the Baltic Sea Area.

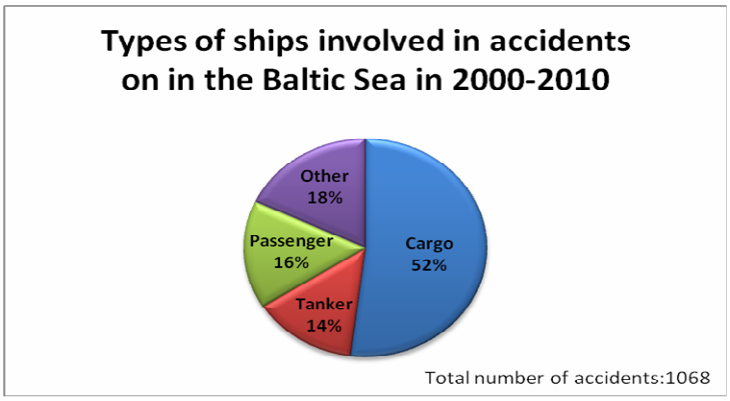

Fig. 6 Types of ships involved in accidents in the Baltic Sea in 2000-2010

Source: *www.helcom.fi*

The main types of shipping accidents in Baltic Sea Area during 2000-2010 were 52% cargo ships, 16% passenger ships, 14% tanker ships and 18% other types of vessels.

4. ICE NAVIGATION TRAINING COURSES

In December 2002, IMO recommended new guidelines for arctic navigation. The recommendation included a two level training regime where simulators can be used to some extent (Kjerstadt and Bjoerneseth, 2003). A recent revision to the Seafarers' Training, Certification and Watchkeeping (STCW) Code provides some training guidance for ice operations. The amendments adopted include new training guidance for personnel serving on board ships operating in polar water.

The Conference adopted a number of resolutions, including Conference Resolution 11 on Measures to ensure the competency of masters and officers of ships operating in polar waters. Furthermore, committee decided to develop training requirements and model course for navigation in polar waters, but no mandatory requirements until Polar Code adopted. But the IMO did not adopt proposals to establish minimum competency requirements for ship officers (http://www.dnv.com, 2012). That's why many enterprises developed their training program in different periods and contents. Different training programs developed by training centers all over the world, briefly explained under Table 2.

Table 2: International Ice Navigation Training Courses

No	Country	Training Centre	Day
1	Finland - Espoo	Icetrain Meriturva- Maritime Safety Training Centre	3
2	Finland - Turku	Aboa Mare	3
3	Finland - Kotka	Kymenlaakso University	3
4	Latvia - Riga	Novikontas Group-Maritime Training Centre	5
5	Latvia - Riga	Lapa Traning Centre	2
6	Denmark - Aoroe	Marstal Maritime Education Centre	4
7	Denmark	Maersk Training Centre	3
8	Philippines - Makati	TMS - Maritime Training Centre	1
9	Philippines - Wartsila	Wartsila	3
10	Russia - St. Petersburg	Admiral Makarov-State Maritime Academy	5
11	India - Mumbai	Anglo -Eartern Maritime Training Centre	3
12	Canada - New Foundland	Marine Institute of Memorial University	5
13	UK	South Tyneside College	5
14	Turkey - Izmir	Dokuz Eylül University	3

Source: Writer, 2012

TMS from Philippines has the minimum period of training structure with only one day training. Baltic countries where ice navigation mostly operated due to sub zero temperatures most of the time, has the longest periods of training structure.

In Turkey, Dokuz Eylul University Maritime Faculty also operates Ice Navigation training program with 3 days periods. Content of training programs developed with reference to codes and regulations mentioned below;

- IMO Arctic & Polar Shipping Guidelines,
- Guidelines For Ships Operating In Polar Waters,
- STCW Requirements Concerning Polar Areas,
- SOLAS Requirements Concerning Polar Areas and Related Guidelines Activities (Chapter V- Navigational Requirements),

- MARPOL Requirements Concerning Polar Areas,
- International Code of Safety for Ships in Polar Waters (Canada),
- The International Ice Navigators Course submitted by Transport Canada,
- CLASS recommendations (Writer, 2012) .

Within this period, many training methods such as simulation, cbt, theoretical and table top exercises have been performed for better solution mentioned in Table 3 and 4.

Table 3: Ice Navigation Training Content in DEU Maritime Faculty

Subject	Therotical	Cbt	Video	Table Top Exercise	Simulation
• Physical properties of ice • Ice conditions and types	❋	❋	❋		
• Navigation in ice • Ship handling in ice • Ship performance in ice. • Meeting and crossing situation • Towing operations and ice pilotage • Convoy formation	❋				❋
• Ice classification • Ice strengthening • Ice class ships design • Propulsion concepts	❋		❋		
• Icebreaker operations • Characteristics of icebreakers • Design of icebreakers • Icebreaker assistance	❋	❋	❋		
• Weather information systems • Ice information systems • Egg Code and ice charts	❋	❋	❋	❋	
• Planning the approach to forthcoming ice fields	❋		❋		❋
• Preparations before entering cold ambient	❋		❋		
• Watchkeeping during ice passage • Positioning methods • Operation and maintenance of bridge accessories	❋				❋
• Routines during navigation in ice infested areas	❋		❋		❋
• Accidents • Ice damage • Avoiding damages to hull and structure	❋		❋		
• Rules and regulations	❋				

Source: Writer, 2012

Table 4: Winterization Training Content in DEU Maritime Faculty

Subject	Therotical	Cbt	Video
• Operation and controlling of ballast tanks and piping systems • Operation of deck and machinery equipments	✲	✲	✲
• Operation, maintenance and protection of deck equipments	✲	✲	✲
• Icing and ship stability	✲	✲	✲
• Ice build-up processes	✲	✲	✲
• Methods for removing of ice	✲	✲	✲
• Effect of cold upon human organism • Proper clothing and outfits • Treatment of cold induced injuries	✲	✲	✲
• Anti Ice and De-Ice Equipments	✲	✲	✲
• Beware of freezing spray	✲	✲	✲
• Living Quarter	✲	✲	✲
• Protective Equipments	✲	✲	✲
• Group and personal survival equipment/kits and techniques	✲		✲

Source: Writer, 2012

Simulation based scenarios of ice navigation training conducted by bridge simulator. Many scenarios such as assisted and unassisted ship handling in ice covered area, berthing and unberthing maneuvering, meeting situation maneuvering, crossing situation maneuvering are conducted.Before advanced ship handling operations, firstly orientation of bridge simulator in ice covered water conducted. First scenario mainly aims at how ship reacts when she entered in ice covered area. This scenario basicly considered on turning circle discrepancies between ice free and ice covered areas highlighted below Figure 7.

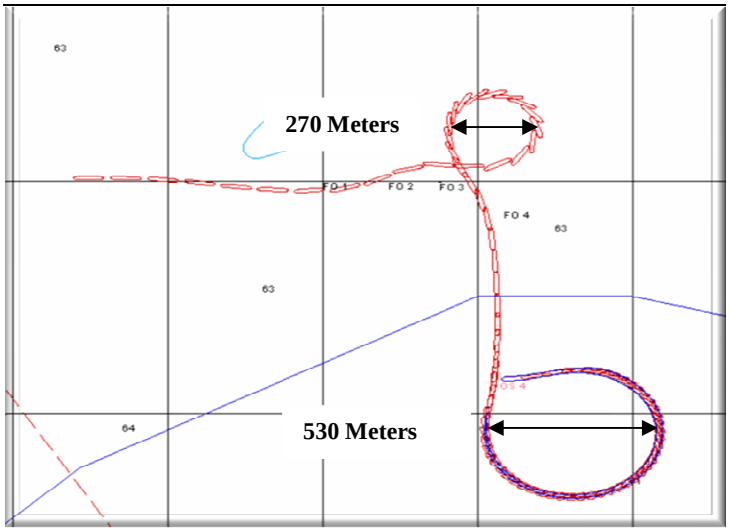

Fig. 7.Scenario 1: Comparison of Turning Circle Diameters in Ice Covered and Ice Free Areas

Source: Writer, 2012

Entering ice fields and proceeding to meeting point with ice breaker are the beginning of unassisted passage in ice navigation. After meeting with icebreaker chase up maneuvering begins and assisted navigation operation is conducted. This practice mainly aims of follow distance calculations, bridge to bridge communication practices and avoiding closing situations in ice canal mentioned in Figure 8.

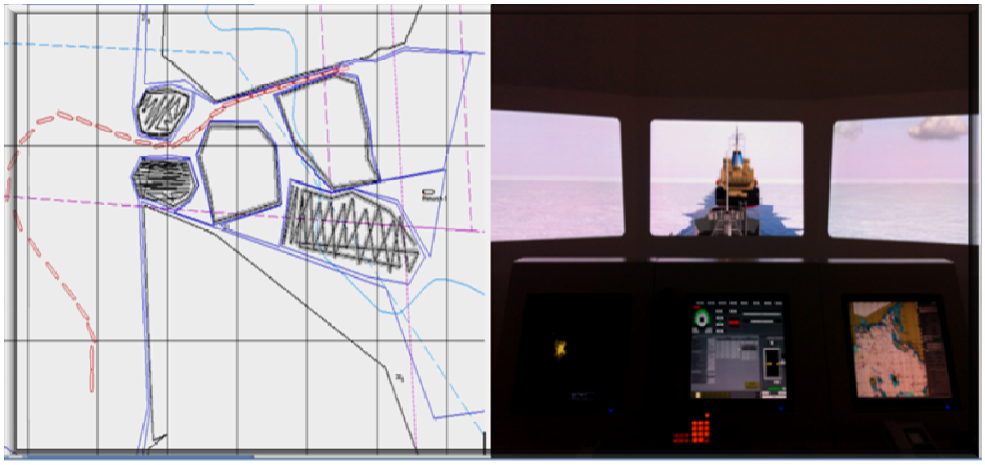

Fig. 8. Scenario 2: To Follow of Ice Breaker in Ice Canal (Assisted Navigation)
Source: Writer, 2012

The main *situations* of collision risk are overtaking, *meeting*, head-on, and crossing. Collision avoidance in ice canals by means of meeting of two ice canals are performed with bridge simulation. This scenario mainly aims to increase in bridge team work efficiency and awareness of collision situations mentioned below Figure 9.

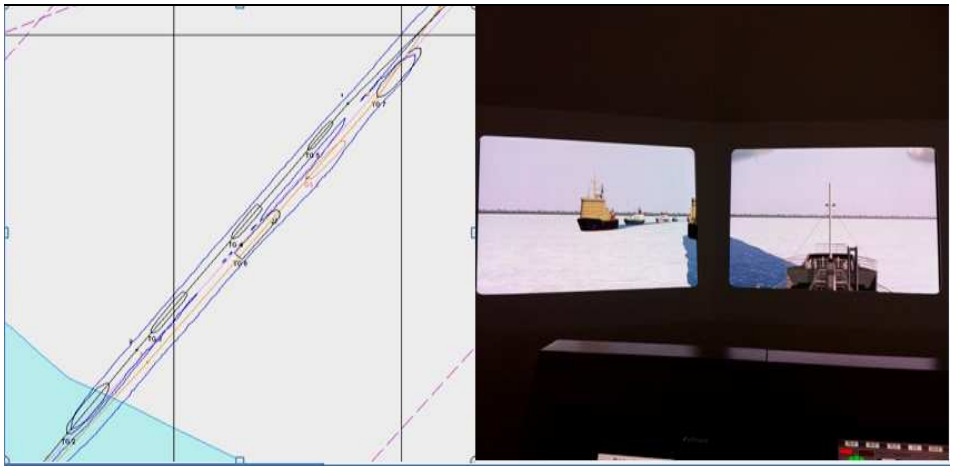

Fig. 9. Scenario 3: Meeting Situation of Ships in Different Ice Canal (Assisted Navigation)

Source: Writer, 2012

Berthing in ice-covered waters can be, and usually is, a long process, particularly in the Arctic where normally there are no tugs. When approaching a berth in ice-covered waters it

is desirable (even if this is not the normal practice) to have an officer stationed on the bow to call back the distance off the wharf or pier because a variation in ice thickness (not observed from the bridge) can result in a sudden increase or decrease in the closing speed of the bow and the wharf. Scenario 4 mainly aims to increase in efficient framework for berthing and unberthing operations.

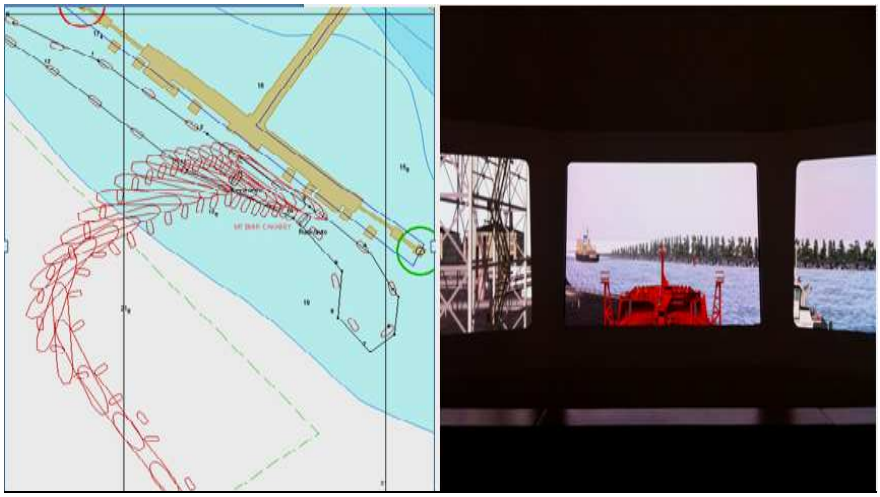

Fig. 10. Scenario 4: Berthing and Unberthing Operation Ship in Ice

Source: *Writer, 2012*

5. CONCLUSIONS

In the past the Northern Sea Route was difficult to pass through, but in recent years, the effects of global warming the potential of the route has emerged in terms of its use for commercial shipping. Increased traffic volumes in the Baltic Sea have created urgent demand for crews with relevant training. The crews are more and more from southern countries with no experience in ice navigation. Virtually minor operational mistakes due to ignorance can have costly impacts in the forms of damages and off-hire and major mistakes cause marine pollution and total losses

The labour situation within the maritime sector today and in the future is a topic that attracts much attention worldwide. Many fear that the maritime industry is entering a period where a massive shortage of qualified personnel can, among other factors, represent a possible threat to both quality and safety standards. Demand for efficient and high quality training of maritime personnel will continue to increase over the next decade. Key applications for simulation, such as training, decision support, procedure and mission planning will continue to be paramount for industry. Real life training using real equipment presents a number of challenges.

Increased risk to personnel and equipment combined with limited access to required marine assets and related escalating costs are creating an increased demand for simulation technology. Simulation under highly realistic circumstances presents a safer and more cost-efficient training alternative. Simulation has already proven its effectiveness and is, without doubt, the future of maritime training. Due to the almost unlimited possibilities provided by simulation, better results can be achieved in a safer, more efficient manner, which in turn produces higher quality personnel. Compared to the conventional training, simulators offer a more structured method of building high levels of competence. During simulation training,

one can isolate and freeze each sub-system to understand and acquire knowledge, perform critical operations over and over again to train skills, and test and develop attitudes by training in situations that demand complex decision making.

REFERENCES

[1]. Bjorgo, E., O. M. Johannessen, and M. W. Miles.- ***Analysis of Merged SSMR/SSMI Time Series of Arctic and Antarctic Sea Ice Parameters,***1978–1995, 413 – 416, 1997.

[2]. Climate Change 2001 - **T*hird Assessment Report of the Intergovernmental Panel on Climate Change - IPCC (WG I & II),*** Cambridge University Press, Cambridge, 2001.

[3]. Cho, Y. - ***The Melting Arctic Changing the World: New Sea Route. A Conference on Energy Security and Geopolitics in the Arctic: Challenges and Opportunities in the 21st Century*****,** 2011.

[4]. Comiso J. C., Parkinson C. L. - ***Arctic Climate Impact Assessment (ACIA),*** 2004.

[5]. Comiso, J. C. - ***A Rapidly Declining Perennial Sea Ice Cover in the Arctic***, Geophys. Res. Lett., 29(20), 2002.

[6]. Fung, I., Tucker , C., and Prentice, K.C. - ***Application of Advanced Very High Resolution Radiometer Vegetation Index to Study Atmosphere-Biosphere Exchange of CO2*****,** J. Geophys. Res. 92, 2999-3015, 1987.

[7]. ***Global Security, Arctic Ocean***, http://www.globalsecurity.org/military/world/war/ arctic.htm, 2012.

[8]. Walther G., Eric P., Peter C., A. Menzel, Camille P., Trevor J. C., Jean-Marc F. - ***Ecological Responses to Recent Climate Change***, 2002.

[9]. Holland, M. M., and C. M. Bitz. - ***Polar Amplification of Climate Change in Coupled Models, Clim. Dyn.***, 21, 221 – 232, 2003.

[10]. ***Helsinki Commission, Ship Accidents in the Baltic Sea Area*****;** IPCC, "Climate Change 2001: http://www.helcom.fi/shipping/accidents/en_GB/accidents/page 6, 2012.

[11]. ***International Requirements for Ships Operating in Polar Waters***, 2009.

[12]. Keeling, C. D., R. B. Bacastrow, A. F. Carter, S. C. Piper, T. P. Whorf, M. Heiman, W. G. Mook, and H. Roeloffzen - ***A Three-Dimensional Model of Atmospheric CO2 Transport Based on Observed Winds: Analysis of Observational Data,***165-236 in D. H. Peterson, editor. Aspects of Climate Variability in the Pacific and The Western Americas. Geophysical Monographs. American Geophysical Union, Washington, D.C., USA, 1989.

[13]. Laiho, L., Rahikainen, P., Jourio, B., Sala, S. - ***Legal and Administrative Issues of Arctic Transportation, Ministry of Trade and Industry,*** Finland, 2005.

[14]. ***Low Temperature Operations Guidance for Arctic Shipping, ABS Winterization Guidelines for LNG/CNG Carriers in Arctic Environments***, 2006.

[15]. ***Maritime, Arctic Shipping Routes***, http://maritime.about.com/od/Climate/a/The-Future-Of-Arctic-Shipping-Operations . htm, 2012.

[16]. Moe, A. and Jensen O. - Fridtjof Nansen Institute. ***Opening of New Arctic Shipping Routes. Belgium,*** 2010.

[17]. N. Kjerstad, O. Bjoerneseth - ***Full-Scale Ice-Navigation Simulator,*** Aalesund University College, Norway, 2002.

[18]. Parkinson, C. L., D. J. Cavalieri - ***A 21 Year Record of Arctic Sea Ice Extents and Their Regional, Seasonal and Monthly Variability and Trends***, 441 – 446, 2002.

[19]. Parkinson, C. L., D. J. Cavalieri, P. Gloersen, H. J. Zwally, and J. C. Comiso - ***Arctic Sea Ice Extents, Areas, And Trends***, 1978 – 1996, J. Geophys. Res., 104, 20,837 – 20,856, 1999.

[20].S. Chernova, A. Volkov - ***Economic Feasibility of the Northern Sea Route Container Shipping Development Logistics and Transport*** , Bodø, 2010.

[21].Stroeve, J., M. M. Holland, W. Meier, T. Scambos, and M. C. Serreze - ***Arctic Sea Ice Decline***: Faster Than Forecast, Geophys. Res. Lett., 34, L09501, doi:10.1029/2007GL029703, 2007.

[22]. ***The IMO Guidelines for Ships Operating in Arctic Ice-covered Waters***, 2007.

[23]. Vitousek, Peter M. - ***Beyond Global Warming: Ecology and Global Change the Robert H. Macarthur Award,*** Madison, Wisconsin Ecology, 75(7), pp. 1861-1876, 1994.

For Authors

Are edited scientific papers in topics, written in English. Papers are selected after a peer review. Each participant is allowed to send maximum 2 papers as first author. Authors should make sure that the manuscripts submitted are ready for refereeing. The papers that are to be published must bring scientific contributions to the journal. The papers also have to contain the results of some of your work. It is strongly recommended an even number of pages, no longer than 6-10 pages. The papers that do not respect the publishing conditions and which are not integrated in the thematic of this journal will be rejected from the start by the Editorial Board. Authors submitting an article affirm that the same manuscript is not concurrently submitted to another publication. The authors are entirely responsible for the content of their papers.

PUBLISHED SINCE 2008
ISSN:1844-6116
ON LINE SINCE: 2008
PUBLISHED BY: Editura Nautica/ Constanta Maritime University